ILLEGITIMATE V(D)J REARRANGEMENT IN γ-IRRADIATION INDUCED T CELL LYMPHOMA IN NEWBORN *scid* MICE

by

Danny Vesprini

A thesis submitted in conformity with the requirements
for the degree of Master of Science
Graduate Department of Immunology
University of Toronto

© Copyright by Danny Vesprini (1997)

Acquisitions and
Bibliographic Services

395 Wellington Street
Ottawa ON K1A 0N4
Canada

Acquisitions et
services bibliographiques

395, rue Wellington
Ottawa ON K1A 0N4
Canada

Your file Votre référence

Our file Notre référence

The author has granted a non-exclusive licence allowing the National Library of Canada to reproduce, loan, distribute or sell copies of this thesis in microform, paper or electronic formats.

L'auteur a accordé une licence non exclusive permettant à la Bibliothèque nationale du Canada de reproduire, prêter, distribuer ou vendre des copies de cette thèse sous la forme de microfiche/film, de reproduction sur papier ou sur format électronique.

The author retains ownership of the copyright in this thesis. Neither the thesis nor substantial extracts from it may be printed or otherwise reproduced without the author's permission.

L'auteur conserve la propriété du droit d'auteur qui protège cette thèse. Ni la thèse ni des extraits substantiels de celle-ci ne doivent être imprimés ou autrement reproduits sans son autorisation.

0-612-29263-0

Canada

Acknowledgments

I would like to thank my supervisor, Jayne Danska, for her guidance, understanding and friendship. I would also like to thank the members of my supervisory committee, Dr. Neil Berinstein, Dr. Susanna Lewis and Dr. Bob Phillips, who all provided excellent counsel throughout my graduate school experience. Thanks to the members of the Danska lab (Priscilla Chiu, Casey Fox, Ildiko Grandal, Christine Williams, Kelly Williams), as well as Cynthia Guidos, for their support and friendship. Finally, I would like to thank my friends and family, who were always there when I needed them.

Dedication

This thesis is dedicated to the memory of grandma Tilly Vesprini.
"Be good to the people."

Note:

The experiments presented in the first section of results, the RAG-2$^{-/-}$ *scid* analysis, were done in collaboration with Christine Williams. The RAG2$^{-/-}$ *scid* mice were bred by Ildiko Grandal at the Hospital for Sick Children. Fluorescent *in situ* hybridization was performed by the author under the direction of Dr Barbara Beatty of the CGAT FISH mapping center, at the Hospital for Sick Children.

Table of Contents

LIST OF TABLES

LIST OF FIGURES

Illegitimate V(D)J Rearrangement in γ-Irradiation-Induced T Cell Lymphoma in Newborn *scid* Mice, Master of Science, 1997, Danny Vesprini, Department of Imunology, University of Toronto

Abstract

The production of DNA double strand breaks during V(D)J recombination, makes developing lymphocytes particularly susceptible to neoplasia. Severe combined immunodeficient (*scid*) mice inefficiently ligate free coding ends generated during V(D)J recombination due to a mutation in the catalytic subunit of DNA-dependent protein kinase (DNA-PK_{cs}). Treatment of newborn *scid* mice with low dose (100 cGy) γ-irradiation restores V(D)J rearrangement at multiple TcR loci and results in the universal development of T cell lymphoma. In this study, we used a genetic approach to determine that V(D)J rearrangement played an obligate role in radiation-induced lymphoma in *scid* mice. We also present evidence of abnormal V(D)J rearrangement in irradiated newborn *scid* (IRNB-SCID) T cell lines. Our results collectively indicate that sequence specific breaks made during V(D)J rearrangement are essential for radiation-induced lymphomagenesis in *scid* mice, and that mutations accumulated during attempted TcRβ locus rearrangement may contribute to the invariant outgrowth of thymic lymphoma.

Background

V(D)J RECOMBINATION AND DNA REPAIR

Clonally distinct T and B cell antigen receptors are generated from the joining of dispersed variable (V), diversity (D), and joining (J) gene segments, in a highly ordered, multi-step process termed V(D)J recombination (reviewed in 1, 2). Recombination signal sequences (RSS), which flank recombinationally active gene segments, target the recombinase machinery to the antigen receptor loci. RSSs consist of conserved heptamer and nonamer motifs separated by a non-conserved spacer sequence of either 12 or 23 bp (3). Recognition of RSS is followed by the introduction of double stranded breaks (DSB) between the RSS and coding sequences, generating two sets of DNA termini: coding ends and signal ends (2). Co-expression of the lymphoid specific, recombinase activating genes, *rag*-1 and *rag*-2, is required for V(D)J recombination, and RAG-1/RAG-2 protein expression in non-lymphoid cells is sufficient to support recombination of extrachromosomal V(D)J substrates (4). Moreover, targeted gene disruption of either *rag*-1 or *rag*-2 prevents V(D)J recombination (5, 6). Consistent with these observations, the RAG-1 and RAG-2 proteins have been determined to be both necessary and sufficient for recognition of RSS, introduction of DSBs and formation of hairpin terminated V(D)J coding ends (7, 8)

Ligation of free DNA termini leads to the creation of coding joints and signal joints (2). Depending on the orientation of the RSSs, recombination results in the inversion or deletion of the intervening DNA sequence. Prior to ligation, coding ends are often subject to nucleotide deletion and/or addition (reviewed in 1, 9). The addition of non-templated (N) nucleotides at coding junctions is catalyzed by the lymphocyte-specific enzyme terminal deoxynucleotidyl transferase (TdT) (10-12).

Though not an obligate participant in the V(D)J recombination process, TdT contributes diversification to the germ-line (11, 12). Coding joins may also contain palindromic (P) nucleotides, which are thought to arise during the resolution of DNA-hairpin intermediates (13, 14). In contrast to coding ends, nucleotide addition or loss at signal ends is rare (15). The asymmetry of these reaction products suggests that coding ends and signal ends are processed differently.

The crucial role of DSB repair in V(D)J recombination was revealed by studies of mice harbouring the severe combined immunodeficiency (*scid*) mutation. In these mice, failure to productively rearrange the antigen receptor genes results in the lack of mature T and B lymphocytes (16). The *scid* V(D)J recombination defect results from a deficiency in DSB repair activity (17-20) which is required for the efficient joining of coding segments (15, 21, 22). In *scid* lymphocyte precursors, DSB are introduced at RSS, (13) but coding ends are ligated inefficiently. Interestingly, though RSS ligation is essentially normal in *scid* mice (15, 23, 24), coding joint formation has been measured to occur at a frequency of approximately 10-100 times less than WT (25). The "leakiness" of the *scid* mutation is illustrated by the fact that rare normal V(D)J coding joints can be isolated from the lymphocytes of aged *scid* mice (25-28). Moreover, coding joints analysed in *scid* mice often display characteristic structural abnormalities. For example, long P nucleotides are often seen in the rare coding joints from "leaky" *scid* (29, 30). In spontaneous *scid* thymic lymphomas and Abelson murine leukemia-virus transformed *scid* bone marrow cells, loss of DNA sequence due to nuclease digestion or illegitimate rearrangement has been observed (21, 22, 31, 32). Therefore, although the *scid* mutation confers a DSB repair defect, it appears that V(D)J rearrangement can occur in *scid* lymphocytes.

In addition to impairing V(D)J recombination, the *scid* mutation causes defective DSB repair in all cell lineages, resulting in hypersensitivity to ionizing

radiation and other agents that induce DSB (17-19). The *scid* mutation has been mapped to the gene encoding the catalytic subunit of the DNA-dependent protein kinase (DNA-PK_{cs} (33-35), which is a 460 kDa member of the phosphatidylinositol (PI)-3 serine/threonine kinase family (36). DNA-PK_{cs} is active when bound to DNA, and this is mediated by the Ku nuclear complex, a heterodimer of 80 and 70 kDa (37). The effects of the *scid* mutation implicate a crucial role for DNA-PK_{cs} in both DSB repair and V(D)J recombination. Though the precise role of DNA-PK in DSB repair is not defined, it has been suggested that DNA-PK phosphorylates downstream target molecules in response to DSBs (38). Compatible with this suggestion, in vitro studies have shown that several DNA binding proteins, including the transcription factors SP1, c-JUN, c-FOS and OCT1, act as substrates for DNA-PK (39). Therefore, the DSB repair defect in *scid* mice maybe due to the inability to effectively respond to DNA lesions.

Until recently, the exact nature of the *scid* mutation was unknown. The leakiness of the *scid* mutation suggested that the DSB repair defect was not due to a null mutation. Recent work done in our lab, in collaboration with Cynthia Guidos, supports the hypothesis that the *scid* phenotype is a result of abnormal co-ordination or regulation of DSB repair (40), as opposed to the absence of DNA-PK activity, which had been suggested by others (33, 35, 41). DNA sequence analysis of the C-terminal kinase domain of DNA-PK_{cs} identified a single base pair substitution, which resulted in a premature ochre stop codon (40, 42). This mutation is predicted to truncate DNA-PK_{cs} by approximately 8 kDa, but leaves intact the motifs thought to be required for kinase activity (40). It was also discovered that expression of DNA-PK_{cs} in *scid* cells was reduced 10-fold relative to that in WT thymocytes. Moreover, the *scid* mutation apparently disturbs DNA-PK_{cs} nuclear localization, which is presumably required for its enzymatic activity (40). Taken together, these data

suggest that the *scid* phenotype results from inefficient DSB repair, rather than the absence of this activity.

ROLE OF V(D)J RECOMBINATION IN LYMPHOCYTE DEVELOPMENT

The successful rearrangement of the immunoglobulin heavy chain (Igμ) and T cell receptor beta chain (TcRβ) play important roles in B and T cell development, respectively. Bone marrow derived progenitor cells which migrate to the thymus do not express CD4 or CD8 co-receptors, and are referred to as co-receptor double negative (DN) cells. Within the DN compartment there is a maturational progression defined by the expression of the IL-2 receptor alpha chain (CD25) and the phagocytic glycoprotein 1 (CD44). Rearrangement at the TcRβ locus occurs as the $CD25^+$ DN cells down-regulate CD44 expression (43, 44). Cells expressing a successfully rearranged TcRβ chain, probably paired with a non-rearranged pre-Tα chain (45), proliferate extensively, downregulate CD25 expression, upregulate CD4 and CD8 co-receptors to become double positive (DP), and initiate rearrangement at the TcRα chain (46). DP thymocytes expressing low levels of the TcRαβ heterodimer undergo maturation into $CD4^+$ or $CD8^+$ single positive (SP) cells which express high levels of the TcRαβ heterodimer. Similarly, in B cell development, the successful rearrangement and expression of Igμ chain, complexed with λ5 and VpreB proteins, mediates signals for developmental maturation of $B220^+$ $CD43^-$ pre B cells from $B220^+$ $CD43^+$ large pro-B cell precursors (47), and promotes rearrangement of the Ig light chain loci (48-50). Mature B cells are produced when rearranged Ig light chains are paired with heavy chains and expressed at the cell surface (51).

Rearrangement at antigen receptor loci is developmentally regulated. For example, in T cells, rearrangement at the TcRβ locus precedes that of TcRα in

normal developing cells (52, 53)., The TcRβ locus consists of at least 22 V gene segments and a constant region that contains two tandemly arrayed clusters of genes. The closely linked Cβ1 and Cβ2 are each preceded by a cluster of six functional Jβ gene segments, one non-functional (pseudo, ψ) Jβ gene segment, and one Dβ gene segment (Fig 1). At the TcRβ locus, the rearrangement of these originally separated gene segments occurs in a developmentally ordered fashion, as joining of D to J is followed by that of V to DJ (54, 55). Consistent with this, DJ rearrangements at the TcRβ locus are seen in mice by day 14 of gestation (55, 56). Moreover, during murine embryogenesis, an ordered program of TcR gene expression takes place in the thymus; TcRγ, δ and β gene expression occurs between days 14 and 16 of gestation, whereas TcRα gene expression is delayed until day 17. These observations demonstrated the tight coupling of V(D)J rearrangement with development, and in particular, implicated a role for TcRβ locus rearrangement in T cell development.

As previously stated, mice bearing the *scid* mutation have a DSB repair defect which affects all cell lineages (17-20). During V(D)J recombination in *scid* mice, RSS-mediated DSB are initiated, but coding ends are unable to join efficiently (15). Mice with a targeted disruption of either the *rag*-1 or *rag*-2 genes are unable to initiate DSB at RSS, and their antigen receptor genes remain in germ-line (5, 6). Lymphocyte development in both *scid* and RAG-deficient mice is therefore arrested at a similar stage: T cell maturation is arrested at the $CD44^-$ $CD25^+$ DN stage, while B cell development is arrested at the $B220^+$ $CD43^+$ large pro B cell (5, 6). Introducing a functionally rearranged TcRβ or Igμ transgene into RAG-deficient or *scid* mice promotes the development and expansion of DP thymocytes (53, 57, 58) or pre-B cells (59, 60), confirming that successful rearrangement of these antigen receptor genes provides essential developmental and proliferative signals in T and B cell development.

Introduction

THE IRRADIATED NEWBORN *scid* MOUSE MODEL

Our lab has studied the effects of DNA damage on T cell development and T cell lymphomagenesis in *scid* mice. Exposure of newborn *scid* mice to 100 cGy o ionizing radiation relieved the block in thymocyte development (61, 62) anc restored the production of highly diverse, in-frame TcRβ chains (61). Surprisingly the developmental block in B cell maturation was unaffected by radiation treatmen and productive Igμ rearrangement was not detected. TcRβ coding joins from irradiated newborn *scid* mice (IRNB-SCID) displayed normal fine structure and lacked anomalies characteristic of "leaky" *scid* antigen receptors (25-28) Furthermore, restoration of V(D)J rearrangement was not specific to the TcRβ locus as normal rearrangement at the TcRδ (63) and TcRγ locus (64) was also detected in IRNB-SCID mice. Collectively, these results revealed that irradiation of newborn *scid* mice induces transient rescue of V(D)J rearrangement, leading to productive TcR rearrangement and thymocyte maturation to the DP stage.

At four to five months post-irradiation, all IRNB-SCID mice displayed DP thymic lymphoma. This invariant progression to lymphoma suggests that growth promoting mutations occurred in some of the rescued DP cells following irradiation. Interestingly, no tumours of other cell lineages have been detected in the IRNB-SCID mice even though the *scid* mutation affects DSB repair in all tissues Taken together, these results suggest that irradiation induced rescue of V(D)J recombination in T cell precursors which harbour a defect in DSB repair may enhance the generation of chromosomal aberrations which promote the invariant development of thymic lymphoma. We hypothesize that γ-irradiation induced

restoration of V(D)J rearrangement leads to an increased frequency of illegitimat rearrangement events at the TcRβ locus, a common feature of lymphocyti malignancies (65).

MECHANISMS OF LYMPHOMAGENESIS

Multiple doses of sub-lethal γ-irradiation repeated at regular intervals (split dose) has been shown to produce thymic lymphoma in susceptible mouse strain (66). This irradiation treatment activates murine leukemia retro-viruses which ac as insertional mutagens (66-70). Integrated retroviruses can activate flankin cellular genes through several mechanisms: 1) promoting transcription from th viral promoter, 2) affecting expression of adjacent cellular genes, 3) disrupting cis acting elements, or, 4) integrating within a transcription unit, thus altering th structure and function of the encoded protein. Through searching for genomi DNA rearrangements, novel murine leukemia virus integration events were no detected in irradiation induced *scid* thymomas (Jolicoeur and Danska, unpublishe observations). Activation of murine leukemia viruses therefore do not appear t account for the invariable development of T cell lymphoma in IRNB-SCID mice.

A recurring theme in the molecular pathogenesis of hematopoieti malignancy is activation of cellular proto-oncogenes by chromosomal aberration the most frequent of which are chromosomal translocations. Analyses o chromosomal translocations in human lymphoid neoplasias have shown that thes aberrations fall into two categories. In the first, the chromosomal translocatio causes the formation of a novel transcriptional unit derived from the fusion o genes at the breakpoint sites (fusion transcripts). A chimeric gene found in bot human chronic myelogeneous leukemia (CML) and acute lymphoblastic leukemi (ALL) is the BCR-ABL fusion gene (71). The resultant fusion protein has enhance

tyrosine kinase activity and tumourigenic properties (72). Another example of chimeric gene creation involves a translocation present in B cell ALL, where the basic-helix-loop-helix transactivation domain of the transcriptional regulator E2A, is fused to the carboxy-terminal portion of PBX1, which contains a DNA-binding homeodomain (73, 74). In translocations such as these, fusion transcript formation leads to chimeric proteins displaying novel biochemical properties distinct from those of the wild-type proteins.

In the second category of aberrations, reciprocal translocation juxtaposes TcR or Ig loci to a gene from another chromosome. In T cells, this ectopic localization causes deregulated expression of the translocated gene, driven by powerful enhancers present in the T cell receptor loci (reviewed in 75). The same mechanism occurs in B cells. For example, in Burkitt's lymphoma, c-*myc* is translocated to the Ig heavy chain locus, resulting in the activation of this proto-oncogene (76-78). The TcRβ locus is also a frequent site for chromosomal translocations in lymphoid cancers. One such translocation juxtaposes the gene encoding the protein tyrosine kinase $p56^{lck}$ (*lck*) and the TcRβ locus, which causes *lck* mRNA levels to become significantly elevated (79). Therefore, in translocations involving antigen receptor loci, the predominant biological consequence is transcriptional deregulation of the juxtaposed gene, resulting in inappropriate levels of the gene product compared to normal cells. Given the prevalence of chromosomal rearrangements at antigen receptor loci in lymphoid malignancies, and our detection of γ-irradiation induced rescue of V(D)J rearrangement in *scid* thymocytes, illegitimate rearrangement of the TcRβ locus could likely play a role in the universal development of T cell lymphoma in IRNB-SCID mice.

Much evidence implicates illegitimate V(D)J recombination in translocations involving the antigen receptor loci. Evidence for V(D)J recombinase mediated translocations can be seen through examination of the translocation breakpoints. In many cases, DNA sequences that resemble the heptamer and/or nonamer RSS are found on the non-antigen receptor locus partner of the translocation (80-85). Though these 'cryptic' RSS differ from the consensus RSS, they may be able to mediate RAG dependent DSB, as a recent study showed that RSS elements that have significant sequence or structural variation still serve as recognition sites for the RAG proteins (86). The observation of cryptic RSS at translocation breakpoints therefore supports the view that abnormal recombination results from mistakes in the process of recombinase mediated joining.

Some characteristics of V(D)J recombinase mediated translocation breakpoints are non-templated 'N' region nucleotide additions (80-82, 84, 85, 87, 88), palindromic 'P' sequence additions (89), and evidence of exonuclease activity (80, 89, 90). In multiple reported cases, one of the products of translocations involving illegitimate rearrangement is not modfied, much like a signal-join, while the reciprocal product manifests coding-join-like modifications (79, 82, 85). The breakpoint characteristics mentioned above are not restricted to translocations involving Ig or TcR loci, but have also been observed in a recurrent site-specific deletion in T-ALL cell lines, that fuses two genes, *scl* and *sil* (83). Normally, the expression of *scl* in hematopoietic tissues is heterogeneous: it is expressed in cells with stem cell attributes but is consistently absent in thymocytes and mature cells (91). *scl* is ectopically expressed as a result of juxtaposition to the *sil* gene, which is constitutively active in thymocytes (92). The recombination event that produces the *scl-sil* fusion displays features suggesting that it is mediated by the action of the V(D)J recombinase

machinery. These observations clearly implicate illegitimate V(D)J rearrangement as being a common contributor to the development of human lymphoid neoplasias.

THE IRRADIATED RAG-DEFICIENT MOUSE MODEL

The rescue of DP T cell development in irradiated *scid* mice was associated with TcRβ rearrangement and expression (61). It remained possible that the DSB repair defect caused by the *scid* mutation also promoted T cell development, which was independent of TcRβ expression. To determine the effect of irradiation on the development of T cells in the absence of TcRβ expression, our lab in collaboration with Cynthia Guidos, treated RAG-1 and RAG-2 deficient mice with γ-irradiation. A single, sublethal dose (750 cGy adults, 400 cGy newborns) of irradiation rescued the development and expansion of DP thymocytes in irradiated RAG-1 and RAG-2 deficient mice in a TcRβ-independent pathway (93, 94). In contrast to the IRNB-SCID mice, T cell development in irradiated RAG-deficient mice occurred in the absence of T cell lymphoma, consistent with the idea that the progression to lymphoma in IRNB-SCID mice was related to restoration of V(D)J rearrangement. Nevertheless, these studies could not rule out the possibility that the invariable development of T cell lymphoma in IRNB-SCID mice was attributable to the imposition of random DNA damage in cells with a DSB repair defect, and thus was independent of the restoration of V(D)J rearrangement.

In the current study we have investigated: 1) the role of RSS cleavage in the development of lymphoma in irradiated newborn *scid* mice, and 2) the putative role of V(D)J recombinase mediated translocation of the TcRβ locus in five IRNB-SCID DP T cell lines; LK3, LK3C, LK6.2, LK8 and SCTL2. Our results support the view that the restoration of V(D)J rearrangement plays an important role in the universal development of lymphoma in IRNB-SCID mice. We also present

evidence of abnormal rearrangement in the IRNB-SCID DP T cell lines, which ir one of the lines appears to have resulted in a chromosomal translocation at the TcRβ locus. Even though chromosomal translocations involving illegitimate V(D)J rearrangement have been well characterized in humans, there is little evidence of this mechanism in murine models of lymphoma or leukemia. Given our evidence that the restoration of V(D)J rearrangement appears to be involved in the invariable development of T cell lymphoma, we postulated that the IRNB-SCID model would prove to be a useful system in which to study illegitimate rearrangement.

Materials and Methods

DNA PROBES

The cDNA and genomic probes used in this study were: murine β-actin (0.59 *PstI/PstI* fragment;(95)); murine TcRCα (0.55 kb *EcoRI/PstI* fragment; (96); murine TcR Cβ (0.4 kb *Hind*III/*EcoRI* fragment; (97)); murine TcR 5'Dβ1 (1.2 kb *PstI/AccI* fragment; (98)); murine TcR 3'Jβ2 (0.8 kb *ClaI/EcoRI* fragment; (98)); murine TcR Vβ2 (0.23 kb *RsaI/RsaI* fragment; (97); murine TcR Vβ3 (0.27 kb *EcoRI/RsaI* fragment; (97); murine TcR Vβ7 (0.3 kb *EcoRI/PstI* fragment; (97); murine TcR Vβ14 (0.3 kb *EcoRI/BglI* fragment; (97); murine Thy-1 (TM8) (0.7 kb *PstI/PstI* fragment; (99)); and murine pTα (0.66 kb *EcoRI/EcoRI* fragment) which was generated by RT-PCR based upon the published sequence (45).

CELL LINES

LK3, LK3C, LK6.2, LK8 and SCTL2 are CD4/CD8 co-receptor double positive (DP) T cell lines derived from irradiated newborn *scid* (IRNB-SCID) mice (61). LK6.2, LK8 and SCTL2 were isolated from individual mice. LK3 and LK3C are distinct clonal T cell lines derived from one mouse. VL3-3M2 (100) is a subclone of BL/VL3 (101), a radiation leukemia virus-induced C57BL6/Ka thymic lymphoma. All cell lines were maintained in RPMI 1640 (Antibiotics, Toronto, ON) supplemented with 5% fetal calf serum (FCS; Gibco BRL, Gaithersburg, MD), 5 X 10^{-5} M β-mercaptoethanol (Sigma, St. Louis, MO), 10 mM L-glutamine (Gibco BRL, Gaithersburg MD) and 10 mM N-2-hydroxyethylpiperazine-N'-2-ethanesulfonic acid buffered saline (HEPES).

MICE

Animals carrying a targeted disruption of the RAG-2 gene coding region [RAG-$2^{-/-}$ mice; (6)] were obtained from GenPharm (Mountain View, CA) and bred at the Hospital for Sick Children. C.B.-17 SCID (16) referred to in the text as *scid* mice, and BALB/c mice were bred and housed at the Hospital for Sick Children. To generate RAG-$2^{-/-}$ *scid* double mutant mice, (RAG-$2^{-/-}$ X *scid*) F1 offspring were backcrossed to *scid* mice. *scid* homozygotes were identified by flow cytometric screening of peripheral blood, for the presence of T cells (anti-CD3ε, 145-2C11, (102)) and B cells (anti-IgM, F 9259, Sigma, St. Louis, MO). Mice deficient in T and B cells were *scid* homozygotes. The RAG-2 mutant and wildtype alleles were identified by PCR amplification of tail DNA using the primer trio of RAG2-3, Neo-3, and RAG2-1 (the sequences of these primers are found in Table 1; (103)). Thermal cycling conditions for this primer trio were 30 cycles of 30 seconds at 94°C, 90 seconds at 60°C, and 120 seconds at 72°C. Under these conditions, RAG2-3 and Neo-3 amplified a 937 bp mutant fragment, and the RAG2-3 and RAG2-1 amplified a 973 bp WT fragment, which were resolved by electrophoresis through a 2% agarose gel. Mice found to be RAG-$2^{+/-}$ *scid/scid* were intercrossed to derive RAG-$2^{-/-}$ *scid* homozygous double mutants, which were bred and housed at the Hospital for Sick Children.

Newborn RAG-$2^{-/-}$ *scid* mice received 100 cGy of irradiation from a ^{137}Cs source within 24 hours of birth. For adoptive transfer experiments, $1x10^6$ cells isolated from the thymus of a 16 week old irradiated newborn RAG-$2^{-/-}$ *scid* mouse, were resuspended in 200 µl of 1X Hanks Buffered Salt Solution (HBSS, Gibco BRL, Gaithersburg, MD; 10X HBSS is 1.4 g/L calcium chloride, 4.00 g/L potassium chloride, 0.60 g/L potassium phosphate, 1.00 g/L magnesium chloride, 1.00 g/L magnesium sulfate, 80.00 g/L sodium chloride, 0.90 g/L dibasic sodium phosphate

and 10.00 g/L D-glucose) and injected (intravenously) into the tail vein of RAG-2 $^{-/-}$ recipients. Twelve weeks post transfer, thymocytes were harvested and analysed by flow cytometry for expression of CD4 and CD8 co-receptors.

FLUORESCENCE ACTIVATED CELL SORTING (FACS) AND ANALYSIS

(i) Preparation of Antibodies

Serum free concentrates of monoclonal antibodies (MAbs) were prepared by affinity purification on a Econo-column (Bio-Rad, Mississauga, Ont.) containing Protein A Sepharose (Pharmacia, Baie d'Urfe, QUE). MAbs were eluted first with two volumes of 0.2 M sodium acetate/1 mM NaN_3 (azide) pH 4.1, followed by one volume of 0.1 M acetic acid. The pooled MAb elutent was dialyzed against phosphate buffered saline (PBS; 150 mM sodium chloride, 2 mM potassium chloride, 10 mM Sodium phosphate, 2 mM potassium phosphate, pH 7.4). MAbs were stored at 1 mg/ml at -70°C. MAbs were biotinylated by adding 100 μL of a 1 mg/ml solution of biotin-XX-succinimydyl ester, P-1606 (Molecular Probes Inc., Eugene, OR) in dimethyl sulfoxide, per ml of MAb solution. Prior to biotin addition, the pH of the MAb solution was adjusted to between 8.2 and 8.6 with 1 M sodium carbonate/bicarbonate buffer, pH 9.2. The biotin/MAb solution was then incubated with mixing for four hours at room temperature (RT), dialyzed against two changes of one L of PBS, and stored at 4°C. MAbs were conjugated to fluorescein isothiocyanate (FITC) by adding 100 μL of a 1 mg/ml solution of FITC (Molecular Probes Inc., Eugene, OR) in 1 M sodium carbonate/bicarbonate buffer, pH 9.2, per ml of MAb solution. This FITC/MAb solution was mixed for two hours at RT with the tube wrapped in tin foil to protect it from the light. The conjugated MAb was then dialyzed against two changes of one liter of PBS, stabilized by adding a 1:10 dilution of 50 mg/ml BSA in 0.1 M azide, and stored at 4°C. Each MAb was

titrated to derive the concentration at which it was to be used in the flow cytometric analysis.

(ii) FACS Analysis

For flow cytometric analysis, T cell lines and freshly isolated lymph node cells or thymocytes were stained with: (i) biotinylated antibody to CD4 (anti-CD4; YTS 191.1; ref 104) and FITC conjugated anti-CD8 (YTS 169-4(104), (ii) biotinylated anti-TCRβ (H57-597; (105)) and FITC-conjugated anti-IL-2Rα (7D4;(106)) or (iii) biotinylated anti-TcRβ and FITC-conjugated anti-TcRVβ5 (MR9-4; (107)) as described (108). Briefly, one to two million cells suspended in PBS were transferred to four ml conical tubes (Bio-Rad, Mississauga, Ont.), underlayed with 0.3 ml of bovine calf serum (CS), pelleted by centrifugation (500 x g, 4°C, five minutes), resuspended in 50 μL of the first step MAb reagents diluted appropriated in staining media [1X HBSS, 2% FCS], and allowed to incubate under aluminum foil, on ice for 30 minutes. The cells were washed by adding 0.5 ml of staining media and underlaying with 0.3 ml of CS. The cells were then pelleted by centrifugation (500 x g, 4°C, five minutes), and the supernatant was removed by aspiration. The cells were resuspended in 50 μL of the second step reagent [phycoerythrin (PE)-conjugated streptavidin (Caltag, Cedarlane Lab. Ltd, Hornby ON)], and allowed to incubate under aluminum foil, on ice for 30 minutes. The cells were then washed as described above, resuspended in 0.5 ml of staining media containing 1-2 μg/ml propidium iodide (Sigma, St. Louis, MO). The cell suspension was then filtered through nytex into four ml round bottom tubes (Falcon). Fluorescence was analyzed on either a FACScan or a FACSCalibur flow cytometer (Becton Dickinson, Mississauga, ON). Dead cells and debris were excluded by gating on cells with high forward scatter and low propidium iodide fluorescence. Lysis II and CELLQuest software was used to analyze fluorescence data (Becton Dickinson, Mississauga, ON).

RADIOLABELING OF DNA PROBES

DNA probes were prepared by adding 11.4 µl of labeling solution [5 mM each dATP, dGTP, dTTP; 62.5 mM Tris pH 8.0; 6.25 mM $MgCl_2$; 5 mM β-mercaptoethanol; 250 mM HEPES pH 6.6; 70 pmol ethylenediamine tetra acetic acid (EDTA); 70 pmol Tris pH 7.5; and $7x10^{-5}$ units of random hexamer oligonucleotides ($p(dN)_6$; Pharmacia, Baie d'Urfe, QUE)], 10 µg BSA, 50µCuries (µCi) ^{32}P-dCTP (Amersham, Oakville, ON) and ten units Klenow DNA polymerase (Promega, Madison, WI), to 100-200 ng of heat denatured double stranded (ds) DNA probe. Reactions were incubated for a minimum of two hours at RT, purified on NucTrap pushcolumns (Stratagene, La Jolla, CA), and stored at -20°C.

RNA EXTRACTION

RNA was isolated from mouse tissue and cell lines using TRIzol (Gibco BRL, Gaithersburg, MD) as per the manufacturers instructions. Briefly, cells were pelleted by centrifugation (500 x g, 4°C, five minutes) and lysed using one ml of TRIzol reagent per $5x10^6$ cells. After five minutes at RT, 0.2 ml of chloroform was added per ml of TRIzol reagent, the samples were agitated for 15 seconds, and allowed to sit at RT for five minutes. The aqueous and organic phases were separated by centrifugation (3000 x g, 4°C, 20 minutes). The RNA was precipitated from the aqueous phase by mixing with one half volume of isopropanol, allowed to sit at RT for ten minutes, and then subjected to centrifugation (3000 x g, 4°C, 20 minutes). The RNA pellet was washed once with ice-cold 75% EtOH, and once with ice-cold 100% EtOH, allowed to air dry for 20 minutes and resuspended in RNase free ddH2O [diethyl pyrocarbonate (DEPC) treated ddH2O].

NORTHERN ANALYSIS

Total RNA was separated according to size by the Northern method (109). RNA samples were prepared as a solution of ten μg of RNA, 1 X -[N-morpholin]propanesulfonic acid buffer (MOPS), 50% formamide (Boehringer Mannheim Corp., Laval, QUE) and 2.2 M formaldehyde (Mallinckrodt Canada Inc.). Prior to loading the samples were heated at 65°C for 5-10 minutes, and immediately placed on ice. Two μl of DEPC-treated gel loading buffer (50% glycerol, 1 mM EDTA, 0.25% bromophenol blue, 0.25% xylene cyanol) was added to each sample while the 1.5% agarose-formaldehyde gel was prerun in 1 X MOPS and 2.2 M formaldehyde running buffer, at 100 V for approximately five minutes. The samples were then loaded and electrophoresed for 600VH. The gel was washed in several changes of DEPC-treated water before the RNA was transferred to nylon membrane (Micron Separations Inc., Westborough, MA) by capillary transfer, overnight in 10 X SSC (20X SSC is 3 M NaCl, 0.3 M NaCitrate). RNA was crosslinked to the filter by exposing it to 1200 μjoules/cm^2 of UV irradiation in a Stratalinker UV crosslinker (Stratagene, La Jolla, CA). Filters were prehybridized for a minimum of two hours in a solution of 2X Denhardt's [1% Ficoll, 1% polyvinylpyrrolidine, and 1% molecular grade bovine serum albumin (BSA; Sigma, St. Louis, MO)], 5 X SSPE (20X SSPE is 3 M NaCl, 0.2 M Sodium Phosphate monohydrate, and 0.02 M EDTA), 0.1% sodium dodecyl sulfate (SDS), and 50% formamide at 42°C. Filters were hybridized for 12-24 hrs in the same solution at 42°C with the addition of heat denatured ^{32}P labeled DNA probe at a final concentration of 1 X 10^6 counts per minute per ml of hybridization solution. Filters were washed for 20 minutes at RT in 1 X SSC, 0.1%SDS, followed by three washes of 20 minutes each at 55°C in 0.2 X SSC, 0.1%SDS. Damp filters were enveloped in plastic wrap, exposed to a phosphorscreen for 12-18 hours, and the radiographic image was digitized by a phosphorscanner

(Molecular Dynamics). Filters were stripped of hybridized probe by incubating in 200 ml of 0.01% SDS, 0.01 X SSC at 100°C, while shaking, for 2-3 minutes. This procedure was repeated three times. After the final wash, the filter was blotted, enveloped in plastic wrap, exposed to a phosphorscreen, and the radiographic image was analysed to ensure stripping was efficient.

REVERSE TRANSCRIPTASE COUPLED POLYMERASE CHAIN REACTION (RT-PCR)

(i) cDNA Synthesis

The sequences of the oligonucleotide primers used in this study are shown in Table 1. Generation of cDNA was accomplished using established methods (110). A 20 μL reaction contained 10.5 μL of reaction mixture (50 mM Tris, pH 8.3; 40 mM KCl; 6 mM $MgCl_2$; 1 mM DTT, 0.1 mg/ml BSA), 0.5 mM of each deoxynucleotide triphosphate (dATP, dCTP, dGTP, dTTP; Promega, Madison, WI); 1 μg/ml oligo $(dT)_{15}$ primer (Promega, Madison, WI); 12 units of ribonuclease inhibitor (RNasin; Promega, Madison, WI); 2.5 units avian myeloblastosis virus reverse transcriptase (AMV-RT; Promega, Madison, WI)]; and two μg of RNA in a volume of 9.5 μL DEPC-treated ddH_2O. RNA/ddH_2O samples were heated at 70°C for five minutes before addition of 10.5 μL of the reaction mixture. cDNA reactions were incubated at 42°C for two hours, after which the cDNA mixture was diluted by the addition of 20 μL of ddH_2O. Mock reactions without AMV-RT were included with each series of reactions to provide negative controls.

(ii) Polymerase Chain Reaction

Two and a half μL of each cDNA sample was subjected to the reverse transcriptase coupled polymerase chain reaction (RT-PCR) in a DNA thermal cycler (Perkin-Elmer 460, Perkin-Elmer, Rexdale, Ontario). PCR reactions included 50 mM

KCl; 1.5 mM $MgCl_2$; 10 mM Tris pH 9.0; 0.1% Triton-X 100; 0.2 mM each of dATP, dCTP, dGTP and dTTP; 0.5 μM of each primer; and 1.65 units of *Taq* polymerase (Perkin-Elmer, Rexdale, Ontario). cDNA quality was confirmed by the detection of a RT-PCR amplification product using β–actin primers. TcRβ cDNA was amplified with a degenerate, consensus Vβ primer specific for sequences in the Vβ1, 2, 5, 6, 8, 10, 12, 13, 15 and 16 genes (61) or primers specific for Vβ 3, 11 and 14, (61, 97) together with a Cβ antisense primer (Cβuni) designed from a conserved sequence in the Cβ1 and Cβ2 genes (61). cDNA containing a TcR Cβ gene segment (TcR Cβ cDNA) was amplified with primers (Cβ sense, Cβ antisense) which were designed from conserved sequences in both Cβ1 and Cβ2 such that cDNA containing both Cβ1 and Cβ2 were amplified. As a negative control for each PCR reaction, mock cDNA template (synthesized without reverse transcriptase) was amplified with the same PCR reaction mix. PCR cycling conditions for Vβ specific/Cβuni, the Cβ sense/Cβ antisense, and the β–actin primers were 30 cycles at 94°C for 30 seconds, 55°C for 60 seconds, and 72°C for 60 seconds. For the Vβ consensus primer, the annealing temperature for the first 3 cycles was 37°C, followed by 30 cycles at 55°C. A final ten minute extension was performed at 72°C for all primer reactions. PCR products were resolved on 1% agarose gels, stained with ethidium bromide, photographed under ultraviolet light, denatured in 1.5 M NaCl/0.5 M NaOH, neutralized in 1 M Tris/1.5 M NaCl, and transferred to nylon membrane in 10XSSC. After overnight transfer, the DNA was crosslinked to nylon membrane and the filters were prehybridized, hybridized and analysed as was described in the Northern Analysis section, with the following exceptions. The hybridization solution was 5X Denhardt's, 6 X SSC, 1% SDS, 50% formamide and 100μg/ml denatured herring sperm DNA. Filters were stripped of hybridized probe by gentle agitation in 0.4N NaOH for 40 minutes, followed by 30 minutes in 0.1X SSC, 0.1% SDS and 0.2 M Tris pH 7.5.

DNA SEQUENCING

PCR products were agarose gel-purified using a QIAEX II gel extraction kit (QIAGEN, Chatsworth, CA) and ligated directly into the vector pCR-2 (Invitrogen) as per the manufacturers instructions. The ligation products were transformed into OneShot^{TM} competent E. coli (Invitrogen, San Diego, CA) as per the manufacturers instructions, and plated on Luria Broth (LB) agar containing ampicillin at 50 μg/ml. Individual colonies were selected, inoculated in cultures of three ml of LB containing ampicillin at 50 μg/ml, and incubated overnight in a 37°C bacterial incubator and shaker. The plasmid DNA was then extracted by the alkaline lysis method (109). Clones containing the PCR product were identified by digesting the DNA isolated from each clone with the restriction enzyme EcoRI (Promega, Madison, WI) and resolving them by gel electrophoresis to determine insert size (PCR products are ligated into the pCR-2 vector such that they are flanked by *EcoRI* sites, allowing easy restriction digest analysis). The DNA sequence of positive clones was determined on a 7% urea-polyacrylamide gel by the dideoxy chain termination method (111) using a T7 sequencing kit (Sequenase, U.S. Biochemicals, Cleveland, OH) as per the manufacturer's instructions. DNA sequence analysis was performed with MacMolly software (Soft Gene, Koln, Germany). Sequences were compared to those in the GenBank database using the NCBI Blast E-mail server (112).

GENOMIC DNA EXTRACTION

DNA was extracted from mouse tissue (kidney, thymus) or cell lines (LK3, LK3C, LK6.2, LK8, SCTL2, VL3-3M2) by resuspending $1x10^7$ cells in 400 μL of solution A (10 mM Tris pH 7.5, 10 mM EDTA, 10 mM NaCl), to which an equivalent volume of solution B (solution A with 2% SDS) was added. Proteinase K (Promega,

Madison, WI) was added to a final concentration of 100 μg/ml and incubated at 50°C for 2-16 hours. The DNA was then extracted sequentially with equal volumes of phenol , phenol/chloroform/isoamyl alcohol (25:24:1), and chloroform. Prior to use, the phenol was equilibrated to a pH greater than 7.8 by washing with Tris pH 8.0 (109) because DNA partitions into the organic phase at acidic pH. At each extraction step, the aqueous phase was transferred to a new tube. The DNA was then precipitated by adding NaCl to a concentration of 200 mM and two volumes of 100% EtOH. DNA was spooled onto a heat sealed micropipette and washed twice with 75% EtOH, followed by one wash with 100% EtOH. The DNA was allowed to air dry for five minutes, and resuspended in ddH2O by gentle rocking for 12-36 hours.

SOUTHERN BLOT ANALYSIS

Heat denatured dsDNA probes were hybridized to genomic DNA using the protocol described by Southern (109, 113). Briefly, 15 μg of DNA was digested with 30 units of the appropriate restriction enzyme and electrophoresed through a 1% agarose gel for approximately 600VH. The DNA in the gel was denatured, neutralized, transferred and crosslinked to nylon membrane, and the filters were prehybridized, hybridized and analysed as was described in the RT-PCR section.

QUANTITATIVE PHOSPHORIMAGING

Southern blots were exposed to a phosphorscreen for 12-18 hours and digitized by a phosphorscanner (Molecular Dynamics). Absolute pixel number in each sample was quantified by volume integration using ImageQuant software (Molecular Dynamics). Pixel number is directly correlated to signal intensity. To determine the copy number of the gene of interest, the ratios of the pixel values

obtained for a given TcRβ probe and a control probe (Thy-1) were compared between the experimental samples and the average of the non-lymphoid tissue controls (kidneyA and kidneyB). The ratio of the kidney control was defined as two alleles of the gene of interest. The average pixel value taken from the outline of the object created around each sample was used to determine background pixel values for each Southern blot. The following formula was used to determine the copy number of the gene of interest: (p.v. = pixel value; l.s. = lymphoid sample; Ka = kidneyA; Kb = kidneyB)

$$\frac{\dfrac{\text{l.s. p.v. for TcR}\beta}{\text{l.s. p.v. for Thy-1}}}{\left(\dfrac{\text{Ka p.v. for TcR}\beta}{\text{Ka p.v. for Thy-1}} + \dfrac{\text{Kb p.v. for TcR}\beta}{\text{Kb p.v. for Thy-1}}\right)} \Big/ 2 \times 2 \text{ alleles} = \#\text{ of alleles represented}$$

The following equation displays how this formula was used to determine the number of Vβ2 alleles present in the IRNB-SCID DP T cell line LK3. The pixel values obtained for LK3, kidneyA, and kidneyB are found in figure 17-A.

$$\frac{\dfrac{15371}{69509}}{\left(\dfrac{16359}{67003} + \dfrac{17754}{86419}\right)} \Big/ 2 \times 2 \text{ alleles} = 1.967435\ \text{V}\beta2 \text{ alleles}$$

FLUORESCENCE in situ HYBRIDIZATION (FISH)

A - PREPARATION OF METHANOL:ACETIC ACID FIXED CELLS

(i)Spleen Cell Preparation:

Mouse spleen was minced into a culture dish with three drops of RPMI 164(supplemented with 20% fetal calf serum (FCS; Gibco BRL, Gaithersburg, MD), 5 X 10^{-5} M β-mercaptoethanol (Sigma, St. Louis, MO), 10 mM glutamine (Gibco BRL Gaithersburg, MD), 10 mM Penicillin/Streptomycin (Gibco BRL, Gaithersburg, MD) and 10 mM HEPES, until no large lumps were visible. The cell suspension wa transferred to a 15 ml conical tube. The cells were pelleted by centrifugation (500 x g 4°C, five minutes), washed two times with PBS, and resuspended in ten ml of media containing three μg/ml concanavalin A (Calbiochem, Behring Diagnostics, La Jolla California). From this suspension, two sets of dilutions were made, one at 1 x 10^{6} cells per ml, and the other at 0.5 x 10^{6} cells per ml. The cells were allowed to incubate at 37°C in a 5% CO_2 incubator for 48 hours.

(ii) Cultured Cell Line Preparation:

The irradiated newborn *scid* (IRNB-SCID) DP T cell lines (LK3, LK3C, LK6.2 LK8, and SCTL2) were cultured starting at a density of 0.5x10^{6} per ml in ten ml o RPMI 1640 supplemented with 10% FCS, 5 X 10^{-5} M β-mercaptoethanol, 10 mM L-glutamine, and 10 mM HEPES. The cells were allowed to incubate at 37°C in a 5% CO_2 incubator for 24 hours.

(iii) Cell Harvesting:

Both cultured cells and spleen cells were pelleted by centrifugation (500 x g 4°C, five minutes), and resuspended in ten ml of RPMI 1640 supplemented with 20% FCS, 5 X 10^{-5} M β-mercaptoethanol, 10 mM glutamine, 10 mM Penicillin/Streptomycin, and 10 mM HEPES, at a density of 2x10^{6} per ml. The cells were then treated with colcemid (Gibco BRL, Gaithersburg, MD) at 0.1 μg/ml

incubated at 37°C in a 5% CO_2 incubator for 30 minutes, transferred to 15 ml conical tubes, washed with ten ml of PBS, and pelleted by centrifugation (500 x g, 4°C, five minutes). The supernatant was decanted, leaving approximately 0.5 ml of fluid in which the cells were resuspended.

(iv) Hypotonic Treatment:

Ten ml of 37°C hypotonic medium (seven ml ddH_2O plus five ml RPMI 1640 media supplemented with 5×10^{-5} M β-mercaptoethanol and 10 mM HEPES) was added to the cells. The first ml of hypotonic solution was added two drops at a time, with mixing between additions. After the first ml was added, hypotonic solution was added in increasing amounts between episodes of mixing. The cells were then incubated in a 37°C incubator for ten minutes.

(v) Fixation:

One ml of 3:1 methanol/acetic acid fixative solution was added to each tube and the cells were pelleted by centrifugation (500 x g, 4°C, five minutes). The supernatant was decanted, leaving approximately 0.5 ml of fluid in which the pellet was resuspended by gently flicking the tube. Ten ml of the 3:1 fixative was slowly added to the tubes. The first ml of fixative solution was added two drops at a time, with mixing in between additions. After the first ml was added, fixative solution was added in increasing amounts between episodes of mixing. The cell suspensions were placed at RT for 20 minutes and then pelleted by centrifugation (500 x g, 4°C, five minutes). The supernatant was decanted, leaving approximately 0.5 ml of fixative solution in which the pellet was resuspended by gently flicking the tube. The cells were then washed two times in the fixative solution. After each wash the cells were pelleted by centrifugation (500 x g, 4°C, five minutes). After the final wash the cells were resuspended in one ml of fresh fixative solution. Fixed cells were either used immediately, or stored at 4°C.

B - SLIDE PREPARATION

(i) Cleaning:

Slides were cleaned by immersing first in acetone, then in HCl:ethanol 1:1, for five minutes each, and then placing under running tap water. The slides were then stored in distilled water at 4°C for a minimum of 30 minutes.

(ii) Metaphase preparation:

The following procedure was performed in a fume hood.

Using a Pasteur pipette, one drop of the fixed cell suspension was dropped on to a slide (removed from cold, 4°C, distilled water) from a height of 1-3 cm. The slide was placed at an angle of 45° so that the drop spread out producing an elliptical area. Excess fluid was removed and the slide was placed onto a hot plate until dry. Remaining large drops of fluid were removed by tapping the slide on gauze. Ambient humidity was critical for this procedure: too dry an atmosphere impaired the quality of metaphase chromosomes, too humid an atmosphere and slow drying time resulted in "ghost" chromosomes, which appeared empty with a dark outline. To increase the humidity, a humidifier was placed into the fume hood during the procedure. After the slides had dried, they were checked under a phase contrast microscope (10X objective) in order to evaluate the number of cells undergoing mitosis (mitotic index) and metaphase quality. Two to three metaphases with no overlapping chromosomes, little cytoplasm, and 50 nuclei per 10X power field was determined to be suitable for analysis. In optimal preparations, the chromosomes appeared dark grey in colour. Chromosomes which were light grey or very black and refractile did not hybridize well. If the mitotic index was sub-optimal, the original cell suspension was either diluted with fixative, or concentrated by centrifugation (500 x g, 4°C, five minutes). The slides were allowed to rest for two days at RT before being hybridized with chromosome "paint" probes (114). The slides were stored at -20°C.

C - HYBRIDIZATION AND DETECTION

(i) Target Slide Denaturation

Cold slides were equilibrated to RT before use to prevent condensation from forming on the slide. The chromosome spreads were treated with 100 µl of 100 µg/ml ribonuclease A (RNase) in 2X SSC for one hour at 37°C in a box humidified with Millipore filtered water soaked Whatman paper. Fifty ml of freshly prepared 70% formamide/2X SSC, was placed in a coplin jar and warmed to 75°C in a water bath. While the formamide solution was warming, the RNase treated chromosome spreads were taken from the incubator and washed three times, for three minutes, in 2X SSC at RT. The chromosome spreads were then dehydrated by washing in an ethanol series of 70% ethanol, 90% ethanol, and 100% ethanol (all at -20°C) for five minutes each, then allowed to air dry for five minutes. The chromosomes were denatured at 75°C for two minutes in the 70% formamide/2X SSC solution. The final desired temperature was 70°C. The temperature of the formamide solution decreased one °C per slide added, thus to denature the chromosomes on five slides, the bath was set to 75°C. If the temperature was <70°C, denaturation was incomplete. After denaturation, the chromosome spreads were placed in cold 70% ethanol for five minutes, dehydrated in an ethanol series as describe above, and allowed to air dry for ten minutes.

(ii) Probe Denaturation

Mouse chromosome paints were obtained from Pamela H. Rabbitts of the Medical Research Council in Cambridge, England (114). Each paint is a complex mixture of DNA probes prepared by PCR amplification of individually sorted chromosomes using partially degenerate primers (degenerate oligonucleotide-primed-polymerase chain reaction, DOP-PCR, (114, 115). The 'paints' are labeled with biotin by a secondary PCR reaction in which biotin dUTP is incorporated into

the probes. This allows subsequent detection with fluorescent antibodies following hybridization of the paint to metaphasic chromosomes. For an in depth explanation on how to produce mouse chromosome specific paints see (114). For each slide seven μl of the chromosome paint probe [50% formamide, 5% Dextran Sulphate 0.1% SDS, 1X Denhardts, 100 μg/ml salmon sperm DNA, 0.1 μg/ml mouse repetitive DNA (CoT_1 fraction), and 15 ng/μl of chromosome probe DNA] was added to eight μl of hybrisol VI (65% formamide/2X SSC; Oncor), and the mixture was warmed in a 37°C incubator. One hundred ng of probe per slide was optimal for hybridization. The chromosome paints were denatured at 75°C for ten minutes, then allowed to prehybridize to mouse CoT_1 DNA for 90 minutes in a 37°C incubator.

(iii) Hybridization

Cover slips and chromosome spreads were prewarmed in a 37°C incubator for ten minutes prior to use. The denatured, CoT_1-prehybridized, chromosome paints were applied to the chromosome spreads and then covered by a 24x40 mm coverslip. The coverslips were then sealed onto the slides with rubber cement, and incubated overnight at 37°C in a box humidified with moist filter paper.

(iv) Washing and Detection

Using tweezers, the rubber cement was removed from the coverslips, and the coverslips were removed from the slides by rinsing in 2X SSC. To remove non-hybridized probe, slides were washed three times in 50% formamide, 1X SSC at 42°C for five minutes each and then three times in 2X SSC at 42°C for five minutes each. The chromosome spreads were then treated with 3% BSA, 4XSSC, 0.1% Tween 20 (BDH, Toronto, ON), to block non-specific hybridization. Forty μL of the blocking solution was pipetted onto each slide, covered by a 24x30 mm coverslip and the chromosome spreads were then placed at 37°C for 20 minutes in a humidified box.

The following steps were done in a dark room as fluorescent-antibody complexes are light sensitive. After treatment with the blocking solution, coverslips

were removed by gently tapping the slides on the edge of a plastic beaker. Forty µl of avidin conjugated to fluoroscein isothiocyanate (FITC-Avidin; Oncor) was added to each slide, covered by a 24x30 mm coverslip and incubated for 30 minutes at 37°C. Chromosome spreads were then washed three times in 4X SSC, 0.1% Tween 20 at 42°C for 5 minutes each. Forty µl of biotinylated goat anti-avidin antibody (Oncor) was then added to each slide, covered with a 24x40 mm coverslip and incubated for 20 minutes at 37°C. The chromosome spreads were then washed three times in 4X SSC, 0.1% Tween 20 at 42°C for five minutes each. Forty µl of FITC-Avidin was then added to each slide, covered with a 24x40 mm coverslip, and incubated for 20 minutes at 37°C. The chromosome spreads were then washed three times in 4X SSC, 0.1% Tween 20 at 42°C for five minutes each, counterstained with 4',6-diamino-2 phenylindole (DAPI) and propidium iodide (PI) by adding 12 µl of a mixture (8:4 v/v) of DAPI/antifade (Oncor; 0.1 µg/ml DAPI, antifade contains 70% glycerol) and PI/antifade (Oncor; 0.6 µg/ml PI) to each slide, covered with a 24x30 mm coverslip, and stored in a dry, light proof container covered with aluminum foil at 4°C until analysed. Fluorescent signals were detected using a confocal laser scanning microscope (Nikon Microphot-FXA) and images were collected and composite images were generated using Adobe Photoshop (Adobe Systems Inc.)

PULSED FIELD GEL ELECTROPHORESIS (PFGE)

(i) Preparation of DNA in agarose blocks:

Cultured cells (LK3, LK3C, LK6.2, LK8, and SCTL2) were washed three times in ice-cold HBSS, resuspended at a concentration of $5x10^7$ cells per ml in buffer (10 mM Tris, pH 7.2, 20 mM NaCl, 100 mM EDTA; TNE), and incubated at 42°C for five minutes. An equal volume of 2% low melt preparative grade agarose (LMP; Bio-Rad, Mississauga, Ont.) in TNE buffer containing 100 µg/ml Proteinase K (Promega,

Madison, WI), was prepared and equilibrated to 42°C. The 42°C molten agarose was mixed with the cell suspension using a sealed pasteur pipette, and transferred to plug molds (Bio-Rad, Mississauga, Ont.) using a micro-pipette fitted with a tip with the end cut off with a razor blade to create a wider opening. The agarose was allowed to solidify at 4°C for 30 minutes, then transferred to 50 ml conical tubes containing Proteinase K Reaction buffer [TNE containing 1 mg/ml proteinase K and 1% N-Lauroyl-Sarcosine (Sigma, St. Louis, MO)], and incubated at 50°C for 24 hours. The digestion mixture was replenished and the plugs were incubated for a further 24 hours at 50°C. The plugs were then incubated for an hour at 50°C in 50 volumes of 10 mM Tris, 1 mM EDTA (TE) pH 7.6. After one hour the TE, pH 7.6 was replaced with fresh buffer and allowed to incubate for another hour. The plugs were then washed one final time in TE, pH 7.6 and stored at 4°C in 0.5 M EDTA pH 8.0. Genomic DNA is these plugs remained stable for approximately two months at 4°C.

(ii) Restriction enzyme digestion of DNA in agarose blocks:

Agarose plugs (stored in 0.5 M EDTA) were incubated in ddH_2O for 30 minutes at 4°C in a 1.5 ml microcentrifuge tube. After 30 minutes the plugs were incubated in fresh ddH_2O for 30 minutes, then incubated in one ml of the appropriate restriction enzyme buffer for one hour at 4°C. After incubation, the buffer was removed and 200 µL of fresh restriction enzyme buffer was added along with 30 units of the restriction enzyme *Nae* I (Boehringer Mannheim), and the tubes were incubated at 4°C for 30 min in order to allow the enzyme to diffuse throughout the agarose plugs. The restriction enzyme reaction was activated by placing the tubes at 37°C and the DNA was digested for 12-16 hours. After digestion was complete, the blocks were incubated in one ml of TE pH 7.6 at 4°C for one hour.

(iii) Gel Electrophoresis

Following digestion, the agarose plugs were transferred into the wells of a 1% agarose gel in 0.5X Tris-borate/EDTA electrophoresis buffer (TBE; 1X TBE is 90 mM

Tris/90 mM boric acid/2.5 mM EDTA), and molten LMP agarose was used to seal the plugs into the sample wells. The gel was electrophoresed in a Chef-DR III (Bio-Rad, Mississauga, Ont.) at 14°C with the following parameters: ramped switch time from 10-45 seconds, voltage at six V/cm, field angle of 120 degrees, and a run-time of 19 hours. These parameters allowed good separation of DNA fragments between 50 kb and 1000 kb. λ phage DNA concatamers embedded in 0.75% LMP agarose (Bio-Rad, Mississauga, Ont.) were applied to the gel as DNA size standards.

(iv) Southern Blot transfer of PFGE gels

Transfer of DNA was performed as described for genomic Southern blots with the following exceptions. After electrophoresis, the gel was depurinated with 0.25 M HCl [prepared from 1N Hydrochloric acid (HCl) stock; Fisher Scientific, Don Mills, ON] for ten minutes before transfer to nylon (Magna nylon transfer membrane; Micron Separations Inc., Westborough, MA) in 10 X SSC for 48 hours. The filter was prehybridized, hybridized and analysed as described for standard Southern blots with the following exception. The filter was exposed to the phosphorscreen for 48-96 hours before the radiographic image was digitized by a phosphorscanner.

Results

(A) Effects of low-dose ionizing radiation on RAG-2 deficient *scid* mice

Irradiation of RAG-2 deficient scid mice induces development of DP thymocytes without rapid development of thymic lymphoma

In order to determine if RAG activity was crucial to the invariable progression to thymic lymphoma in irradiated newborn *scid* (IRNB-SCID) mice, we analysed the effects of irradiation on RAG-2-deficient *scid* mice (RAG-2$^{-/-}$ *scid* mice). These animals bear the *scid* DSB repair defect, but are unable to introduce DSB at RSS adjacent to V, D and J coding ends. By uncoupling the ability to cut at RSS from the generalized DSB repair defect, we tested whether abrogating RAG mediated cleavage at RSS would impact susceptibility to thymic lymphoma in irradiated newborn RAG-2$^{-/-}$ *scid* mice. If RAG-deficiency had a protective effect, a role would be implicated for illegitimate V(D)J rearrangement in the invariable progression to T cell lymphoma in IRNB-SCID mice.

We found that a single dose of γ-irradiation was able to rescue DP T cell development and expansion in the RAG-2$^{-/-}$ *scid* mice. By three weeks post-irradiation, RAG-2$^{-/-}$ *scid* thymocytes were 20-60% DP (Table 2). Thymus cellularity in three week old irradiated double mutant mice was 10-100 times greater than in non-irradiated, age-matched controls. The loss of CD25 expression, which occurs during the DN to DP transition (52), was also observed in RAG-2$^{-/-}$ *scid* mice by three weeks post irradiation, concomitant with the appearance of DP cells in the thymus. By six weeks of age, thymus cellularity and frequency of DP thymocytes declined (Fig 2) as had been previously observed in irradiated RAG-1 and RAG-2 deficient mice (93). Therefore, the kinetics of irradiation induced T cell development

in RAG-2$^{-/-}$ *scid* mice were similar to those observed in irradiated RAG-1 or RAG-2 deficient mice (93).

Evidence for the development of T cell lymphoma was not observed in the irradiated newborn RAG-2$^{-/-}$ *scid* mice analyzed at later time points post-treatment. By 10-16 weeks post-irradiation, two phenotypes ('A' and, 'B'), were observed in the irradiated RAG-2$^{-/-}$ *scid* animals. 'A' mice resembled the non-irradiated, three week old, RAG-2$^{-/-}$ *scid* controls, with low thymus cellularity and few DP thymocytes (Table 2, Fig 3). 'B' mice displayed greater than 50% DP thymocytes, and thymus celullarity was 10-60 fold greater than non-irradiated controls (Table 2, Fig 3). None of the analysed RAG-2$^{-/-}$ *scid* mice displayed thymus cellularity or development that was comparable to that observed in IRNB-SCID animals 10-16 weeks post irradiation (Fig 2, and ref 61). We therefore found no evidence of development of DP T cell lymphoma in irradiated RAG-2$^{-/-}$ *scid* mice.

It is possible that the DP thymocytes detected in 'B' mice were preneoplastic cells with the potential to develop into a thymic lymphoma. Previous studies have shown that preneoplastic lymphocytes can develop into thymic tumours after explantation to a compatible host (116-118). To determine if 'B' mice had preneoplastic cells, one million thymocytes were isolated from a 16 week old 'B' mouse and transferred intravenously into two RAG-2 deficient recipients. Twelve weeks post-transfer, no DP cells were observed in the thymus of the recipient mice (data not shown). The thymus cellularity of these recipients was identical to non-treated RAG-2 deficient, or RAG-2$^{-/-}$ *scid* mice, as they had less than 1 x 10^6 cells in the thymus. We cannot exclude the possibility that the absence of donor cells was due to their failure to reach a suitable microenvironment and expand. Alternatively, the DP thymocytes taken from the irradiated RAG-2$^{-/-}$ *scid* donor may have reached the thymus but were unable to develop into a thymic tumour. This possibility is supported by a failure of DP thymocytes derived from 'B'

irradiated RAG-2$^{-/-}$ *scid* mice to adapt to tissue culture, whereas thymic tumours explanted from IRNB-SCID mice were readily adapted in this manner (61). This analysis supported the view that the DP thymocytes isolated from the 'B' irradiated RAG-2$^{-/-}$ *scid* mouse were not preneoplastic.

These results suggest that RAG-2 deficiency protects irradiated *scid* mice from T cell lymphoma presumably by abrogating cleavage at RSS. In thymocytes of IRNB-SCID mice, oligoclonal TcRβ rearrangements were detected as early as 6 weeks post irradiation (61). Therefore, thymocytes harbouring oligoclonal TcRβ rearrangements expanded from an initially polyclonal pool, suggesting preferential survival and/or proliferation of pre-lymphoma cells. Taken together, these results implicate a role for rescued V(D)J rearrangement at the TcRβ locus in lymphomagenesis in IRNB-SCID mice. We therefore decided to determine if aberrant V(D)J rearrangement had occurred at the TcRβ locus in five IRNB-SCID DP T cell lines that were established from primary radiation-induced *scid* thymic lymphomas (61).

(B) Characterization of *scid* $CD4^+CD8^+$ T cell lymphoma lines

The IRNB-SCID DP T cell lines are blocked at an early stage of T cell development

Five cell lines (LK3, LK3C, LK6.2, LK8 and SCTL2) were established from primary irradiation induced tumours from individual irradiated newborn *scid* (IRNB-SCID) mice (61). Previous characterization for T cell developmental markers found each line to be $CD4^+CD8^+CD25^-$ (61; Guidos and Danska, unpublished observations). If illegitimate TcRβ locus rearrangement played a role in IRNB-SCID lymphomagenesis, we would have expected each cell line to have a common pattern of gene expression reflecting their developmental level of clonal expansion and maturation arrest.

As discussed in the background of this thesis, cells expressing a successfully rearranged TcRβ chain, paired with the invariant pre-Tα chain (45), initiate rearrangement at the TcRα chain locus (46). The pTα gene is expressed at varying amounts at successive stages of T cell development (45). In immature, DP T cells, pTα expression is high, but as DP thymocytes mature into single positive (SP; $CD4^+CD8^-$ or $CD4^-CD8^+$) thymocytes, pTα mRNA expression is downregulated. TcRα expression is also coupled to T cell development, as exemplified by the finding that DP thymocytes which lack expression of the TcRα gene do not progress to the SP stage of development (57). Rearrangement and expression of the TcRα locus therefore plays a role in the transition from the DP stage to the SP stage of T cell development. In our study, the detection of pTα message, coupled with the lack of TcR Cα expression would have indicated that the IRNB-SCID lines were blocked at the DP stage of development just after TcRβ rearrangement. This result would support the view that illegitimate rearrangement at the TcRβ locus played a role in the universal development of lymphoma in IRNB-SCID mice.

Through Northern blot analysis, we found that all of the IRNB-SCID lines expressed high levels of pTα message, as compared to the BALB/c thymus control (Fig 4-A). Low expression of pTα in normal thymus has been previously shown and is thought to be due to the fact that the majority of cells in a wildtype thymus are small DP cells which have presumably downregulated pTα expression (45). In contrast, the IRNB-SCID lines each represent a clonal population of DP cells that retain pTα expression, but lack expression of the TcR Cα gene (Fig 4-B). Based on the fact that TcRα rearrangement normally initiates after productive TcRβ rearrangement (44), we propose that the IRNB-SCID lines were blocked at a stage of development where TcRβ rearrangement had occurred, but TcRα rearrangement had either not been initiated, or rearrangement at this locus was non-functional (out-of-frame). Consistent with this interpretation, hairpin-terminated TcRα coding end molecules were detected in *scid* DP thymocytes, 1 week post-irradiation (63), indicating that RSS specific DSB had been introduced at the TcRα locus. These results support the view that illegitimate TcRβ locus rearrangement played a role in the rapid development of DP lymphoma in IRNB-SCID mice.

(C) Expression of TcRβ genes in irradiated newborn *scid* DP T cell lines

Detection of TcR Cβ expression in irradiated newborn scid DP T cell lines

In human lymphoid neoplasms, translocations involving antigen receptor loci can lead to the production of chimeric mRNA species (fusion transcripts) that encode portions of the TcR or Ig loci (81, 90, 119-122). Chromosomal translocation at the TcRβ locus in the IRNB-SCID DP T cell lines may have resulted in abnormally sized mRNA species containing either of the TcRβ constant genes (Cβ1 or Cβ2). To address this possibility, we examined TcR Cβ containing messages in the IRNB-SCID lines by both Northern blot and RT-PCR analysis.

In wildtype thymocytes, two TcR Cβ containing mRNA species of 1.3 kb and 1.0 kb have been defined (54). The 1.3 kb species is the full length V-D-J-C TcRβ transcript, while the 1.0 kb message represents an incomplete D to J rearrangement. This 1.0 kb message appears early in T cell development, and may precede full V(D)J rearrangement (123, 124). Our Northern blot analysis revealed that one of the five IRNB-SCID lines, LK3C, expressed a 1.0 kb TcR Cβ containing message (Fig 4-C). The presence of this TcR Cβ mRNA species was confirmed by RT-PCR, using a strategy (Fig 5; 5' Cβ-sense and 3' Cβ-antisense primers) that detected Cβ containing transcripts (Fig 6-A). Although we cannot rule out that the 1.0 kb transcript represented a fusion transcript, the size suggested it was the result of incomplete D-J rearrangement ((54)). SCTL2 contained an apparently full length 1.3 kb TcRβ message (Fig 4-C). A RT-PCR strategy which detected rearranged TcRβ V-D-J-C cDNA templates (Fig 5; 5' specific Vβs or Vβ consensus, 3' Cβ uni primers) supported the interpretation that this transcript was a full length TcRβ chain (Fig 6-B). Therefore, by both Northern blot and RT-PCR analysis, we did not detect abnormally sized TcRCβ containing transcripts, suggesting that a fusion transcript

containing a TcRβ constant gene segment was not present in any of the IRNB-SCID DP T cell lines.

TcRβ chain expression in SCTL-2

We then examined whether the 1.3 kb TcR Cβ transcript in SCTL2 was the result of a productive (in-frame) rearrangement. If the TcRβ message was the product of normal V(D)J recombination, we expected to observe a DNA sequence with normal modifications (small deletions and few N nucleotide additions) at the coding ends. We therefore RT-PCR amplified, cloned and sequenced the TcR Cβ chain from SCTL2. Our sequence analysis showed that the RT-PCR fragment amplified in SCTL2 corresponded to an in-frame TcRβ transcript, of the Vβ5.1, Jβ2.5 and Cβ2 gene segments (Fig 7). The V(D)J joining sequence notably did not contain P nucleotides, or evidence of extensive exonuclease degradation as have been observed in TcR genes from *scid* thymocytes (21). To confirm that the TcRβ transcript detected in SCTL2 was translated into protein, we analysed intracellular expression of TcRβ protein using a MAb specific for a TcR Vβ5 determinant (MR9-4; (107)1). We found that SCTL2 cells expressed TcR Vβ5 protein (Fig 8).

Taken together, these results show that none of the IRNB-SCID lines expressed abnormally sized TcRβ mRNA species, and one line displayed a productive TcRβ rearrangement presumably produced during the irradiation-induced transient restoration of TcRβ locus rearrangement. The lack of TcRβ expression in the other IRNB-SCID lines could be explained if rearrangement had either not occurred, or was out-of-frame. Alternatively, illegitimate V(D)J rearrangement may have resulted in a chromosomal translocation that disrupted the TcRβ locus. We therefore decided to look for abnormal rearrangement at the TcRβ locus in the IRNB-SCID lines through Southern blot analysis.

(D) Rearrangement at the TcRβ locus in irradiated newborn *scid* DP T cell lines

TcRβ locus rearrangement in the irradiated newborn scid DP T cell lines.

Was there a chromosomal translocation at the TcRβ locus in any of the IRNB-SCID lines? To explore this possibility, we first sought to confirm that the TcRβ locus had undergone rearrangement in all of the *scid* lines through Southern blot analysis of *Pvu*II digested genomic DNA using a TcR Cβ probe specific for both Cβ1 and Cβ2 genes (TcRCβ; (97)). Because the *Pvu*II sites located on the 5' side of Cβ1 and Cβ2 lie within the Jβ1 and Jβ2 gene clusters respectively (Fig 9-B), non-germ-line restriction fragments hybridizing to the TcR Cβ probe represented rearrangement events occurring 5' of Cβ1 or Cβ2.

When *Pvu*II digested BALB/c kidney and thymus DNA was analysed, two closely migrating germ-line fragments (6.2 kb and 6.5 kb; Cβ1 and Cβ2 respectively), were observed (Fig 9-A). The reduced intensity of the germ-line bands in the BALB/c thymus DNA , relative to the kidney DNA, was indicative of polyclonal TcRβ locus rearrangements. All of the IRNB-SCID DP T cell lines were found to have rearranged both TcRβ locus alleles, as indicated by the absence of a germ-line restriction fragment hybridizing to the TcR Cβ probe (Fig 9-A).

The analysis described above did not resolve Cβ1 from Cβ2 rearrangements. In order to detect rearrangements involving the Cβ1 cluster (ie. Dβ1, one of Jβ1.1-1.6, and Cβ1; depicted in Fig 1) the same TcR Cβ specific probe used in the previous analysis was hybridized to *Hind*III digested genomic DNA. This mapping strategy took advantage of the position of the *Hind*III sites which flank the Cβ1 and Cβ2 genes (Fig 10-B). The 3.1 kb *Hind*III restriction fragment that contains the Cβ2 gene is not altered during normal V(D)J rearrangement because the 5'*Hind*III site is located 3' of the Jβ2 cluster. In contrast, rearrangements involving the Cβ1 cluster alter the size of the Cβ1 containing restriction fragment because the 5'*Hind*III site is

located upstream of the Jβ1 cluster. Therefore, any restriction fragments which were not 3.1 kb in size corresponded to rearrangements involving the Cβ1 cluster.

The germ-line (kidney) configuration of the Cβ1 cluster produced a 9.6 kb *Hind*III fragment (Fig 10-A). Most rearrangements to the Cβ2 cluster involve deletion of the Cβ1 cluster. Therefore, in lines that deleted both Cβ1 alleles, the TcR Cβ probe detected only the 3.1 kb, Cβ2 containing restriction fragment. This analysis showed that LK3, LK3C and LK6.2, had deleted both Cβ1 alleles, while LK8 and SCTL2 had restriction fragments which represented rearrangements involving the Cβ1 cluster (Fig 10-A).

These results showed that rearrangement had occurred on both alleles of the TcRβ locus in all of the IRNB-SCID lines. As SCTL2 was the only cell line that expressed full length TcRβ mRNA, we wanted to determine why the rearrangements detected in the other IRNB-SCID lines did not result in transcription of TcRβ message. One possibility was that abnormal rearrangement had occurred, resulting in a chromosomal translocation. This possibility was supported by our detection of Cβ1 gene segment deletion. Although this deletion could have been the result of rearrangement to the Cβ2 cluster, Cβ1 gene deletion resulting from abnormal rearrangement has been detected in *scid* thymocytes (21), and T cells harbouring a chromosomal aberration involving the TcRβ locus (79, 84, 87). We therefore wanted to determine if abnormal rearrangement had occurred at the TcRβ locus in any of the IRNB-SCID DP T cell lines.

Abnormal rearrangement at the TcRβ locus

We wanted to determine if abnormal V(D)J rearrangement had deleted the Cβ1 gene segments in the IRNB-SCID T cell lines. The DNA sequence found 3' of the Jβ2 gene segments is not deleted during normal V(D)J rearrangement because there are no recombinationally active gene segments situated between the Jβ2

cluster and Cβ2 (Fig 1). Previous work showed that abnormal Cβ region rearrangement in *scid* lymphocytes often resulted in deletions that covered the entire Jβ2 region and extended to the flanking sequence (21, 125). We therefore examined the Jβ2 gene segments by Southern blot analysis using a probe situated 3' of the Jβ2 gene segments (3'Jβ2; (98)). Loss of the sequence 3' of Jβ2 indicated that abnormal rearrangement had occurred at the TcRβ locus.

When *Pvu*II digested DNA from the IRNB-SCID T cell lines was hybridized with a 3'Jβ2 probe, one or more new restriction fragments, corresponding to Cβ2 cluster rearrangements, were observed (Fig 11-A). In LK3C, no fragment hybridizing to the 3'Jβ2 probe was detected (Fig 11-A), suggesting that an abnormal rearrangement had occurred in this cell line. 3'Jβ2 probe hybridization of genomic DNA digested with other restriction enzymes similarily failed to detect a restriction fragment in LK3C (data not shown). The possibility that the entire TcR constant region was deleted in LK3C was excluded by the fact that we detected two distinct TcR Cβ containing *Pvu*II fragments (Fig 9). These restriction fragments likely represented Cβ2 cluster rearrangements, as LK3C had deleted both Cβ1 genes (Fig 10). Collectively, these results revealed that LK3C harboured abnormal deletion of the sequence 3' of the Jβ2 cluster on both TcRβ alleles.

In both LK6.2 and LK8, analysis of the Cβ2 gene cluster with a 3'Jβ2 probe resolved a single *Pvu*II restriction fragment (Fig 11-A). This observation may have been due to deletion of the Jβ2 gene cluster on one TcRβ allele in each cell line. In order to rule out the possibility that these single *Pvu*II fragments represented two 3'Jβ2 cluster alleles, we performed quantitative phosphorimaging. Calibration of the phosphorimaging (Materials and Methods), validated this means of detecting one versus two alleles of a given gene (Fig 12). Our analysis revealed that the single bands detected for both LK6.2 and LK8 represented one Jβ2 allele (Fig 13), suggesting that sequences 3' of Jβ2 were deleted on one TcRβ allele in both of these cell lines.

In order to determine if the Jβ2 cluster deletion detected in LK6.2 and LK8 included the Cβ2 gene segment, quantitative phosphorimaging was performed on the 3.1 kb, Cβ2 containing, *Hind*III restriction fragment seen in Fig 10-A. We found that one copy of Cβ2 had been deleted in both LK6.2 and LK8 (Fig 14). Taken together, these results show that LK6.2 and LK8 had abnormal deletions of the sequence found 3' of the Jβ2 cluster, which included the Cβ2 gene segment.

Southern blot analysis revealed abnormal rearrangement in 3 of the 5 IRNB-SCID DP T cell lines. In LK3C, LK6.2 and LK8, sequences 3' of Jβ2 were deleted on either one (LK6.2 and LK8) or both (LK3C) alleles, as has been documented for several chromosomal translocations involving antigen receptor loci (79-81, 84, 87). Our results are also consistent with abnormal rearrangements resulting from inefficient V to DJ rearrangement at the TcRβ locus in *scid* thymocytes, (21). We therefore wanted to determine if the rearrangements in the IRNB-SCID T cell lines were the result of V to DJ rearrangement, or chromosomal translocation.

(E) TcRβ variable gene rearrangement in irradiated newborn *scid* DP T cell lines

Attempted Vβ to DJβ rearrangement on both TcRβ alleles in all of the irradiated newborn scid DP T cell lines.

Could abnormal V to DJ rearrangement account for the TcRβ deletions we observed in the IRNB-SCID T cell lines? To address this question, we sought to determine if Vβ to DJβ rearrangement had been attempted in any of these cell lines by examining a DNA sequence which is lost during deletional rearrangement (reviewed in 2). We performed Southern blot analysis on *Pvu*II digested genomic DNA, using a probe (5'Dβ1; (98)) that is situated 5' of the Dβ1 gene (Fig 15-B), and is therefore lost during V to DJ rearrangement. Loss of a restriction fragment hybridizing to this probe was indicative of attempted Vβ to Dβ rearrangement.

We observed deletion of the 5' Dβ1 region on both TcRβ alleles in all of the IRNB-SCID lines by probing genomic DNA digested with *Pvu*II (Fig 15-A) and other restriction enzymes (data not shown). In the germ-line DNA configuration, the 5' Dβ1 sequence was represented by a 5.7 kb germ-line *Pvu*II fragment (Fig 15-A). The absence of this restriction fragment in the IRNB-SCID lines could have been due to exonuclease digestion of exposed DNA double strand breaks, which has been postulated to play a role in the abnormal deletions observed in *scid* thymocytes (21). The 5'Dβ1 region could also have been lost if V to DJ rearrangement had been attempted on both TcRβ alleles in all of the IRNB-SCID lines. Alternatively, a chromosomal translocation could have deleted the 5' Dβ1 region, as exemplified by a chromosomal translocation involving the TcRβ locus in a human neoplasm (79). In this aberrant rearrangement, a non-TcR gene (*lck*) rearranged upstream of the TcRβ constant region, and the sequence found between the V and D genes was deleted. Therefore, instead of resulting from V to DJ deletional rearrangement, the 5' Dβ1 region may have been deleted in the IRNB-SCID lines due to chromosoma

translocation upstream of the constant region. We therefore wanted to determine if V to DJ rearrangement had deleted the 5′ Dβ1 sequence in the IRNB-SCID lines

Vβ gene deletion in irradiated newborn scid DP T cell lines.

To determine if V to DJ rearrangement had deleted the 5′ Dβ1 region, we looked at Vβ gene deletion in the IRNB-SCID cell lines. The Vβ genes situated proximal to the TcRβ constant region are often deleted as a result of V to DJ rearrangement. Nineteen of the twenty-one known murine Vβ genes that rearrange by deletion are found upstream of Vβ7 (Fig 16), so Vβ7 has a high likelihood of being deleted in T cells that have rearrangements at both TcRβ alleles. The absence of Vβ7 in any or all of the IRNB-SCID T cell lines would therefore have suggested that V to DJ rearrangement had occurred on both TcRβ alleles.

*Pvu*II digested DNA contains two germ-line fragment which hybridize to a probe specific for Vβ7, sized 1.0 kb and 2.4 kb (only the 1.0 kb band is shown in Fig 17-A). The wildtype DP T cell line, VL3-3M2, was negative for a Vβ7 fragment, suggesting that V(D)J rearrangement had deleted both copies of Vβ7. All of the IRNB-SCID T cell lines had at least one copy of Vβ7 in germ-line configuration (Fig 17-A). Quantitative phosphorimaging showed that in LK3, LK3C and SCTL2, one copy of Vβ7 had been deleted, while in LK6.2 and LK8 both Vβ7 alleles were in germ-line configuration (Fig 18-A). Vβ7 was therefore present on seven of ten TcRβ alleles that, having deleted the sequence 5′ of Dβ1, appeared to have undergone V to DJ deletional rearrangement.

To ensure that the deletion of Vβ7 in LK3, and LK3C was due to attempted V to DJ rearrangement, rather than deletion of the entire TcR Vβ gene region, we examined another segment of the large Vβ gene cluster. Deletion of Vβ2 is indicative of loss of the entire Vβ gene region because it is the V gene most distal to the constant region (Fig 16), and therefore is not deleted during normal V to DJ

rearrangement. Through quantitative Southern blot analysis of Vβ2, we found that all of the IRNB-SCID cell lines retained two Vβ2 alleles (Fig 17-B; Fig 18-B), indicating that the Vβ7 deletion observed in LK3 and LK3C did not reflect deletion of the entire TcR Vβ locus.

To explore the possibility that V to DJ rearrangement had occurred on those TcRβ alleles that retained Vβ7 in germ-line configuration, we performed Southern blot analysis on *Pvu*II digested genomic DNA, using a Vβ14 probe. Vβ14 is the only known Vβ gene that rearranges by inversion (126), and unlike deletional rearrangement, no DNA is lost during inversional rearrangement (reviewed in 2). Our analysis suggested that Vβ14 had not been involved in a rearrangement in any of the IRNB-SCID lines, as both Vβ14 alleles were in germ-line configuration (Fig 17-C; Fig 18-C). These results indicated that inversional rearrangement had not occurred at the TcRβ locus in any of the *scid* lines.

The results presented in this section reveal that in the IRNB-SCID DP T cell lines, either one (LK3, LK3C, SCTL2) or two (LK6.2, LK8) Vβ7 alleles remained in germ-line configuration, but deletions of the locus 5′ to DJ had occurred. There are several possible explanations for these observations. One is that Vβ18, the Vβ gene which is situated most proximal to the 5' end of the TcRβ constant region, was involved in the apparent V to DJ rearrangements, leaving Vβ7 in germ-line configuration (Fig 16). Although we did not exclude this possibility, it is unlikely that Vβ18 was involved in rearrangement of seven of ten TcRβ alleles in the five IRNB-SCID cell lines.

Deletion of the sequence just 5' of the TcRβ constant region could have resulted from excessive exonuclease activity (21), which could explain why it appeared as if V to DJ rearrangement had occurred on both alleles of the TcRβ locus without deletion of the proximal Vβ7 gene. Another possibility, consistent with the possibility of illegitimate TcRβ rearrangement is that a translocation occurred 5' of

the TcRβ constant region, and the Vβ genes (including Vβ7) were translocated to another chromosome. We therefore decided to determine if a chromosomal translocation had disrupted the physical integrity of the TcRβ locus in the IRNB-SCID cell lines.

(F) Physical integrity of the TcRβ locus in irradiated newborn *scid* DP T cell lines

Fluorescent in situ hybridization analysis of metaphase chromosomes

Having established that abnormal rearrangement had occurred in LK3C LK6.2 and LK8, we sought to determine if a chromosomal translocation hac occurred at the TcRβ locus on chromosome 6 in any of the IRNB-SCID DP T cel lines. We performed fluorescent in situ hybridization (FISH) using mous chromosome paint probes (114). Chromosome specific "paints" are a comple mixture of 200-2000 bp DNA probes (127), spaced approximately four kb apart (115) which allow the visualization of entire chromosomes. These probes enabl detection of gross abnormalities such as translocations or large insertions (115). Tc detect chromosome 6 abnormalities, we examined metaphase spreads of the IRNB SCID cell lines, in comparison to BALB/c splenocyte controls.

Metaphase spreads of each cell line were prepared and analysed thre independent times. Approximately 50 spreads were scored per cell line on eacl occasion. We found no detectable abnormalities involving chromosome 6, as all o the metaphasic spreads analysed clearly displayed two chromosomes that hybridizec strongly to the chromosome 6 paint probes (Table 3 and Fig 19). We did detec several other chromosomal abnormalities in the *scid* lines. Mouse chromosome are acrocentric. The presence of metacentric chromosomes is therefore indicative o chromosomal instability. There were two metacentric chromosomes in LK3, anc one metacentric chromosome in LK6.2 (Fig 19, white arrows). We also notec abnormal chromosome number (aneuploidy) in LK3 and SCTL2 (Table 3). Thus although chromosomal abnormalities were present in several of the IRNB-SCII lines, those we detected did not appear to involve chromosome 6.

It has been shown that irradiation of newborn *scid* mice also transientl rescues V(D)J rearrangement at the TcRδ (63) and TcRγ (64) loci. Having access t

paint probes specific for mouse chromosome 14, on which the TcRα/δ locus is situated, we explored the possibility that the TcRα/δ locus was involved in a chromosomal translocation. As observed in our chromosome 6 analysis, all of the IRNB-SCID lines had two copies of chromosome 14 (data not shown). As an added control, chromosome 11, which does not harbour an antigen receptor locus, was similarly analysed and revealed no evidence of chromosomal translocation (data not shown). We therefore concluded that none of the IRNB-SCID T cell lines harboured a gross abnormality involving chromosome 6, 14 or 11.

Pulsed field gel electrophoresis analysis of the TcRβ locus

We considered the possibility that chromosomal abnormalities involving the TcRβ locus existed in the IRNB-SCID T cell lines, but were not detected in our FISH analysis due to the limitations of using whole mouse chromosome paint probes. These probes hybridize along the length of the whole chromosome, and abnormalities that do not alter the hybridization pattern are not detectable. Therefore, our analysis would have missed most deletions and inversions involving chromosome 6. Although the limits of resolution for murine whole chromosome paints have not been carefully analysed, small insertions might have been obscured by the contiguous hybridization signals emitted by the probes (Fig 19). In order to address the possibility that our FISH analysis failed to detect small TcRβ locus abnormalities, we performed pulsed field gel electrophoresis (PFGE), to examine potential chromosomal translocations (128), deletions (129, 130), and inversions (131).

Illegitimate rearrangement at the TcRβ locus in human lymphoid tumours can result in a chromosomal aberration that dislocates the Vβ genes from the constant region (79). We therefore used PFGE to determine if the Vβ gene cluster remained linked to the Cβ region in the IRNB-SCID T cell lines. The enzyme *Nae*I

has been useful in mapping the TcRβ locus (132, 133). Due to variable restriction site methylation, and the fact that *Nae*I uses a two site binding mechanism to cleave substrate DNA (134), *Nae*I generates a defined pattern of partial digestion products that allow linkage of genes located far apart. The Vβ7 and Cβ gene segments reside on a 360 kb *Nae*I restriction fragment (Fig 20). Due to *Nae*I site methylation within the TcRβ constant region, Vβ7 and Vβ14 may also remain on a single 430 kb restriction fragment (Fig 20). Demonstration of linkage between Vβ7 and Cβ, or Vβ7 and Vβ14, would therefore suggest that a chromosomal translocation had not occurred between these gene segments.

Using this PFGE strategy, we determined that Vβ7 remained linked to the Cβ and Vβ14 genes in SCTL2, LK8, LK6.2 and LK3C (Fig 21 A-D, Table 4). In each of these cell lines, a 430 kb restriction fragment co-hybridized to a Vβ7 and Vβ14-specific probe. The linkage of Vβ7 and Vβ14 indicated that Vβ7 was also linked to the Cβ region (Fig 16). In SCTL2, LK8 and LK3C, linkage was confirmed by a 430 kb fragment that also hybridized to a TcR Cβ probe (Fig 21-A,-B and -D, respectively). The TcR Cβ probe did not hybridize to the 430 kb fragment in LK6.2 (Fig 21-C), probably because LK6.2 had deleted three of four Cβ gene segments, reducing the TcR Cβ hybridization signal below detectable levels.

These PFGE data suggest that both TcRβ alleles were intact in LK6.2 and LK8. In LK3C, which had deleted one copy of Vβ7 (Fig18), our results are limited to the interpretation that the TcRβ locus was physically intact on the allele that retained Vβ7 in germ-line configuration. We cannot resolve whether the allele lacking Vβ7 (600 kb *Nae*I fragment; Fig 21-D), was involved in an aberrant rearrangement. In SCTL2, which had lost one copy of Vβ7 as a result of a functional Vβ5.1 rearrangement, the allele lacking Vβ7 was not detected. It is possible that the compression zone (CZ, zone where DNA migrates independently of electrophoresis parameters), which migrated as a diffuse band (Fig 21 A-E) obscured the detection of

this allele. Consistent with this possibility, a faint restriction fragment was visible just below the CZ in *Nae*I digested SCTL2 DNA (Fig 21).

Unlike what was observed for LK3C, LK6.2, LK8 and SCTL2, PFGE analysis of LK3 could not link Vβ7 with either the Cβ region or Vβ14. When *Nae*I digested genomic DNA from LK3 was hybridized with the Vβ7 probe, a 360 kb restriction fragment was revealed (Fig 21-E). This 360 kb restriction fragment was not revealed by either the TcR Cβ or Vβ14 probe, suggesting that Vβ7 was no longer linked to the TcRβ constant region. One piece of evidence to support this interpretation is that the Vβ7 probe did not hybridize to the 430 kb fragment representing partial digestion of the *Nae*I sites within the Cβ region (Fig 20), which was detected in all of the other analysed IRNB-SCID T cell lines (Fig 21 A-D). If Vβ7 had remained linked to the constant region, the Vβ7, Cβ and Vβ14 probes would have co-hybridized to the 430 kb fragment. Alternatively, it is possible that the *Nae*I sites within the Cβ region were digested to completion in LK3. In order to exclude this possibility, further pulsed field gel electrophoresis using a different restriction enzyme would have to be done to ensure Vβ7 was no longer linked to the Cβ region. Nevertheless, we showed that Vβ7 could no longer be linked to the same *Nae*I restriction fragment as the constant region in the IRNB-SCID T cell line, LK3.

Our analysis of the physical integrity of the TcRβ locus revealed no gross abnormalities involving chromosome 6, but in at least one of the IRNB-SCID T cell lines, Vβ7 was discontiguous with the TcR Cβ region and Vβ14. These results suggest a chromosomal aberration caused the Vβ genes in LK3 to dissociated from the constant region. In previous sections we presented evidence that V(D)J rearrangement played a role in the invariable progression to rapid onset lymphoma in IRNB-SCID mice, and that abnormal rearrangement at the TcRβ locus was a common feature of the IRNB-SCID DP T cell lines. Collectively these results suggest that in LK3, an illegitimate rearrangement at the TcRβ locus may have occurred and

contributed to a proliferative/survival advantage, which eventually lead to the development of lymphoma.

Discussion

This study investigates the putative role of illegitimate V(D)J rearrangemen in the universal development of T cell lymphoma induced by irradiation o newborn *scid* mice (61). As described previously, treating newborn *scid* mice with a single dose (100cGy) of γ-irradiation, resulted in the appearance of $CD4^+CD8^+$ (DP) T cells in the thymus (61, 62), as well as the restoration of V(D)J rearrangement at the TcRβ (61), TcRδ (63) and TcRγ loci (64). In addition, the universal development of T cell lymphoma was observed in irradiated newborn *scid* (IRNB-SCID) mice by 16-20 weeks post irradiation. Similar treatment of newborn RAG-1 and RAG-2 deficient mice rescued the block in T cell development, in the absence of restoration of V(D)J rearrangement. Strikingly, none of the irradiated RAG deficient animals developed lymphoma (93). Activation of murine leukemia virus was investigated and appeared not to contribute to lymphomagenesis in the IRNB-*SCID* mice, as no novel viral integration sites were detected in several IRNB-SCID T cell lines (P Joliceour and J. Danska, unpublished observations). Collectively, these results suggested that irradiation of lymphocyte precursors with a DSB repair defect enhances the generation of oncogenic events which lead to the universal, rapid development of T cell lymphoma. We therefore attempted to determine the role of V(D)J rearrangement in this invariable progression to lymphoma in IRNB-SCID mice.

(A) V(D)J rearrangement plays a role in the rapid onset T cell lymphoma in irradiated newborn *scid* mice

In order to determine the contribution of the *scid* DSB repair defect to the development of lymphoma in the absence of V(D)J rearrangement, we bred RAG-2 deficient *scid* (RAG-2$^{-/-}$ *scid*) mice. These double mutant mice were unable to generate DSB at RSS, but retained the DSB repair defect conferred by the *scid* mutation. We found that treatment of newborn RAG-2$^{-/-}$ *scid* mice with a single dose (100 cGy) of γ-irradiation did not lead to the universal development of rapid onset lymphoma (Figs 2 and 3), as was the case for IRNB-SCID animals (61). This result suggests that disabling RSS-specific DNA cleavage is protective against irradiation induced lymphoma, even in the context of the *scid* DSB repair defect.

Since introduction of the RAG-2 mutation reduced the susceptibility to irradiation-promoted thymic lymphoma, we favour the interpretation that V(D)J recombinase activity plays a critical role in lymphomagenesis in IRNB-SCID mice. However, it is possible that the protective effect was not dependent on the RAG-2 deficiency, but conferred by some other gene(s) derived from the RAG-2 deficient background that was inadvertently crossed onto the *scid* background. Consistent with this possibility, there is one report that the response to DNA-damaging agents is heterogeneous between mouse strains (135). In that study, differences in the rate of repair in a given gene were observed in different inbred strains of mice. For example, UV-induced DNA damage in c-*myc* is rapidly repaired in B lymphoblasts from DBA/2N mice, but is poorly repaired in B cells from BALB/c mice (136). However, if the protective effect on lymphomagenesis was conferred by another unlinked gene from the RAG-2 deficient background, random segregation would have occurred. If such a protective genetic element functioned in a dominant fashion, and was not linked to the *rag*-2 gene, the frequency at which it would co-segregate with the disrupted *rag*-2 gene would have been approximately 20%.

Therefore, we would have expected four of five irradiated RAG-2$^{-/-}$ *scid* mice to develop rapid onset lymphoma. By 10-16 weeks post-irradiation in IRNB-SCID mice, thymus cellularity was 50-150 X10^6, while none of the 16 analysed 10-16 week old RAG-2$^{-/-}$ *scid* mice had a comparable number of cells in the thymus (Table 2; Fig2). The absence of irradiation induced T cell lymphoma in RAG-2$^{-/-}$ *scid* mice therefore appears to have been the result of the inability to initiate V(D)J rearrangement.

(B) Detection of abnormal rearrangement at the TcRβ locus in irradiated newborn *scid* T cell lines

This study revealed that rearrangement had occurred on both alleles of the TcRβ locus in all of the IRNB-SCID lines (LK3, LK3C, LK6.2, LK8 and SCTL2; summarized in Table 5). Results obtained from Southern, and pulsed field gel analyses were used to generate physical maps of both alleles of the TcRβ constant locus in these IRNB-SCID DP T cell lines (Figure 22 A-E). The majority of the rearrangements were non-productive, as only SCTL2 and LK3C expressed TcRβ mRNA (Figs 4 and 6). Attempts to determine if the lack of expression of TcRβ in the remaining *scid* lines was due to abnormal V(D)J rearrangement revealed that three of the five IRNB-SCID lines analysed had deleted the Jβ2 gene cluster. In LK3C, both alleles had been deleted while one allele was missing in LK6.2 and LK8 (Fig 11). During normal V(D)J rearrangement the deletion of all of the Jβ2 gene segments does not occur, as there are no gene segments 3' of this cluster that are involved in rearrangement (Fig 1). Jβ2 gene cluster deletion is thus uncommon in wildtype T cells, as reported in a study of T cell lines and lymphomas (125). Of the 34 T cell lines tested in that study, only three had deleted the Jβ2 cluster on one allele. Moreover, the data could not exclude that the loss of the Jβ2 cluster was actually due to the loss of chromosome 6, on which the TcRβ locus is located. Therefore, we

suggest that abnormal rearrangement had deleted this Jβ2 gene cluster in the LK3C, LK6.2 and LK8 lines.

Our observations are similar to those previously reported in spontaneous thymic lymphomas from *scid* mice (21), where 8 of 12 lymphomas examined had deleted the Jβ2 gene cluster. Of these eight lines, five had also deleted the Jβ1 cluster and the Cβ1 gene segment. The fact that the Cβ2 gene was immediately downstream of the Dβ1 gene in these five cell lines suggested that the deletions detected in the spontaneous *scid* lymphomas probably reflected imprecise ligation of the Dβ1 element to a Jβ2 gene segment (21). These results thus implicate the *scid* defect in mediating abnormal TcRβ rearrangements which result in the deletion of sequences within the constant region.

The abnormal rearrangements in the IRNB-SCID lines do not appear to have been caused by the imprecise ligation mechanism stated above because the sequence 5' of Dβ1 had been deleted on both TcRβ alleles in all of the cell lines (Fig 15). The loss of this sequence suggested that attempted V to DJ rearrangement had occurred on both alleles in every line. Although this is true, we found Vβ7, one of the Vβ genes most proximal to the constant region (Fig 16), to be in germ-line configuration on either one (LK3, LK3C, SCTL2) or both alleles (LK6.2, LK8) (Figs 17 and 18). One unlikely explanation for this observation is that Vβ18, the only Vβ gene situated between Vβ7 and the constant region (Fig 16), was involved in the V to DJ rearrangement in all of the alleles that had not deleted Vβ7. Thus Vβ18 to DJβ rearrangement does not delete Vβ7. A more likely scenario is that V to DJ rearrangement had not occurred in the IRNB-SCID cell lines, but that loss of the sequence 5' of Dβ1 was the due to excessive exonuclease activity. Such an analysis would fit with the idea that normal rearrangement between D to J had been transiently restored following irradiation, but V to DJ rearrangement manifested the inefficiency the *scid* mutation, including excessive exonucleolytic degradation of

coding ends. As most studies examining V(D)J rearrangement in *scid* mice have focused on D to J rearrangements (21, 25, 31, 32), the IRNB-SCID cell lines would allow a more detailed examination of V to DJ rearrangement.

The putative exonuclease activity invoked above does not preclude the possibility of an illegitimate rearrangement at the TcRβ locus in the IRNB-SCID lines. In fact, such modification of free signal and coding ends may contribute to the infidelity of the V(D)J recombinase activity. Evidence has been reported that the DNA sequences that flank signal sequences (86), as well as the sequence of the coding elements themselves (137), influence V(D)J rearrangement. Therefore, modification of the DNA sequence flanking the DSBs at the TcRβ locus may have altered the efficiency of V(D)J rearrangement in the IRNB-SCID thymocytes, and increased the frequency of illegitimate rearrangement events. This possibility among others, is consistent with the role of abnormal rearrangement at the TcRβ constant locus, a common characteristic of our IRNB-SCID T cell lines, in the invariable progression to lymphoma in irradiated *scid* mice.

(C) Expression of truncated TcRβ chains: a role in lymphomagenesis?

As described above, our TcR locus mapping analysis showed that deletions, including Cβ1, Dβ2 and the Jβ2 cluster, had occurred in both TcRβ alleles in LK3C (depicted in Fig 22-B). In this regard, it is interesting that LK3C expressed a 1.0 kb TcR Cβ containing mRNA species (Figs 4 and 6) which may have resulted from translocation of a foreign enhancer into the TcRβ locus. Such an event would support a role for V(D)J rearrangement in the development of lymphoma in IRNB-SCID mice.

Alternatively, the 1.0 kb Cβ containing transcript detected in LK3C may have been a germ-line transcript, as it has been proposed that transcription at the TcRβ locus does not require D to J rearrangement (138, 139). This transcript may have also

represented a Dβ1-Jβ1-Cβ2 transcript, resulting from deletion of the Cβ1 gene segment and the Jβ2 cluster. Dβ1-Jβ1-Cβ2 transcripts can arise due to V(D)J rearrangement, and have been documented in New Zealand White (NZW) mice, which carry an 8.8 kb germ-line deletion which includes Cβ1, Dβ2 and the Jβ2 cluster (140). Although the T cell repertoire of NZW mice is more limited, they express functional TcRβ protein (140, 141), representing functional rearrangements despite the large deletion.

Transcripts resulting from Dβ1 to Jβ rearrangement are thought to result from a promoter 5' of Dβ1 (54, 125). In LK3C, we showed that the region 5' of Dβ1 had been deleted (Fig 15), making it unlikely that the 1.0 kb mRNA species was initiated from this 5' Dβ1 promoter. Further characterization of LK3C would be required to determine which of the mechanisms presented above is responsible for the 1.0 kb transcript in LK3C. If non-TcRβ DNA sequence was found upstream of the constant region, illegitimate V(D)J rearrangement would be implicated as having occurred in this T cell line.

In addition to the possibility that the LK3C 1.0 kb transcript was the result of a chromosomal abnormality at the TcRβ locus, production of an abnormal protein from this transcript may have contributed to oncogenesis. A recent study showed that expression of a TcRβ protein lacking a Vβ domain (TcRβΔV) elicits DP T cell lymphomas in transgenic mice (142). In this study, it was found that the TcRβΔV protein mediated allelic exclusion of the endogenous TcRβ loci and thymocyte development was blocked at the DP CD25$^-$ stage. Interestingly, TcRβΔV transgenic mice had very low thymus cellularity compared to normal TcRβ transgenic mice. The possibility that ongoing recombinase activity may have been contributing to the high occurrence of T cell lymphoma was excluded when it was found that crossing the TcRβΔV transgene onto a RAG-1$^{-/-}$ background did not prevent tumour development. It is possible that the absence of a wildtype thymic

microenvironment may be created in which TcRβΔV expressing thymocytes can accumulate mutations leading to lymphoma (142). For example, TcRβΔV thymocytes which develop into DP T cells (142, 143) may not receive signals to cause them to die due to their lack of a variable domain. In this scenario the DP TcRβΔV T cells could persist in the thymus long enough to attain oncogenic mutations. In the context of a DSB repair defect, the number of oncogenic mutations accumulated by the TcRβΔV T cell would be exaggerated. The investigation of such an oncogenic mechanism in a non-transgenic animal would be valuable in understanding how similar mutant TcR or Ig chains contribute to T or B cell neoplasia. Therefore, chromosomal aberrations involving the TcRβ locus may have contributed to lymphomagenesis by creating a truncated TcRβ protein. Such an oncogenic mechanism would clearly implicate illegitimate V(D)J rearrangement in the transformation of this cell line.

(D) The TcRβ locus is not involved in a gross reciprocal translocation in the irradiated newborn *scid* T cell lines

As was discussed above, the abnormal rearrangements detected in the IRNB-SCID DP T cell lines may have been the result of inefficient ligation of coding ends associated with the *scid* DSB repair defect (1, 21, 31, 32), opposed to some other mechanism such as a translocation event occurring 5' of the constant region. Our fluorescent in situ hybridization (FISH) analysis using mouse chromosome 6 paint (114) supported this hypothesis. In this analysis we found no evidence of gross translocation involving chromosome 6 in any of the IRNB-SCID lines (Fig 19). A similar chromosome paint probe analysis of chromosome 14, containing the TcRα/δ locus, did not reveal evidence of a translocation (data not shown).

This analysis could have failed to resolve several types of TcR locus chromosomal abnormalities. The sensitivity of detection using whole chromosome

paints has not been systematically examined, but evidence from studies on human chromosomes suggests the limitations of this type of analysis. Although whole human chromosome paints have been shown to be useful in identifying certain chromosomal abnormalities (144, 145), a deletion, or small translocation may not be detectable (146). In our study, deletion of a portion of chromosome 6 might not have been detectable. If an insertion of a segment from another chromosome had occurred we might have observed the translocated DNA on chromosome 6 because the whole chromosome paint would not have hybridized to this ectopic DNA. Detection of such an event would depend upon the size of the inserted DNA segment. In analyses of human chromosomal abnormalities, translocations that occur close to the centromeric regions are difficult to detect using whole chromosome paints (147), and telomeric regions are often under-represented in human chromosome paint probes (148). Therefore, our FISH analysis using whole chromosome painting may have failed to detect subtle chromosomal aberrations involving the TcRβ locus. Nevertheless, gross translocations of chromosome 6 were not observed in any of the IRNB-SCID T cell lines.

(E) TcRβ locus disruption in irradiated newborn *scid* T cell lines

We performed pulsed field gel electrophoresis (PFGE) to further resolve the physical integrity of the TcRβ locus. PFGE analysis is useful in mapping syntenic genes that are separated by distances which are too great to be linked by traditional agarose gel electrophoresis(128). PFGE has been instrumental in establishing the organization of the TcR loci in both humans and mice (132, 133, 149), as well as the detection of deletions in other genetic loci (150-153). We reasoned that PFGE analysis might enable the detection of chromosomal abnormalities not visible by FISH analysis.

PFGE analysis revealed that the TcRβ locus may have been disrupted in one of the IRNB-SCID T cell lines, LK3. Here we observed discontiguity between the V gene segments and the constant region of the TcRβ locus, as Vβ7 was not linked to either the constant region, or Vβ14 (Fig 21-E), an element downstream of the Cβ2 region (Fig 16). It may be possible that abnormal rearrangement at the TcRβ locus lead to alterations in the methylation patterns of the *Nae*I sites in LK3. Consistent with this possibility, changes in DNA methylation patterns have been documented at the *bcr-abl* chromosomal translocation locus (154). Additionally, excessive methylation of CpG islands has been observed in cells grown in culture for many generations (155). Similarily, it has been shown that alteration of the sequences flanking the *Nae*I restriction sequences modifies cleavage by *Nae*I (156). Therefore, alterations within the TcRβ locus could have resulted in complete digestion of the *Nae*I restriction sites, thus explaining our inability to link Vβ7 to the constant region. Alternatively, the disruption of the TcRβ locus in LK3 could have resulted from an insertion or inversion that separated the Vβ gene segment region from the constant region. Further pulsed field analysis, using other restriction enzymes will have to be done to determine if the TcRβ locus is disrupted in LK3. To determine the nature of such a disruption, future studies would have to examine the DNA sequence found upstream of the constant region. For example, an LK3 genomic library could be generated, TcR Cβ containing clones isolated, and analysed to determine the sequence upstream of the constant region. If this DNA was not from the TcRβ locus, it would confirm the view that an illegitimate V(D)J rearrangement event contributed to the transformation of this cell.

(F) Chromosomal aberrations associated with abnormal TcRβ locus rearrangement

As has been suggested throughout this thesis, we favour the view that chromosomal translocations explain the abnormal TcRβ rearrangements observed in the IRNB-SCID DP T cell lines. Translocations involving antigen receptor loci often display abnormal deletions. For example, analysis of T-ALL cells showed that a TcRβ locus translocation involved a deletion from 5' of Dβ1 to 3' of the Jβ2 cluster (85). Similarly, in the T-ALL cells of a ataxia-telangiectasia patient, a 17kb deletion was found 3' of the translocation breakpoint within the TcRα locus (80). The abnormalities we observed within the TcRβ constant region in the IRNB-SCID lines are very similar to those cited above, supporting the hypothesis that γ-irradiation of *scid* lymphocyte precursors increases the frequency of illegitimate rearrangement at the TcRβ locus, and contributes to lymphomagenesis in IRNB-SCID mice.

(G) Conclusions

We used a genetic approach to examine the role of illegitimate V(D)J rearrangement in lymphomagenesis in IRNB-SCID mice. Our data revealed that introducing the RAG-2 deficiency onto *scid* mice protects irradiated newborn RAG-$2^{-/-}$ *scid* mice from the universal development of rapid onset lymphoma. There are two possible explanations for our data. The first, which has been discussed in detail, is that the ability to introduce DSB at RSS has no role in lymphomagenesis, rather the protective effect of crossing the RAG-2 deficiency onto *scid* mice is due to an unknown genetic factor contributed by the RAG-2 mouse background. To determine if this statement is true, RAG-$2^{+/-}$ *scid* mice should be irradiated and assayed for T cell tumour development. Development of lymphoma will verify that initiation of V(D)J rearrangement plays an obligate role in IRNB-SCID lymphomagenesis.

The second possibility is that aberrant V(D)J rearrangements are promoted by irradiation of *scid* lymphocytes. In this view, aberrant V(D)J rearrangement contributes to an oncogenic mutation which promotes progression to T cell neoplasia in the IRNB-SCID mice. For example, the RAG proteins create DSB at the 5' RSS of the Dβ gene segment and the 3' end of the Vβ gene segment, but the *scid* recombinase machinery fail to unite the free coding ends. As DNA-PK is involved in both V(D)J rearrangement and general DSB repair, a free DNA end generated by γ-irradiation could be ligated 5' of the Dβ element. If a growth promoting gene were found adjacent to the non-TcR free DNA end, the powerful enhancers found in the TcRβ locus could then ectopically drive expression of the translocated gene.

This type of mutation may not be restricted to the TcRβ locus, as V(D)J rearrangement is transiently restored at multiple TcR loci in IRNB-SCID mice (63, 64). In fact, the oncogenic event may not involve a TcR locus at all, as aberrant V(D)J rearrangement involving cryptic RSS elements can occur between two non-antigen receptor loci (83). Regardless of the loci involved in illegitimate V(D)J rearrangements, this illegitimate joining model explains why irradiated RAG$^{-/-}$ *scid* mice are protected from irradiation induced lymphoma, owing to a failure to initiate either bonafide or cryptic RSS cleavage.

The second major aspect of our work, the characterization of the TcRβ locus in five IRNB-SCID lines, supports the illegitimate joining model. The abnormal TcRβ rearrangements in these lines share characteristics observed in chromosomal translocations involving antigen receptor loci. For example, deletions of antigen receptor constant regions such as those we observed in the TcR Cβ region have been observed in human neoplasias (80, 157). More support for the illegitimate joining model is revealed when the abnormal rearrangements found in the IRNB-SCID lines are compared to those analysed in spontaneous *scid* thymic lymphomas and Abelson murine leukemia virus transformed *scid* bone marrow cells (21). For

example, although Jβ2 cluster deletion was observed in both our study and that of Schuler et al., Cβ2 gene deletion was only observed in the IRNB-SCID T cell lines. The 5'Dβ1 region was not deleted in spontaneous/Abelson transformed thymomas with Jβ2 cluster deletion, as was observed in the IRNB-SCID line. These differences suggest that the abnormal rearrangements detected in the IRNB-SCID lines were not the same as those observed in spontaneous *scid* thymomas (21). The illegitimate rearrangement model is further strengthened by our results that suggest disruption of the physical integrity of the TcRβ locus may have occurred in one of the IRNB-SCID lines. This study thus implicates a role for illegitimate V(D)J rearrangement in the invariable development of rapid onset lymphoma in IRNB-SCID mice.

The study of chromosomal translocations in human lymphoid malignancies has revealed an enormous number of novel proto-oncogenes (reviewed in 65, 158). If the model of illegitimate V(D)J recombinase mediated development of lymphoma proves to be correct, the IRNB-SCID system could provide numerous cell lines that harbour rearrangements involving known proto-oncogenes, thus allowing for their analysis. IRNB-SCID mice could also prove to be a rich source for the identification of unknown proto-oncogenes. This possibility is true if the translocation involves one partner that was generated by RSS specific cutting, while the other partner was generated by an irradiation induced DSB. If the irradiation induced DSB occurs adjacent to a proto-oncogene, and the free broken end is then ligated next to the RSS mediated breakpoint, the IRNB-SCID system could theoretically allow for the identification of virtually every proto-oncogene in the mouse genome. Using this "proto-oncogene engine", one could study genes that are integral to normal lymphocyte development as well as to neoplasia.

Table 1 **Oligonucleotides used in this study**

Oligonucleotides	Sequence[a]
RAG2-3[b]	GCC TGC TTA TTG TCT CCT GGT ATG
RAG2-1[b]	TTA ATT CAA CCA GGC TTC TCA CTT
Neo-3[b]	CCA ACG CTA TGT CCT GAT AGC GGT
5'β-actin[c]	TGG GTC AGA AGG ACT CCT ATG
3'β-actin[c]	CAG GCA GCT CAT AGC TCT TCT
Vβ consensus[d]	TAA GCG GCC GCA TGS LYT GGT AYW XXC [S=G or T; L=A, G, or T; Y=C or T; W = A or C; X=A or G]
Cβuni[d]	CAG CTC AGC TCC ACG TGG T
TcRVβ3[e]	AAG ATA TCT GGT GAA AGG GC
TcRVβ11[e]	GCT GGT GTC ATC CAA ACA CC
TcRVβ14[d]	TGG CCA GTT GCC GAG ATC AA
Cβ-antisense	ATA GAG GAT GGT GGC AGA CAA GAC
Cβ-sense	GCT GAG CTG GTG GGT GAA TG

[a]All primer sequences are written in the 5'-3' orientation

[b] - reference 103

[c] - reference 95

[d] - reference 61

[e] - reference 97

Table 2 **Effects of low dose ionizing irradiation on newborn RAG-2$^{-/-}$ *scid* mice**

Age Post-Irradiation	Cellularity[a]	%CD4^{+}CD8^{+}[b]	%CD25^{-}[c]
10 d (n=4)	$2.1 \times 10^6 \pm 2.6 \times 10^6$	17 ± 31	29 ± 35
3 wks (n=8)	$3.2 \times 10^7 \pm 4.1 \times 10^7$	40 ± 26	58 ± 23
6 wks (n=3)	$1.8 \times 10^6 \pm 1.4 \times 10^6$	5 ± 4	20 ± 10
10 wks 'A' (n=1)	1.0×10^6	40	54
'B' (n=4)	$6.3 \times 10^6 \pm 4.8 \times 10^6$	76 ± 21	93 ± 11
16 wks 'A' (n=6)	$7.3 \times 10^5 \pm 2.2 \times 10^5$	0.5 +/- 0.8	25 ± 4 (N=4)
'B' (n=5)	$2.3 \times 10^7 \pm 1.6 \times 10^7$	90 ± 5	98, 3
NIR Controls	$6.1 \times 10^5 \pm 1.5 \times 10^5$	< 1	10 +/- 2

-[a]whole thymocyte suspensions were stained with trypan blue, and viable cells were counted under th microscope

-[b]thymocytes were analysed for expression of CD4 (YTS-191.1) and CD8 (YTS 169-4) by multiparamte flow cytometry as described in Materials and Methods

-[c]thymocytes were analysed for expression of CD25 (7D4) by multiparameter flow cytometry a described in Materials and Methods

-numbers shown are means +/- standard deviation of results obtained from the number (n) of mice per tim point (d=days, wks=weeks)

-when only one or two mice were analysed, the numbers for those mice are shown

-'A', and 'B' are distinct thymocyte developmental phenotypes

Table 3 **Fluorescent In Situ Hybridization analysis of irradiated newborn *scid* DP T cell lines, using mouse chromosome 6 paint probes**

cell type	chromosome 6 equivalents[a] at metaphase	total # of chromsomes at metaphase[b]	# of abnormal chromosome
BALB/c splenocyte	2	40	0
LK3	2	38	2
LK3C	2	40	0
LK6.2	2	40	1
LK8	2	40	0
SCTL2	2	41	0

[a]Two chromosome 6 equivalents per cell means two chromosomes strongly hybridizing to the murine chromosome 6 paint at metaphase

[b]including metacentric chromosomes, each metacentric chromosome was counted as being one chromosome

[c]Metacentric chromosomes visually detected by DAPI staining of entire chromsomes

Table 4 - **Pulsed field gel electrophoresis analysis of irradiated newborn *scid* DP T cell lines**

IRNB-SCID cell line	Fragment size (kb)	Vβ7	Cβ	Vβ14	Interpretation
SCTL2	430	+	+	+	Vβ7 linked to Cβ, Vβ14
	360	+	+	-	Vβ7 linked to Cβ, Vβ14
	75	-	+	+	Cβ linked to Vβ14
LK8	430	+	+	+	Vβ7 linked to Cβ, Vβ14
	360	-	-	-	*Nae*I sites within constant region are deleted
	75	-	-	-	
LK6.2	430	+	?	+	Vβ7 linked to Cβ, Vβ14
	360	+	?	-	Vβ7 linked to Cβ, Vβ14
	75	-	+	+	Cβ linked to Vβ14
LK3C	600	-	+	+	600 kb fragment represents allele with Vβ7 deleted
	430	+	+	+	Vβ7 linked to Cβ Vβ14
	360	+	?	-	
	75	-	+	+	Cβ linked to Vβ14
LK3	430	-	-	-	
	360	+	-	-	Vβ7 is not linked to Cβ or Vβ14
	75	-	+	+	Cβ linked to Vβ14

Table 5 - **Summary of restriction fragment mapping of constant region in IRNB-SCID DP T cell lines**

IRNB-SCID line	Vβ2	Vβ7	5'Dβ1	Cβ1 cluster[a]	Jβ2 cluster[b]	Cβ2	Vβ14
LK3	2 - GL	1 - Δ 1 - GL	2 - Δ	2 - Δ	2 - RR	2 - GL	2 - GL
LK3C	2 - GL	1 - Δ 1 - GL	2 - Δ	2 - Δ	2 - Δ	2 - GL	2 - GL
LK6.2	2 - GL	2 - GL	2 - Δ	2 - Δ	1 - Δ 1 - RR	1 - Δ 1 - GL	2 - GL
LK8	2 - GL	2 - GL	2 - Δ	2 - RR	1 - Δ 1 - RR	1 - Δ 1 - GL	2 - GL
SCTL2	2 - GL	1 - Δ 1 - GL	2 - Δ	1 - Δ 1 - RR	2 - RR	2 - GL	2 - GL

[a] - Cβ1 cluster represents Dβ1, Jβ1.1-1.6, Cβ1
[b] - Jβ2 cluster represents Jβ2.1-Jβ2.6
GL - germline configuration
Δ - deleted
RR - rearranged

Figure 1

The constant region of the murine TcRβ locus

Genomic organization of the constant region of the murine TcRβ locus, which is located on chromosome 6. The two diversity (D) segments are indicated by vertical lines. Each D segment is associated with a cluster of seven joining (Jβ1.1-1.7 and Jβ2.1-2.7) segments (indicated by the filled boxes), and one constant (Cβ1 and Cβ2) gene segment (indicated by the open boxed). Each J cluster has six functional, and one pseudo-gene (denoted by ψ). Cβ1 and Cβ2 cluster designations cited in this work are indicated.

Fig 1

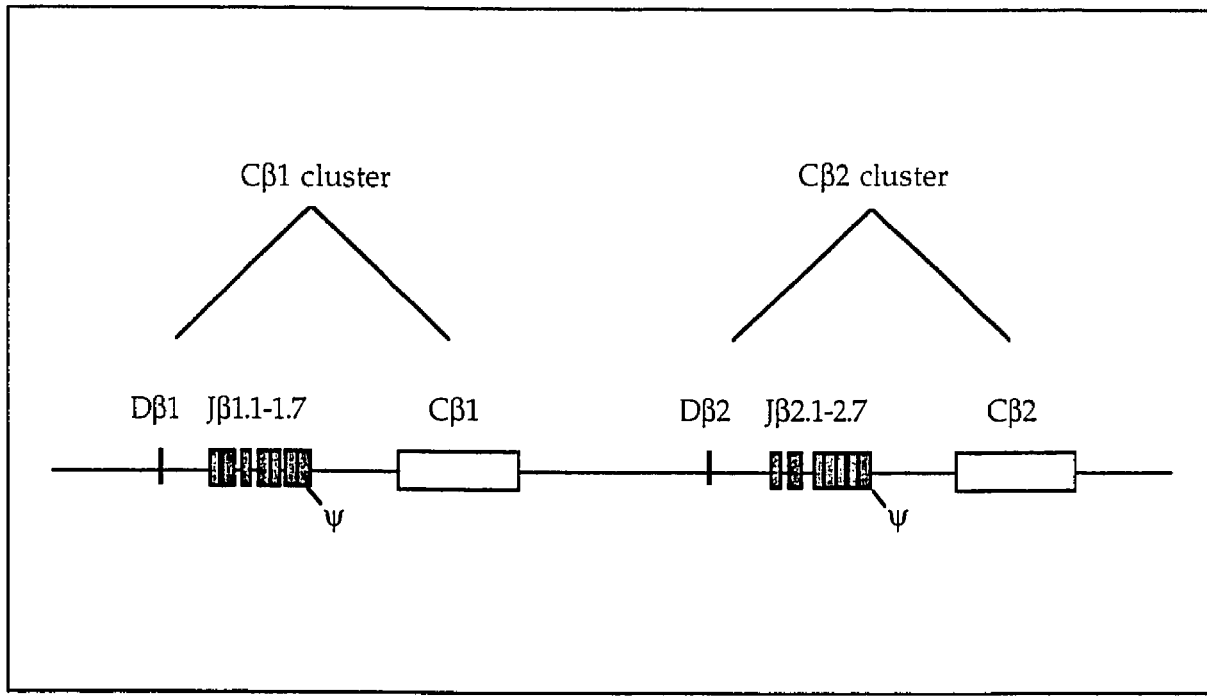

Figure 2

Thymocyte expansion and development in irradiated RAG2 deficient *scid* mice

Thymocyte suspensions were stained with trypan blue, and viable cells were counted under a microscope. Thymocytes were obtained at various time points after irradiation (100cGy) of newborn RAG2$^{-/-}$ *scid* mice and analysed for expression of CD4 (YTS-191.1) and CD8 (YTS 169-4) by multiparameter flow cytometry as described in the Materials and Methods. Data is presented as thymus cellularity as a function of time (top graph), and frequency of CD4/CD8 double positive (DP) thymocytes as a function of time (top graph). Each circle represents one irradiated RAG2$^{-/-}$ *scid* mouse. At 10 and 16 weeks post irradiation open circles (o) represent mice of phenotype A, filled circles (●) represent mice of phenotype B. The number of mice (n) analysed for each time point is indicated on the X axis. Mean values obtained from irradiated newborn (100cGy) *scid* mice are displayed as hatched line. Each triangle represents 4-24 mice (61), and standard deviation is represented as error bars

.

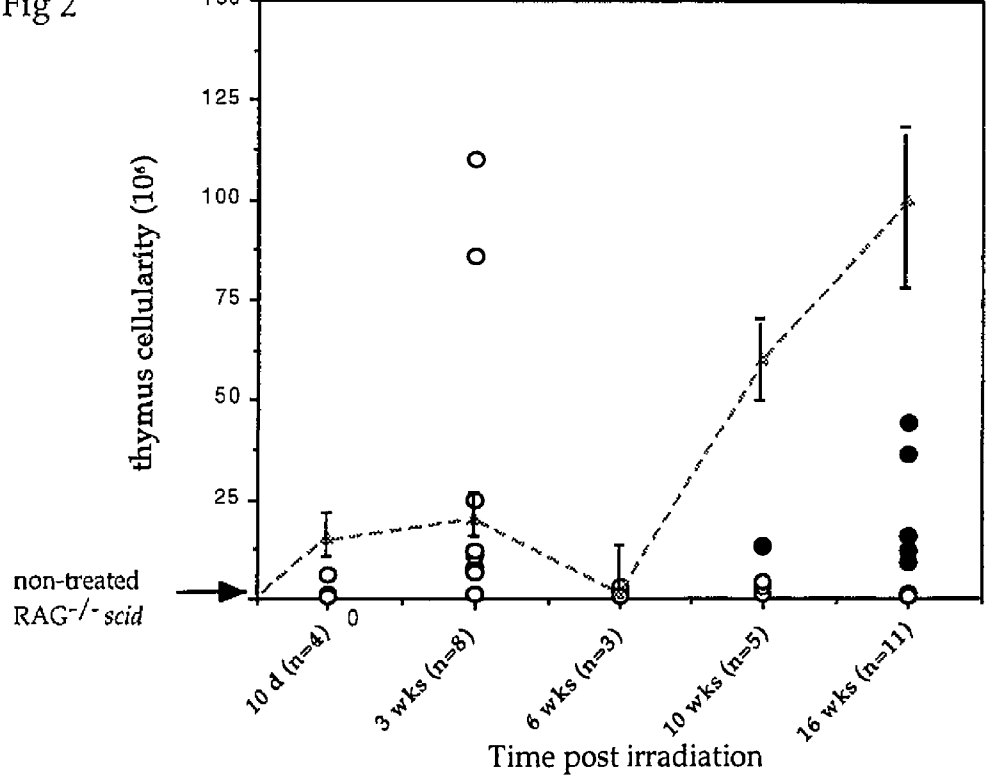
thymus cellularity (10⁶)
125
100
75
50
25
0
non-treated
RAG-/- scid
10 d (n=4)
3 wks (n=8)
6 wks (n=3)
10 wks (n=5)
16 wks (n=11)
Time post irradiation

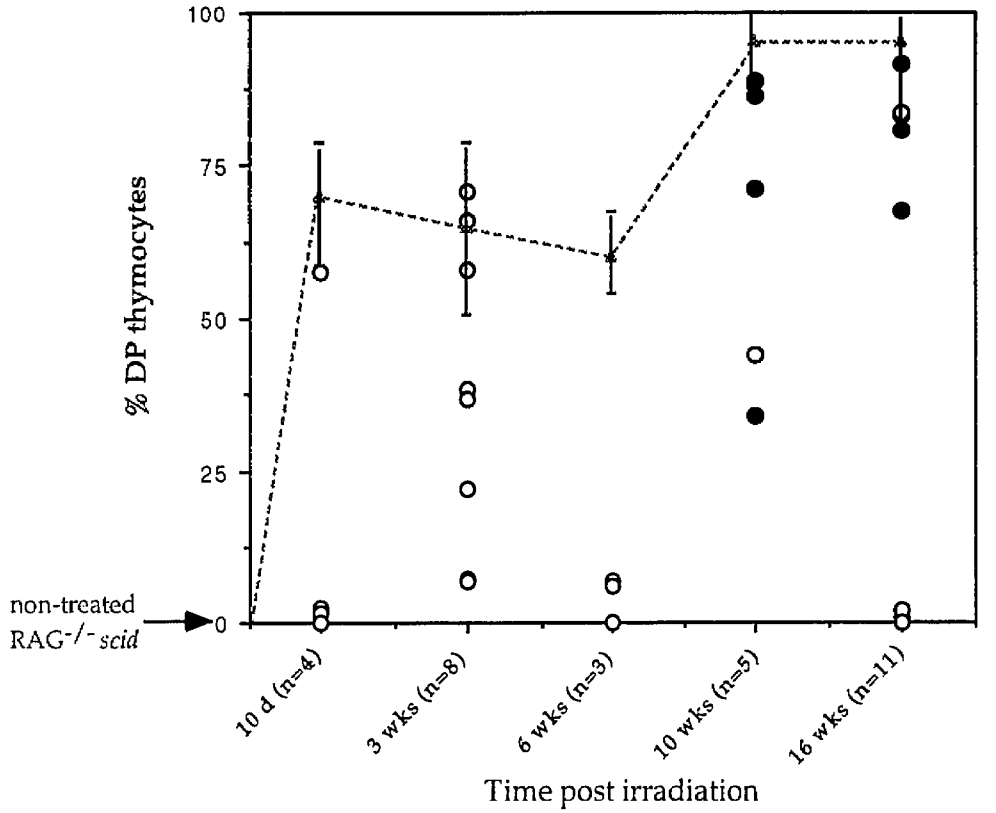
% DP thymocytes
100
75
50
25
0
non-treated
RAG-/- scid
10 d (n=4)
3 wks (n=8)
6 wks (n=3)
10 wks (n=5)
16 wks (n=11)
Time post irradiation

Figure 3

Phenotypic analysis of T lymphocyte development in irradiated newborn RAG2$^{-/-}$ *scid* mice

Thymocytes were obtained at 10 or 16 weeks after irradiation (100cGy) of newborn RAG-2$^{-/-}$ *scid* mice and analysed for forward scatter (FSC) and expression of CD4 (YTS-191.1), CD8 (YTS 169-4), or CD25 (7D4) by multiparameter flow cytometry as describedin Materials and Methods. Two-parameter contour plots (7% probability) show CD4 versus CD8 expression (far left). Single-parameter histograms show the expression of CD25 (middle), compared to staining with isotype-matched control antibodies (shaded histograms), and FSC (far right). Two distinct phenotypes are labeled 'A' and 'B' (see also Table 2). Staining of BALB/c, irradiated newborn RAG-2$^{-/-}$, irradiated newborn *scid* and untreated control RAG-2 $^{-/-}$ *scid* thymocytes are shown for comparison.

Fig 3

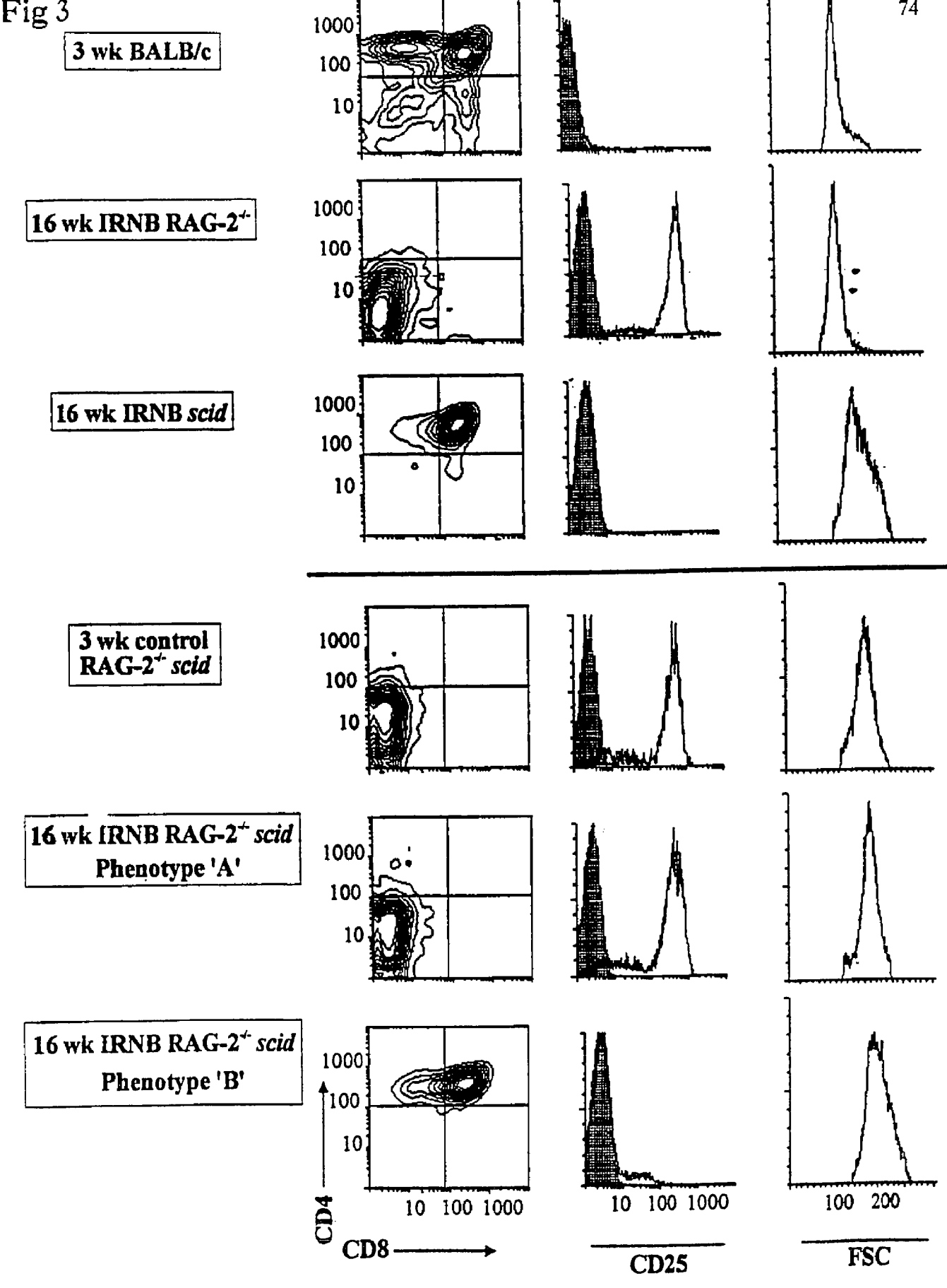
3 wk BALB/c
16 wk IRNB RAG-2-/-
16 wk IRNB scid
3 wk control RAG-2-/- scid
16 wk IRNB RAG-2-/- scid Phenotype 'A'
16 wk IRNB RAG-2-/- scid Phenotype 'B'
1000
100
10
CD4
10 100 1000
CD8
10 100 1000
CD25
100 200
FSC

Figure 4

Northern blot analysis of TcR expression in irradiated newborn *scid* T cell lines

(A) Ten μg of total RNA from the IRNB-SCID DP T cell lines LK3, LK3C, LK6.2, LK8 and SCTL2, as well as from BALB/c thymus, BALB/c bone marrow and the C57Bl/6 DP T cell line VL3-3M2 were electrophoresed through a 1.5% agarose-formaldehyde gel and transferred to nylon membrane. Hybridization was performed with a ^{32}P labeled pTα DNA probe. The same filter was hybridized sequentially with **(B)** a ^{32}P labeled TcR Cα probe; **(C)** a ^{32}P labeled TcR Cβ probe; and **(D)** a β-actin probe. Hybridized filters were exposed to a phosphorscreen for 12-24 hours, and digitized on a Molecular Dynamics Phosphorimager. The position and size of detected mRNA species are indicated to the left edge of each panel.

Fig 4

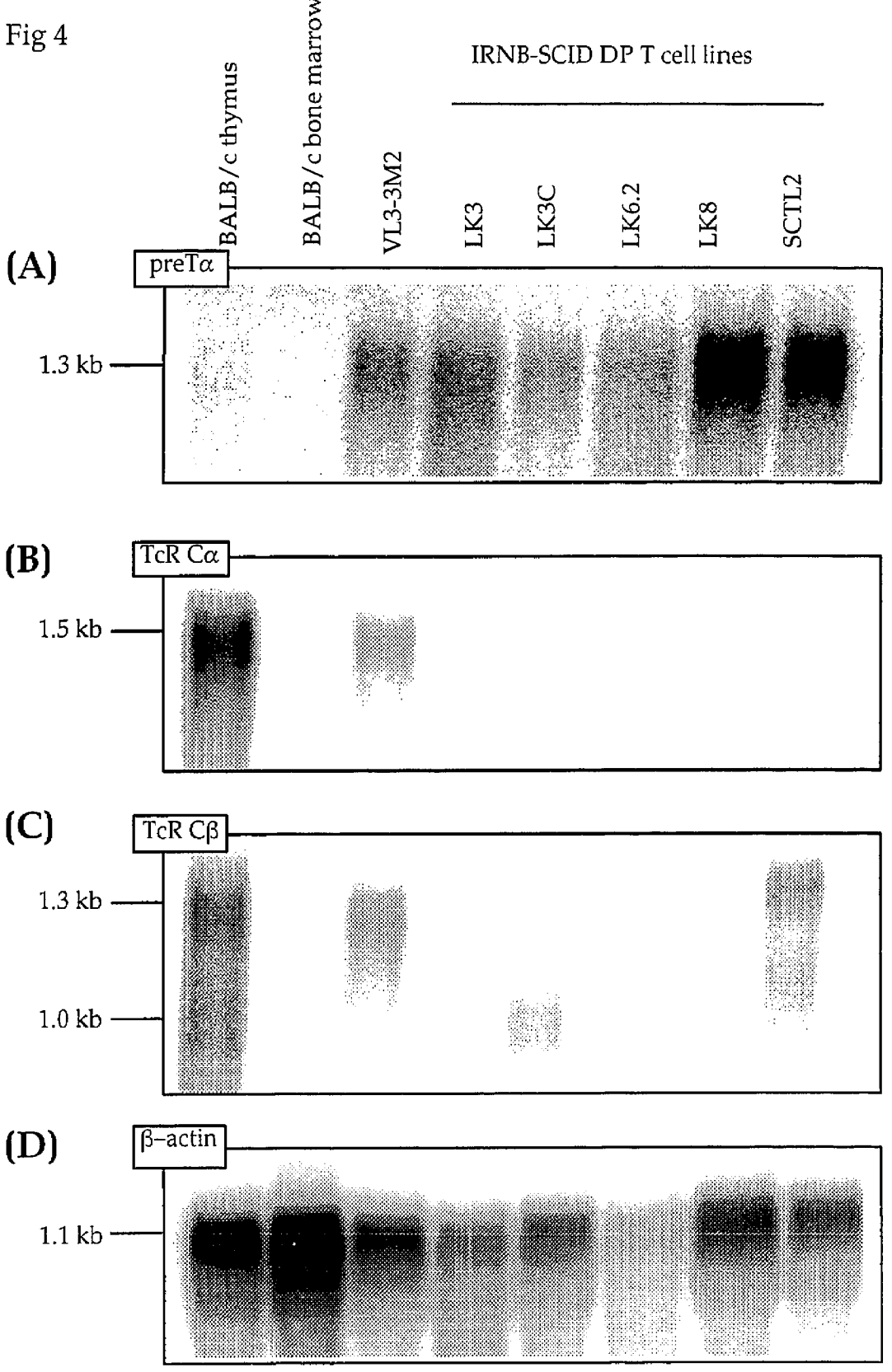
IRNB-SCID DP T cell lines
BALB/c thymus
BALB/c bone marrow
VL3-3M2
LK3
LK3C
LK6.2
LK8
SCTL2
(A)
preTα
1.3 kb
(B)
TcR Cα
1.5 kb
(C)
TcR Cβ
1.3 kb
1.0 kb
(D)
β-actin
1.1 kb

Figure 5

RT-PCR strategy for amplification of TcRβ mRNA

Schematic representation of the RT-PCR strategy utilized to detect TcRβ chain cDNA prepared from DP T cell lines. OIigonucleotides used as PCR primers are represented by arrows. Oligonucleotide sequences are found in Table 1, and their use are described in the Methods and Materials.

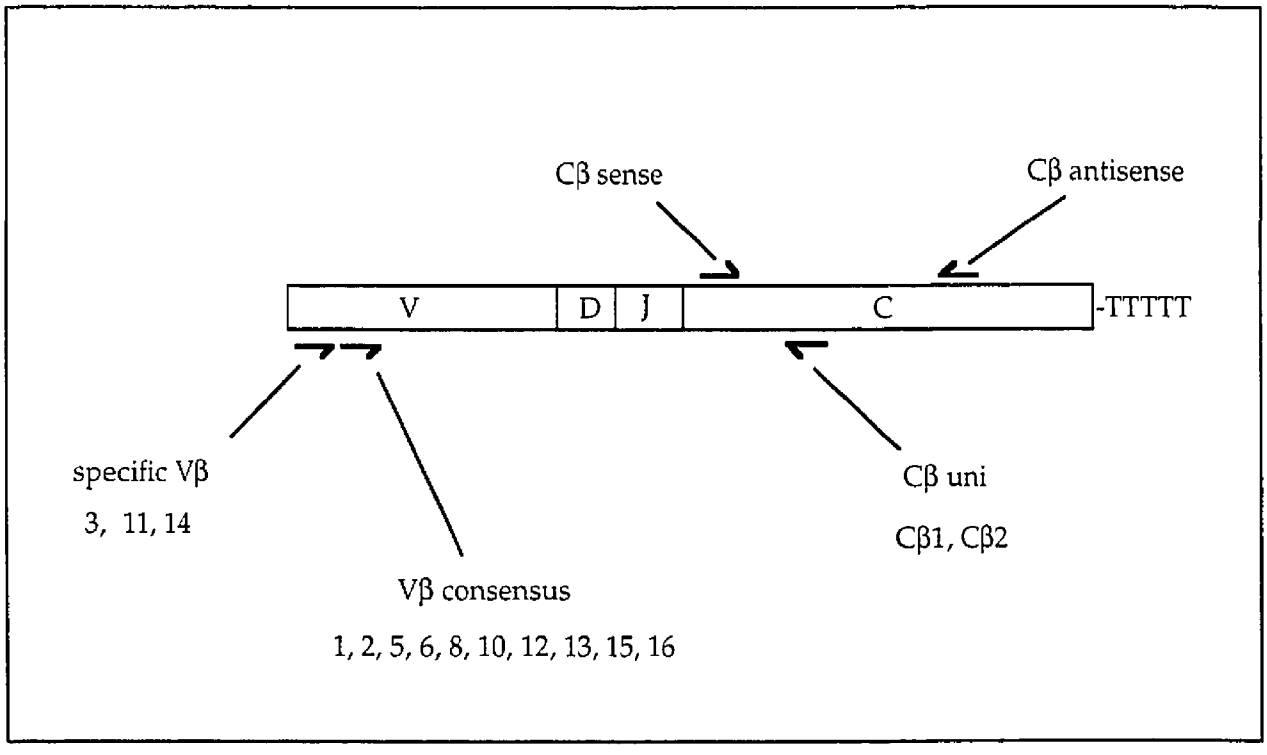
Cβ sense
Cβ antisense
V
D
J
C
-TTTTT
specific Vβ
3, 11, 14
Vβ consensus
1, 2, 5, 6, 8, 10, 12, 13, 15, 16
Cβ uni
Cβ1, Cβ2

Figure 6

TcRβ expression in *scid* DP T cell lines

RNA from IRNB-SCID lines LK3, LK3C, LK6.2, LK8, and SCTL2, BALB/c thymocytes and the C57Bl/6 line VL3-3M2 was isolated using TRIzol as directed by the manufacturer (Gibco). cDNA was prepared by reverse transcription and supplied as template for PCR reactions. For evaluation of Cβ-region expression, cDNA was amplified with the primers Cβ antisense and Cβ sense, which were designed to amplify an internal sequence in both Cβ1 and Cβ2 (panel A). For evaluation of TcR Vβ-region expression, cDNA was amplified with either the Vβ consensus primer (panel B) or V-region specific primers (panel C-Vβ3; panel D-Vβ11; panel E-Vβ14) in conjunction with the Cβ uni primer. β-actin primers (panel E) were used as a positive control for the quality of cDNA. The PCR products were resolved on agarose gels, transferred to nylon membranes, hybridized to ^{32}P-labeled TcR Cβ or β–actin probed, exposed to a phosphorscreen, and the signal was digitized on a Molecular Dynamics Phosphorimager. The position and size of the RT-PCR amplification products are indicated on the left edge of each panel.

Fig 6

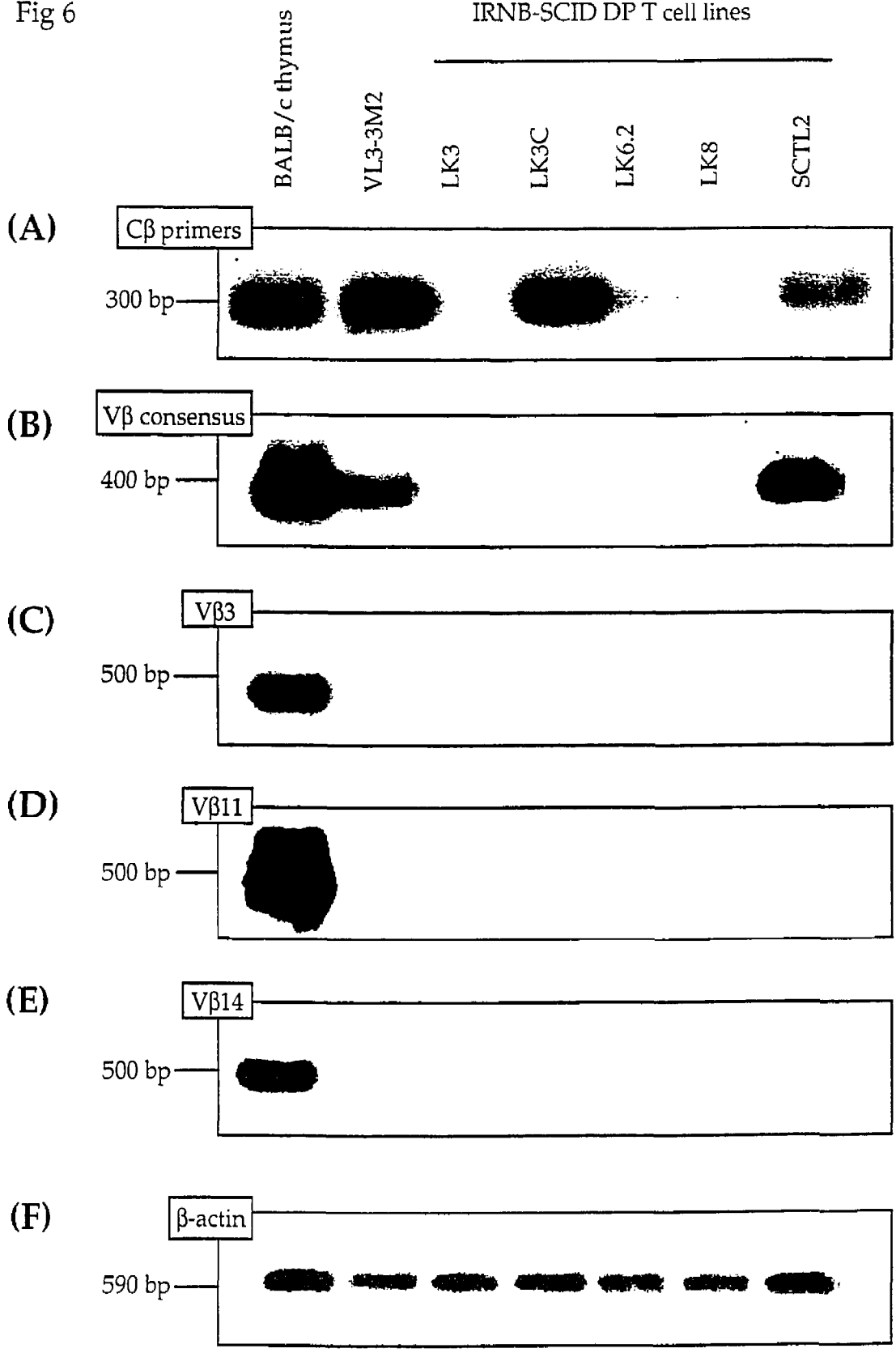
IRNB-SCID DP T cell lines
BALB/c thymus
VL3-3M2
LK3
LK3C
LK6.2
LK8
SCTL2
(A)
Cβ primers
300 bp
(B)
Vβ consensus
400 bp
(C)
Vβ3
500 bp
(D)
Vβ11
500 bp
(E)
Vβ14
500 bp
(F)
β-actin
590 bp

Figure 7

DNA sequence analysis of TcRβ transcripts in *scid* DP T cell line, SCTL2

The TcRβ transcript expressed by the IRNB-SCID DP T cell line SCTL2 was amplified by RT-PCR using the consensus Vβ primer in conjunction with the Cβ uni primer. The product was cloned into the pCR-2 vector (Invitrogen), and was used as a template in a dideoxy-sequencing reaction (Sequenase, U.S. Biochemicals). The nucleotide sequence is compared with germ-line Vβ5.1 and Jβ2.5 gene segments (underlined). The predicted amino acid sequence is also shown (**bold**).

	Vβ sequence	*DβN region*	*Jβ sequence*
Vβ5.1	TGTGCCAGCTCTCTC		Jβ2.5 AACCAAGACACC
SCTL2	TGTGCCAGCTCTCTC	GCTGTG	AACCAAGACACC
protein	**C A S S L**	**A V**	**N Q D T..**

Figure 8

TcRβ protein expression in the *scid* DP T cell line, SCTL2

Freshly isolated BALB/c thymocytes, the *scid* DP T cell lines LK3C andSCTL2 as well as the WT control VL3-3M2 were analysed for expression of TcRβ using biotin-conjugated H57-597 (anti-Cβ) and FITC-conjugated MR9-4 (anti-Vβ5) by multiparameter flow cytometry as described in the materials and methods. Two-parameter contour plots (7% probability) show TcRβ versus Vβ5 expression (far left). Single-parameter histograms show the expression of TcRβ (middle, clear histograms) and Vβ5 (far right, clear histograms) compared to staining with isotype-matched control antibodies (shaded histograms).

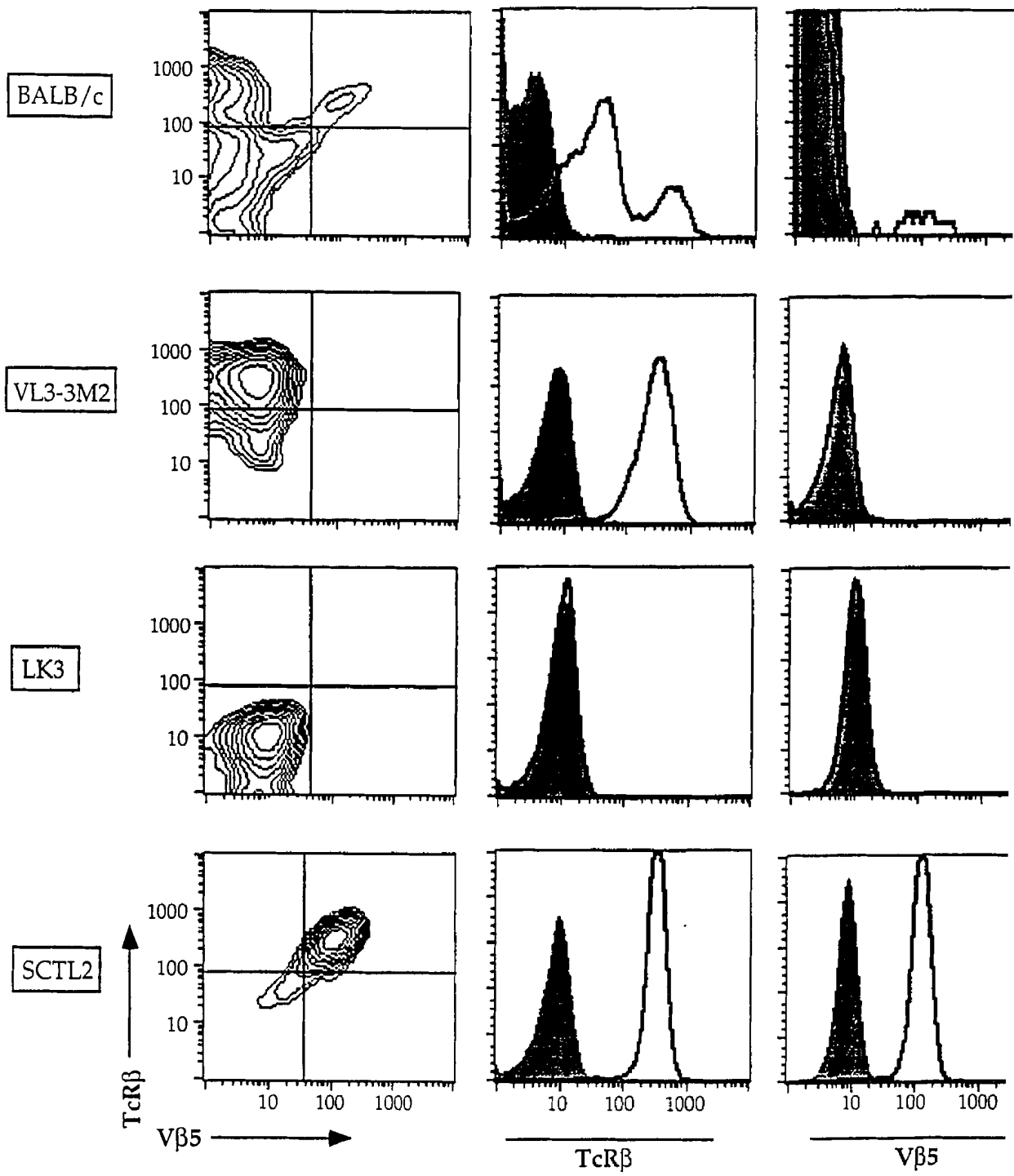
BALB/c
VL3-3M2
LK3
SCTL2
1000
100
10
10
100
1000
TcRβ
Vβ5
TcRβ
Vβ5

Figure 9

Analysis of TcRβ gene rearrangements in the constant region

(A) DNA (15μg) from IRNB-SCID DP T cell lines LK3, LK3C, LK6.2, LK8 and SCTL2, BALB/c kidney, BALB/c thymus and VL3-3M2 was digested with *Pvu*II, electrophoresed through a 1% agarose gel, transferred to nylon membrane, and hybridized to a ^{32}P labeled TcRCβ DNA probe. Phosphorimages were obtained after a 24 hour exposure with the use of a Molecular Dynamics imaging system. The position and size of unrearranged germ-line fragments are indicated on the left edge of the panel. The two closely migrating germ-line fragments are not resolvable in this image. **(B)** A *Pvu*II restriction digest map (not to scale) and the positions of the Cβ probe are included to illustrate the germ-line configuration of the Cβ region.

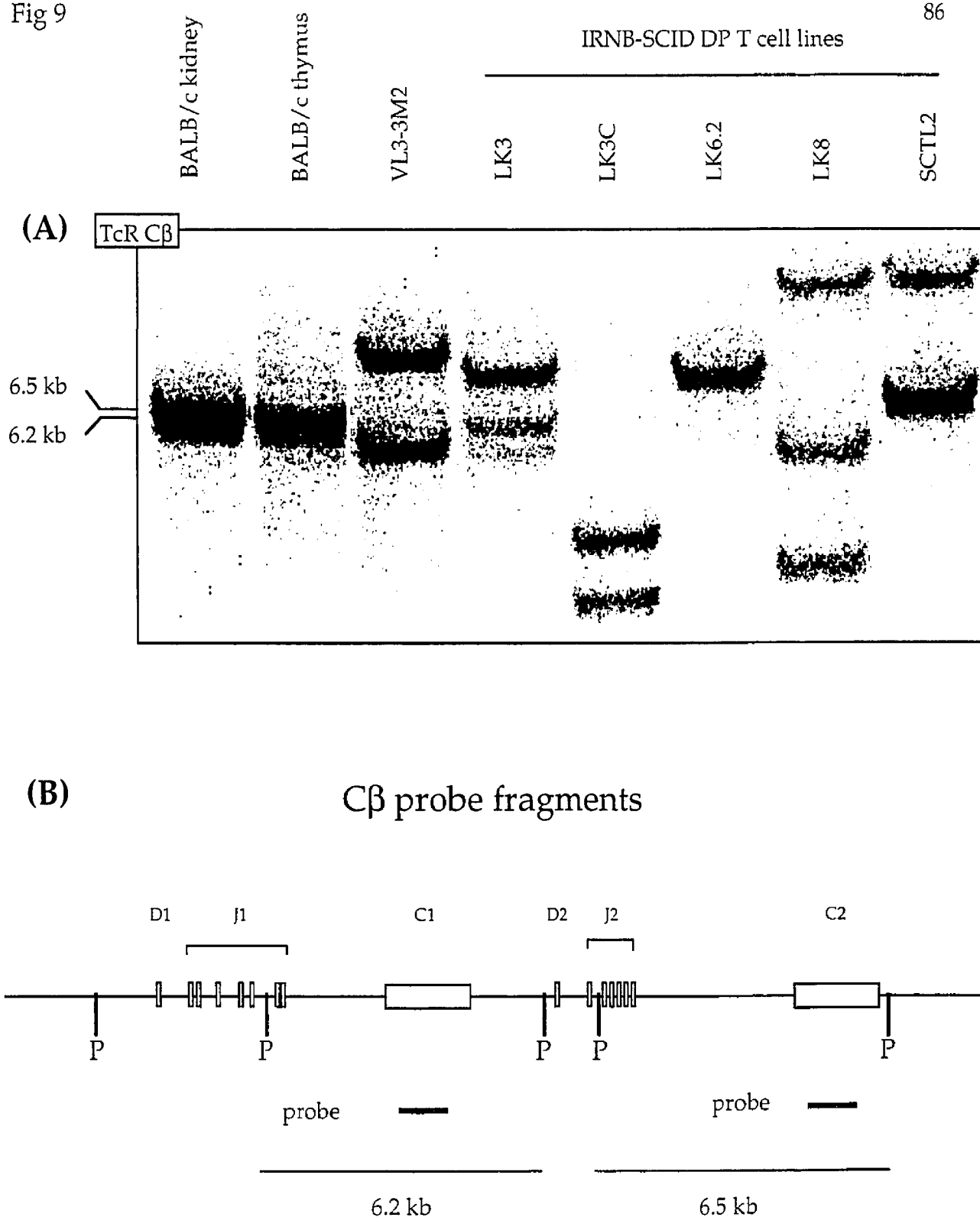
IRNB-SCID DP T cell lines
BALB/c kidney
BALB/c thymus
VL3-3M2
LK3
LK3C
LK6.2
LK8
SCTL2
(A)
TcR Cβ
6.5 kb
6.2 kb
(B)
Cβ probe fragments
D1
J1
C1
D2
J2
C2
P
P
P
P
P
probe
probe
6.2 kb
6.5 kb

Figure 10

Analysis of TcR Cβ1 cluster rearrangements

(A) DNA (15μg) from IRNB-SCID DP T cell lines LK3, LK3C, LK6.2, LK8 and SCTL2, BALB/c kidney, BALB/c thymus and VL3-3M2 was digested with *Hind*III, electrophoresed through a 1% agarose gel, transferred to nylon membrane, and assayed for hybridization to a ^{32}P labeled TcR Cβ probe. Phosphorimages were obtained after a 24 hour exposure with the use of a Molecular Dynamics imaging system. The position and size of the unrearranged germ-line fragments are indicated on the left edge of the panel. **(B)** A *Hind*III restriction digest map (not to scale), and positions of the Cβ probe are included to illustrate the germ-line configuration of the Cβ region.

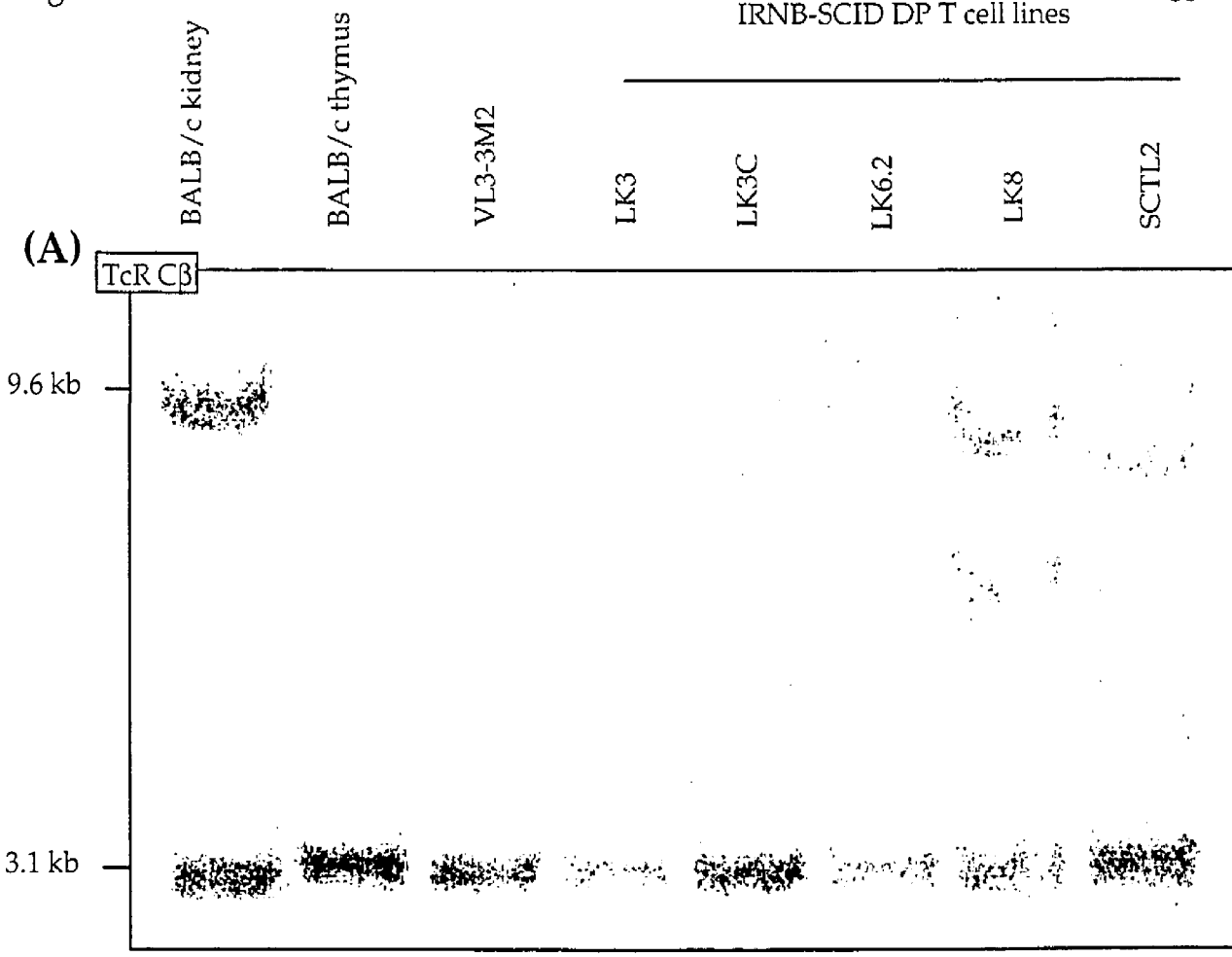
IRNB-SCID DP T cell lines
BALB/c kidney
BALB/c thymus
VL3-3M2
LK3
LK3C
LK6.2
LK8
SCTL2
(A)
TcR Cβ
9.6 kb
3.1 kb

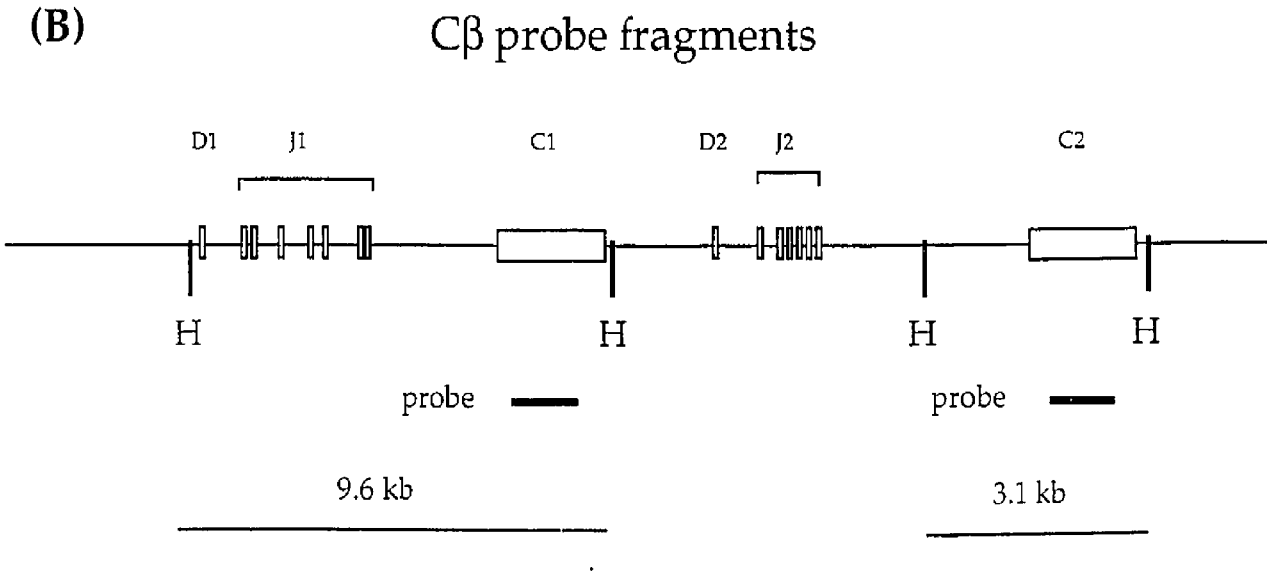
(B)
Cβ probe fragments
D1
J1
C1
D2
J2
C2
H
H
H
H
probe
probe
9.6 kb
3.1 kb

Figure 11

Analysis of TcR Jβ2 cluster rearrangements

(A) DNA (15μg) from IRNB-SCID DP T cell lines LK3, LK3C, LK6.2, LK8 and SCTL2, BALB/c kidney, BALB/c thymus and VL3-3M2 was digested with *Pvu*II, electrophoresed through a 1% agarose gel, transferred to nylon membrane, and assayed for hybridization to a ^{32}P labeled 3'Jβ2 probe. **(B)** The same Southern blot was stripped of 3'Jβ2 probe and hybridized sequentially with a ^{32}P labeled Thy-1 probe to provide a single copy gene control. Phosphorimages were obtained after a 24 hour exposure with the use of a Molecular Dynamics imaging system. The position and size of the unrearranged germ-line fragments are indicated on the left edge of the panel. **(C)** A *Pvu*II restriction digest map (not to scale), and position of the 3'Jβ2 probe are included to illustrate the germ-line configuration of the Cβ region.

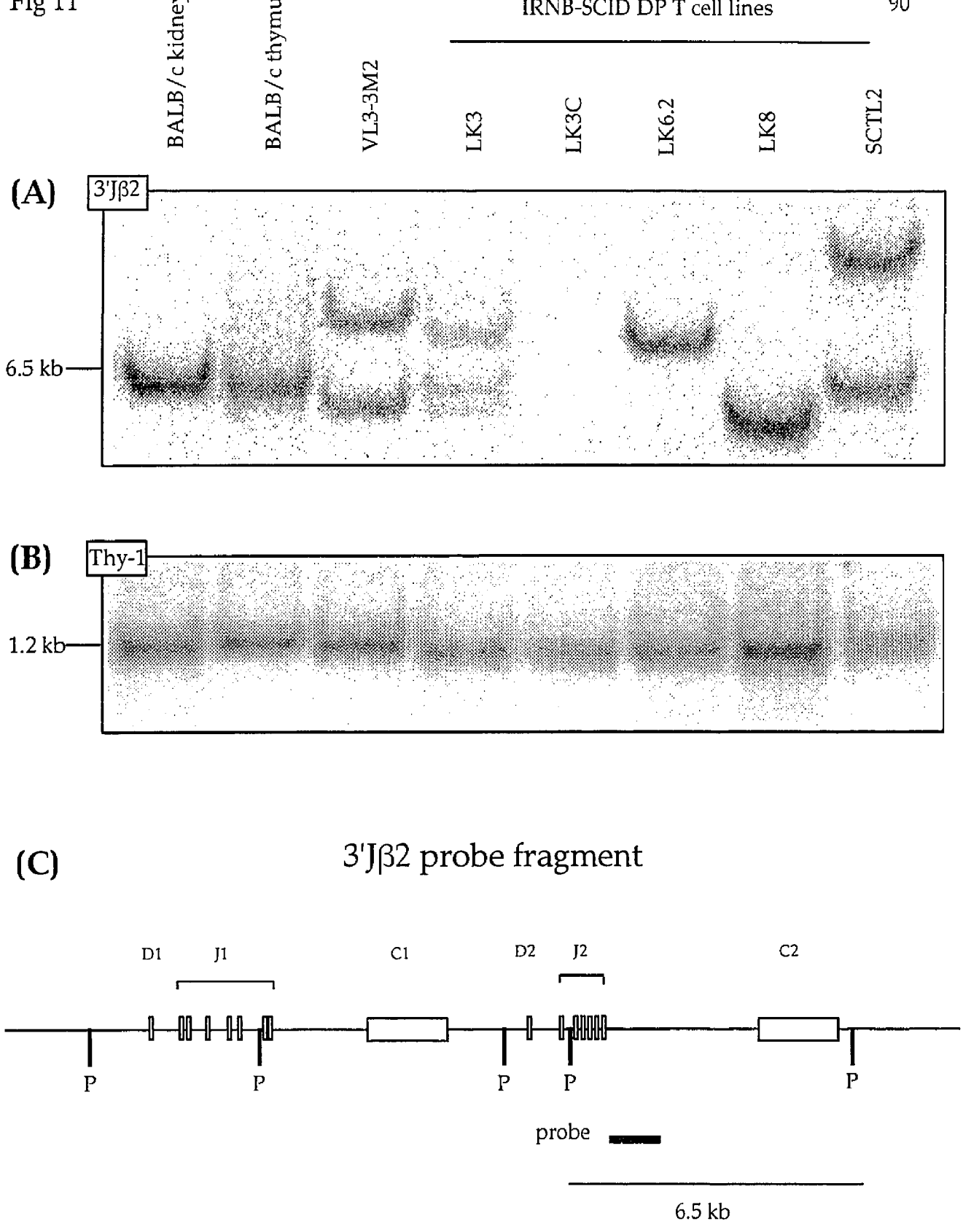
IRNB-SCID DP T cell lines
BALB/c kidney
BALB/c thymus
VL3-3M2
LK3
LK3C
LK6.2
LK8
SCTL2
(A)
3'Jβ2
6.5 kb
(B)
Thy-1
1.2 kb
(C)
3'Jβ2 probe fragment
D1
J1
C1
D2
J2
C2
P
P
P
P
P
probe
6.5 kb

Figure 12

Quantitative phosphorimaging

Varying amounts of BALB/c thymus DNA was digested with *Pvu*II, electrophoresed through an agarose gel, transferred to nylon membrane, and assayed for hybridization to a ^{32}P-labeled Thy-1 DNA probe. The different amounts of DNA (15 μg, 7.5μg, 5μg, 1μg and 0μg) were used to represent different allele copy numbers (2, 1, 1/3, 1/15, and 0, respectively). The hybridized filter was exposed to a phosphorscreen, digitized by a Molecular Dynamics phosphorscanner, and absolute pixel number in each sample was quantified by volume integration using ImageQuant software (Molecular Dynamics). The expected number of alleles represented, pixel value, and calculated number of alleles represented, are displayed under each band. To determine the calculated number of alleles, the pixel value for the sample was compared to the pixel value obtained for the 15μg sample (which represented two alleles of the *thy*-1 gene). See the Materials and Methods for a detailed description.

Fig 12

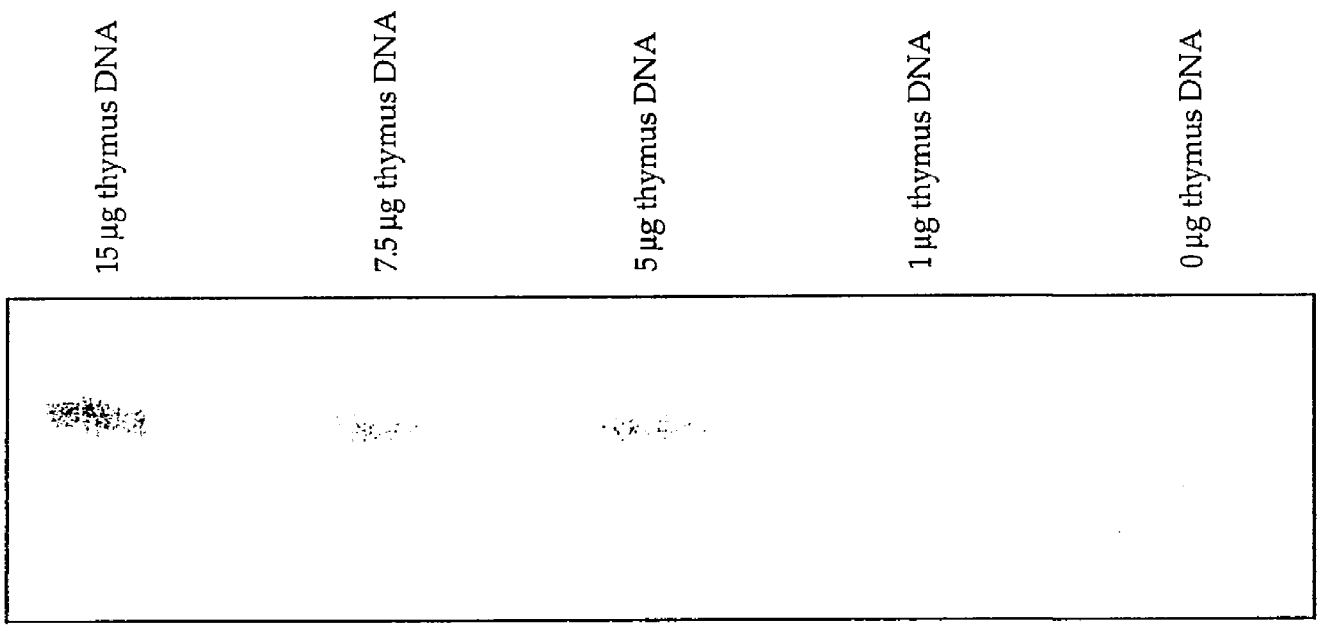

Expected number of alleles	2	1	0.66	0.13	0
Pixel Value	12558	6297	5475	2763	1923
Caculated number of alleles	2	1.00	0.87	0.44	0.31

Figure 13

Quantitative phosphorimaging of the TcR Jβ2 gene cluster in *scid* DP T cell lines

(A) DNA (15μg) from IRNB-SCID DP T cell lines LK3, LK3C, LK6.2, LK8 and SCTL2, BALB/c kidney, BALB/c thymus and VL3-3M2 was digested with *Pvu*II, electrophoresed through a 1% agarose gel, transferred to nylon membrane, and assayed for hybridization to a ^{32}P labeled Thy-1 probe. **(B)** The same Southern blot was hybridized sequentially with a ^{32}P labeled 3'Jβ2 probe. Phosphorimages were obtained after a 24 hour exposure with the use of a Molecular Dynamics imaging system. Densitometry was performed on the restriction fragments hybridizing to either probe. Absolute pixel number in each sample was quantified by volume integration using ImageQuant software (Molecular Dynamics). In order to determine the copy number of the 3'Jβ2 sequence, the ratios of the pixel values obtained for 3'Jβ2 and Thy-1 were compared between the experimental samples (IRNB-SCID T cell lines) and the average of non-rearranging tissue controls (BALB/c kidney). The predicted number of alleles is represented above each band analysed. **(C)** The pixel values for each sample is shown in the bottom panel, along with the ratios used to calculate the predicted number of alleles. Samples denoted by an asterix '*' had two different sized bands hybridizing to the 3'Jβ2 probe, of which one was analysed. The method of calculating the predicted number of alleles is explained fully in the Methods and Materials section.

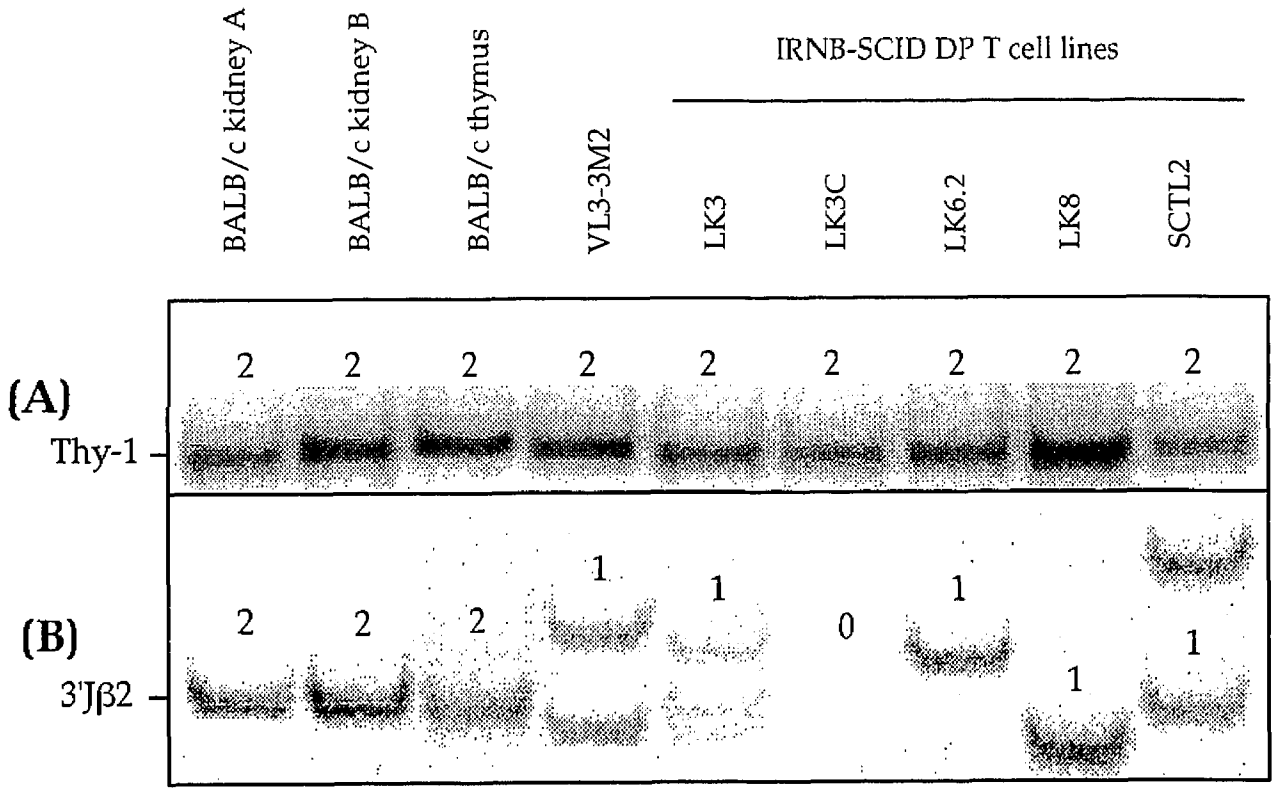

(C)

sample	p.v. Thy-1	p.v. 3'Jβ2	3'Jβ2/Thy-1	# of alleles
kidney A	67003	13631	0.20343865	2.05235464
kidney B	86419	16684	0.1930594	1.94764536
thymus	74093	10133	0.13676056	1.37968455
VL3*	81788	8933	0.1092214	1.10186067
LK3*	69509	5104	0.07342934	0.74077883
LK3C	58184	734	0.01261515	0.12726572
LK6.2	77893	8705	0.11175587	1.12742921
LK8	118041	10550	0.08937573	0.9016511
SCTL2*	62369	5911	0.09477465	0.95611717

Figure 14

Quantitative phosphorimaging of the TcR Cβ2 gene in *scid* DP T cell lines

(A) DNA (15μg) from IRNB-SCID DP T cell lines LK3, LK3C, LK6.2, LK8 and SCTL2, BALB/c kidney, BALB/c thymus and VL3-3M2 was digested with *Hind*III, electrophoresed through a 1% agarose gel, transferred to nylon membrane, and assayed for hybridization to a ^{32}P labeled Thy-1 probe. **(B)** The same Southern blot was hybridized sequentially with a ^{32}P labeled TcRCβ probe. Phosphorimages were obtained after a 24 hour exposure with the use of a Molecular Dynamics imaging system. Densitometry was performed on the restriction fragments hybridizing to either probe. Absolute pixel number in each sample was quantified by volume integration using ImageQuant software (Molecular Dynamics). In order to determine the copy number of the Cβ2 gene, the ratios of the pixel values obtained for Cβ2 (3.1 kb fragment, Fig 10) and Thy-1 were compared between the experimental samples (IRNB-SCID T cell lines) and the average of non-rearranging tissue controls (BALB/c kidney). The predicted number of alleles is represented above each band analysed. **(C)** The pixel values for each sample is shown in the bottom panel, along with the ratios used to calculate the predicted number of alleles. The method of calculating the predicted number of alleles is explained fully in the Methods and Materials section.

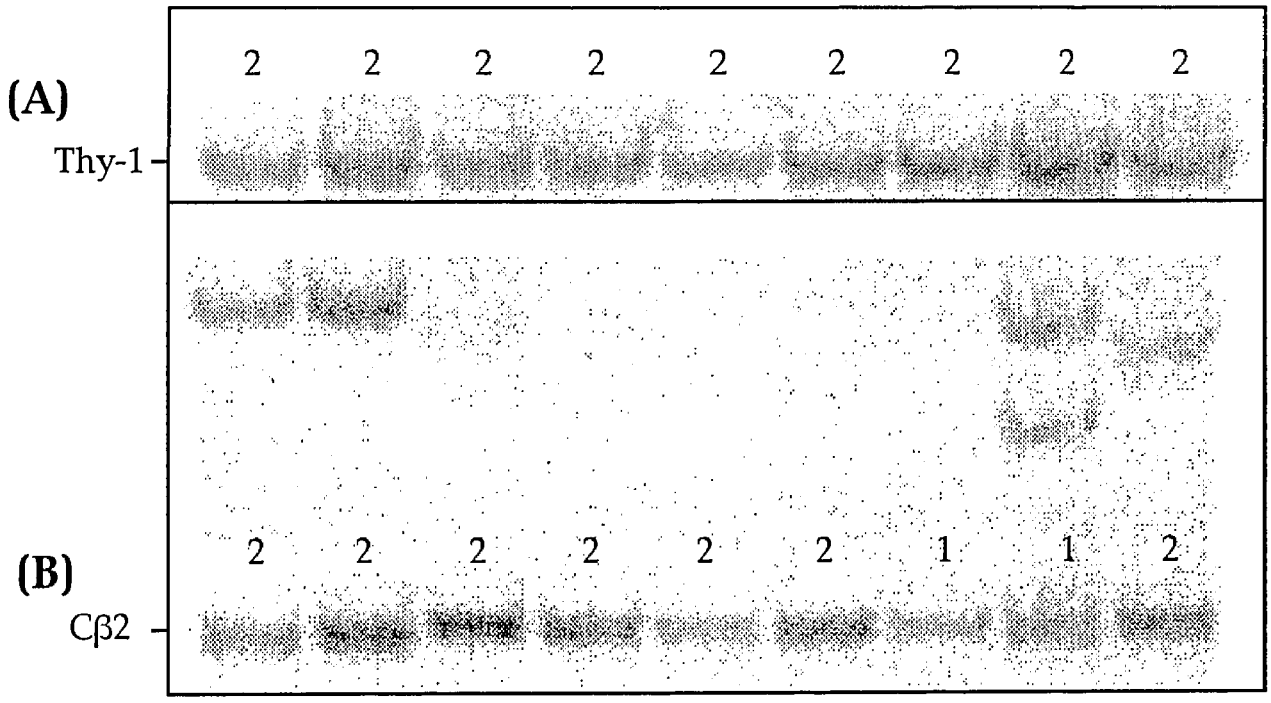

(C)

sample	p.v. Thy-1	p.v. Cβ2	Cβ2/Thy-1	# of alleles
kidney A	12820	8020	0.62558502	1.98745988
kidney B	20078	12719	0.63347943	2.01254012
thymus	15829	13270	0.8383347	2.66335754
VL3	13613	10742	0.78909866	2.50693649
LK3	10612	5841	0.55041462	1.74864638
LK3C	15061	10375	0.68886528	2.18849886
LK6.2	17196	5339	0.31047918	0.98638058
LK8	25604	9473	0.36998125	1.1754164
SCTL2	19841	11605	0.58489995	1.85820496

Figure 15

Analysis of TcRβ locus rearrangement

(A) DNA (15μg) from IRNB-SCID DP T cell lines LK3, LK3C, LK6.2, LK8 and SCTL2, BALB/c kidney, BALB/c thymus and VL3-3M2 was digested with *Pvu*II, electrophoresed through a 1% agarose gel, transferred to nylon membrane, and assayed for hybridization to a ^{32}P labeled 5'Dβ1 probe. **(B)** The same Southern blot was stripped of hybridized probe and hybridized with a ^{32}P labeled Thy-1 probe to provide a single copy gene control. Phosphorimages were obtained after a 24 hour exposure with the use of a Molecular Dynamics imaging system. The position and size of the unrearranged germ-line fragments are indicated on the left edge of each panel. **(C)** A *Pvu*II restriction digest map (not to scale), and position of the 5'Dβ1 probe are included to illustrate the germ-line configuration of the Cβ region.

Fig 15

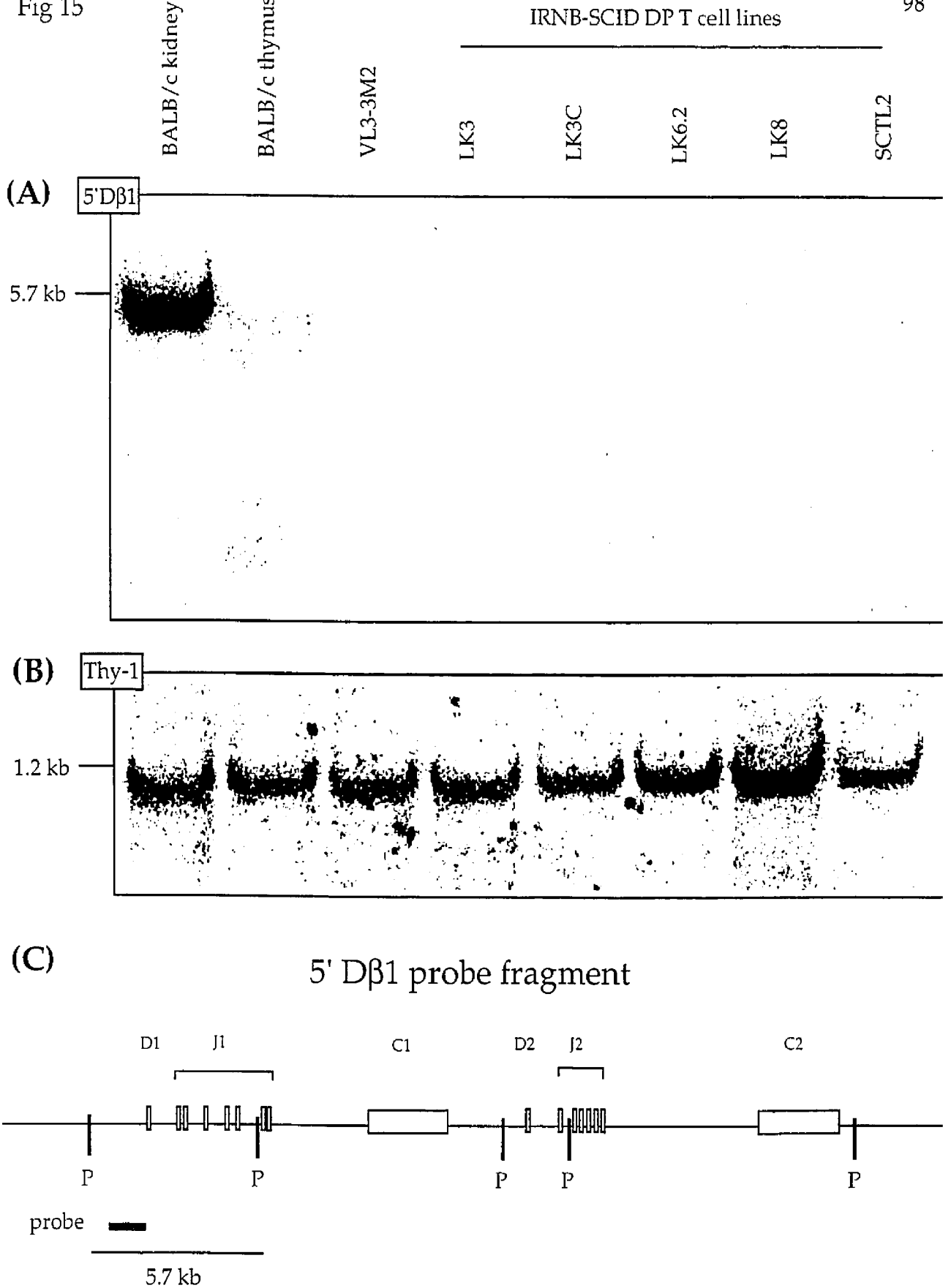
BALB/c kidney
BALB/c thymus
VL3-3M2
IRNB-SCID DP T cell lines
LK3
LK3C
LK6.2
LK8
SCTL2
(A)
5'Dβ1
5.7 kb
(B)
Thy-1
1.2 kb
(C)
5' Dβ1 probe fragment
D1
J1
C1
D2
J2
C2
P
P
P
P
P
probe
5.7 kb

Figure 16

The murine TcRβ chain locus

Physical map of the β-chain gene locus of the murine T cell receptor, which is situated on chromosome 6. The approximate positions of variable regions and the kilobase scale in this figure are based on the data presented in Lindsten et al., 1987, and Lee and Davis, 1988. Vβ and Dβ genes are represented as vertical lines (**|**). The Jβ1 and Jβ2 gene clusters are represented as open boxes. The Cβ genes are represented as filled boxes. The Cβ region (including the Vβ14 gene) has been expanded for clearer representation.

Fig 16

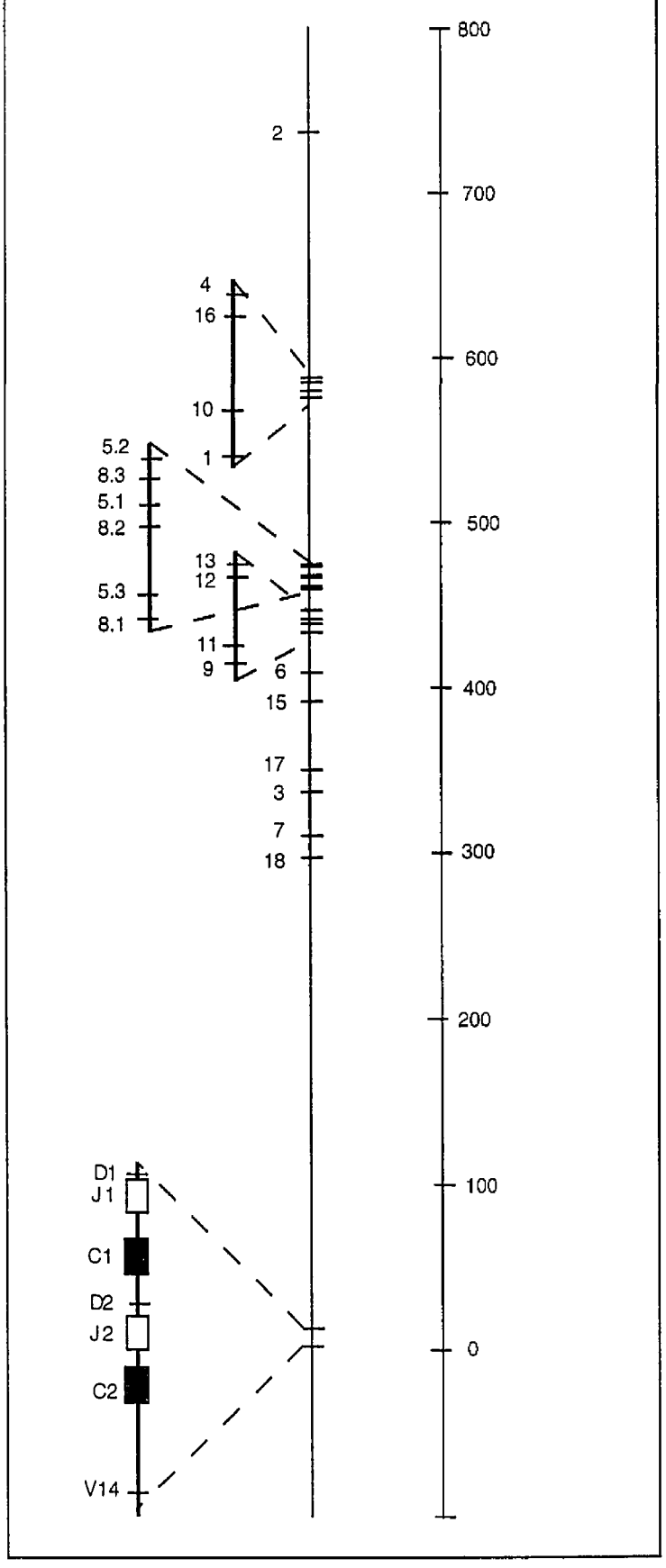
100
800
700
600
500
400
300
200
100
0
2
4
16
10
1
5.2
8.3
5.1
8.2
5.3
8.1
13
12
11
9
6
15
17
3
7
18
D1
J1
C1
D2
J2
C2
V14

Figure 17

Analysis of TcR Vβ gene deletion

(A) DNA (15μg) from IRNB-SCID DP T cell lines LK3, LK3C, LK6.2, LK8 and SCTL2, BALB/c kidney, BALB/c thymus and VL3-3M2 was digested with *Pvu*II, electrophoresed through a 1% agarose gel, transferred to nylon membrane, and assayed for hybridization to a ^{32}P labeled Vβ7 probe. Although two *Pvu*II fragments (2.4 kb and 1.0 kb) were detected with the Vβ7 probe, only the 1.0 kb fragment is shown. **(B)** The same DNA blot was stripped of hybridized probe and hybridized sequentially with a ^{32}P labeled Vβ2 probe. **(C)** The same DNA blot was stripped of hybridized probe and hybridized sequentially with a ^{32}P labeled Vβ14 probe. Phosphorimages were obtained after a 24 hour exposure with the use of a Molecular Dynamics imaging system. The position and size of the unrearranged germ-line fragments are indicated on the left edge of each panel.

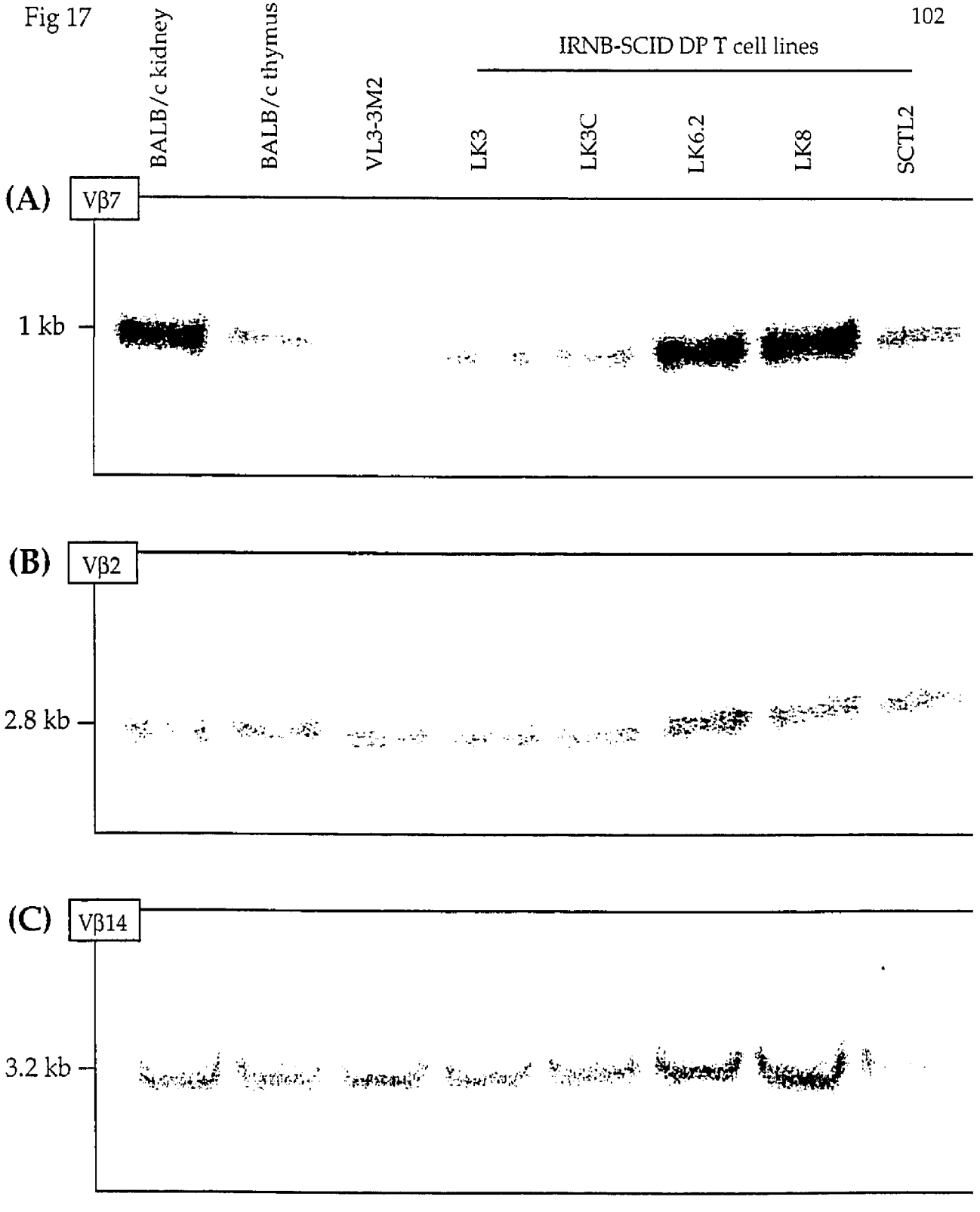
BALB/c kidney
BALB/c thymus
VL3-3M2
IRNB-SCID DP T cell lines
LK3
LK3C
LK6.2
LK8
SCTL2
(A)
Vβ7
1 kb
(B)
Vβ2
2.8 kb
(C)
Vβ14
3.2 kb

Figure 18

Quantitative phosphorimaging of TcR Vβ genes in *scid* DP T cell lines

A: (i) DNA (15μg) from LK3, LK3C, LK6.2, LK8 and SCTL2, BALB/c kidney, BALB/c thymus and VL3-3M2 was digested with *Pvu*II, electrophoresed through a 1% agarose gel, transferred to nylon membrane, and assayed for hybridization to a ^{32}P labeled Thy-1 probe. **(ii)** the same filter was sequentially hybridized with a ^{32}P labeled Vβ2 probe. **(iii)** densitometry/volume integration results **B: (i)** The same DNA samples described above were digested with *Pvu*II, electrophoresed through a 1% agarose gel, transferred to nylon membrane, and assayed for hybridization to a ^{32}P labeled Thy-1 probe. **(ii)** the same filter was sequentially hybridized with a ^{32}P labeled Vβ14 probe. **(iii)** densitometry/volume integration results **C: (i)** The same DNA samples described above were digested with *Pvu*II, electrophoresed through a 1% agarose gel, transferred to nylon membrane, and assayed for hybridization to a ^{32}P labeled Thy-1 probe. **(ii)** the same filter was sequentially hybridized with a ^{32}P labeled Vβ7 probe. **(iii)** densitometry/volume integration results. Densitometry was performed on the restriction fragments hybridizing to the Thy-1 and Vβ probes. Absolute pixel number in each sample was quantified by volume integration using ImageQuant software (Molecular Dynamics). In order to determine the copy number of the Vβ gene of interest, the ratios of the pixel values obtained for that Vβ and Thy-1 were compared between the experimental samples (IRNB-SCID T cell lines) and the average of non-rearranging tissue controls (BALB/c kidney). The predicted number of alleles is represented above each band analysed. The pixel values for each sample is shown in the bottom panel, along with the ratios used to calculate the predicted number of alleles. The method of calculating the predicted number of alleles is explained fully in the Methods and Materials section.

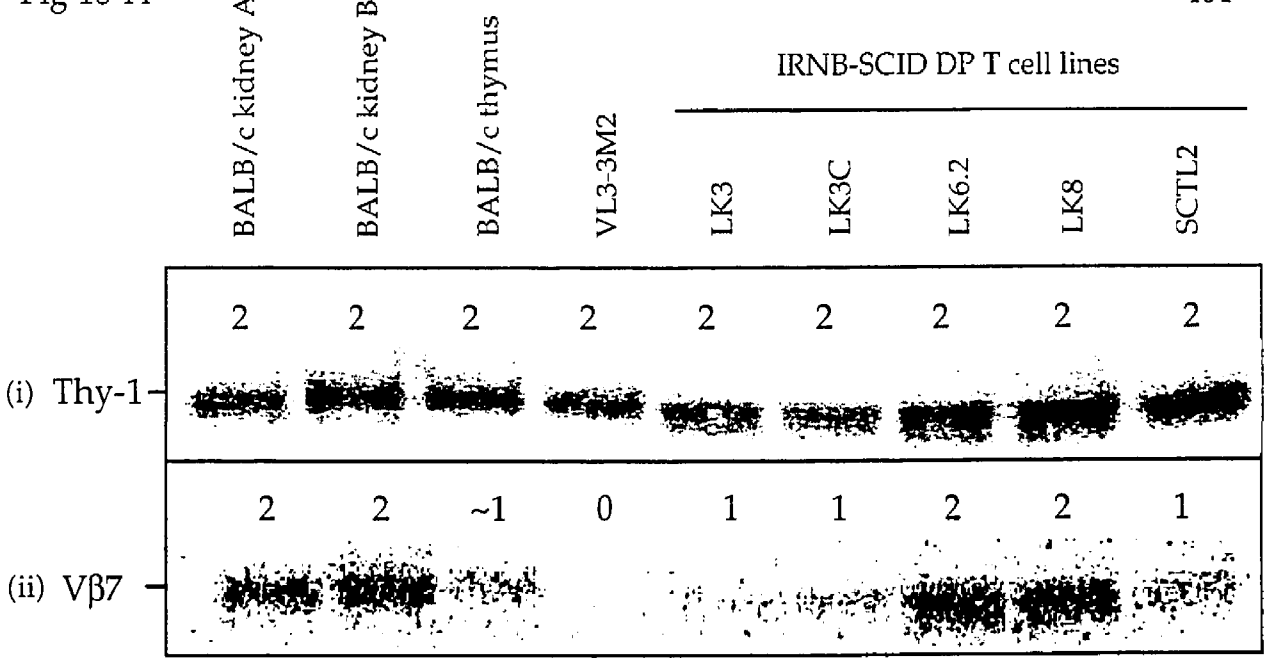

(iii)

sample	p.v. Thy-1	p.v. Vβ7	Vβ7/Thy-1	# of alleles
kidney A	27498	5618	0.20430577	1.91770551
kidney B	32893	7297	0.22184051	2.08229449
thymus	31283	2730	0.08726785	0.85428665
VL3	26302	878	0.03338149	0.31333365
LK3	24748	2943	0.1189187	1.11622422
LK3C	21548	2725	0.12646185	1.18702763
LK6.2	30889	7382	0.23898475	2.33948121
LK8	47446	8733	0.18406188	1.72768731
SCTL2	35893	3293	0.09174491	0.86115883

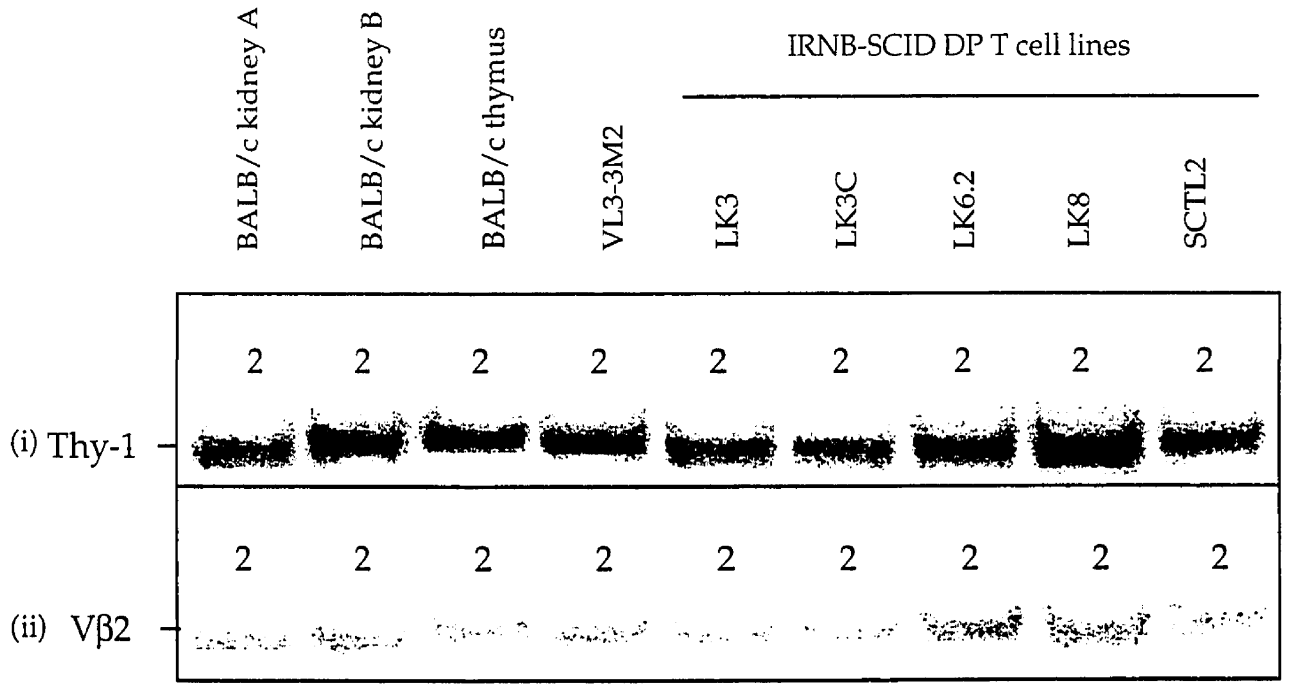

(iii)

sample	p.v. Thy-1	p.v. Vβ2	Vβ2/Thy-1	# of alleles
kidney A	67003	16359	0.24415325	2.17221003
kidney B	86419	17754	0.20544093	1.82778997
thymus	74093	15943	0.21517552	1.91439776
VL3	81788	17638	0.21565511	1.91866459
LK3	69509	15371	0.22113683	1.967435
LK3C	58184	13485	0.23176475	2.06199063
LK6.2	77893	20545	0.26375926	2.34664301
LK8	118041	26137	0.22142306	1.96998159
SCTL2	62369	15478	0.24816816	2.20793036

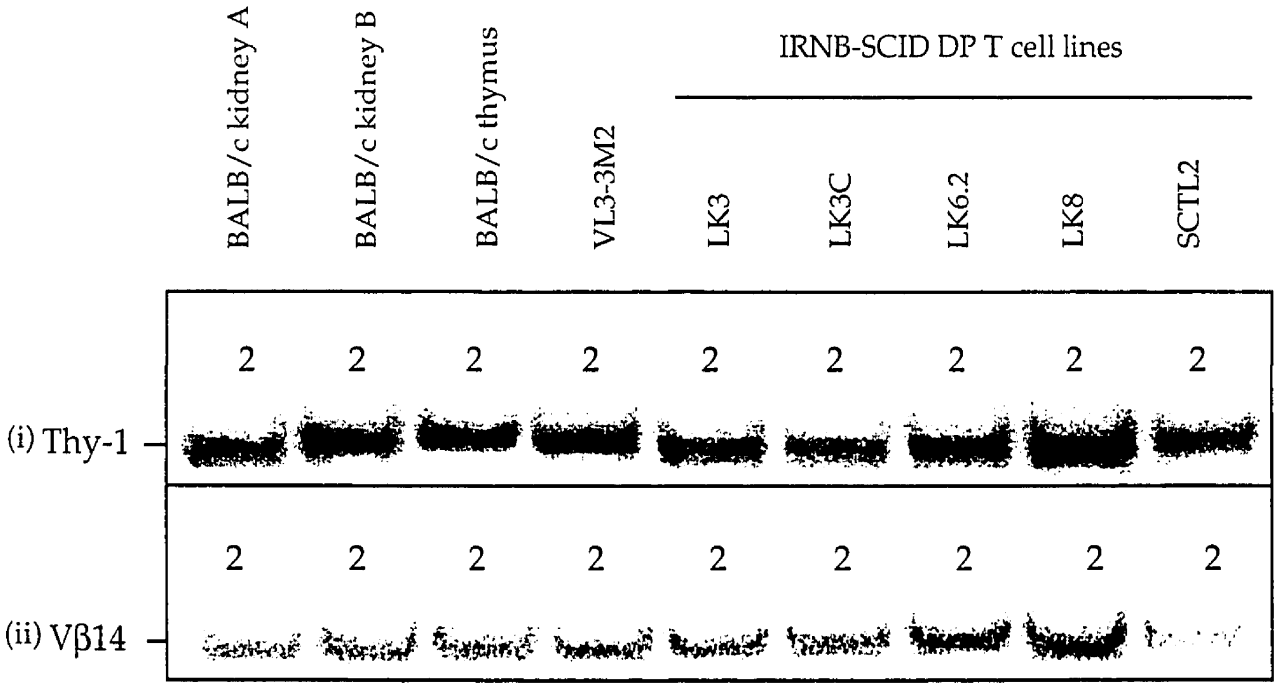

(iii)

sample	p.v. Thy-1	p.v. Vβ14	Vβ14/Thy-1	# of alleles
kidney A	67003	11978	0.17876811	1.94945965
kidney B	86419	16250	0.18803735	2.05054035
thymus	74093	15332	0.20692913	2.25655447
VL3	81788	13941	0.17045288	1.8587823
LK3	69509	14068	0.20239106	2.20706696
LK3C	58184	11266	0.19362711	2.11149649
LK6.2	77893	17134	0.21996842	2.39874743
LK8	118041	22382	0.18961208	2.06771273
SCTL2	62369	9726	0.15594286	1.70055105

Figure 19

Fluorescent In Situ Hybridization

Murine chromosome 6 paint was hybridized to metaphasic spreads prepared from BALB/c spleen cells (BALB/c) and the IRNB-SCID DP T cell lines LK3, LK3C, LK6.2, LK8 and SCTL2. Metaphasic spreads were prepared and assayed for hybridization to the murine paint as described in the Materials and Methods. Chromosomes that hybridized to the chromosome 6 paints are yellow. White arrows indicate metacentric chromosomes.

Fig 19

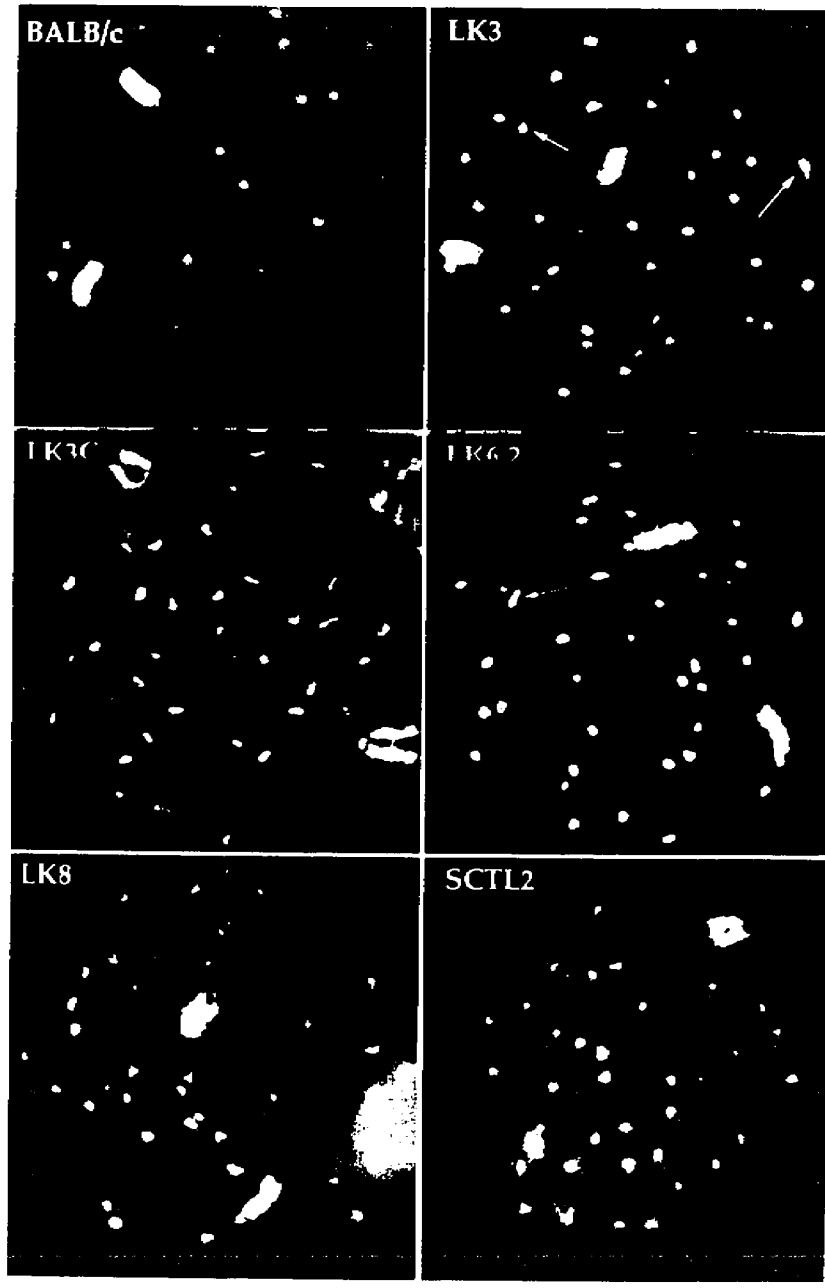

Figure 20

Pulsed Field Gel Electrophoresis Strategy

*Nae*I restriction map of the murine TcRβ locus (not to scale). The horizontal lines below the map indicate *Nae*I restriction fragments of germ-line DNA that contain Vβ7, Cβ1, Cβ2 or Vβ14. The hatched lines represent possible products resulting from partial digestion of the *Nae*I sites within the constant region. Numbers to the right of the horizontal brackets indicate the size of each particular DNA fragment.

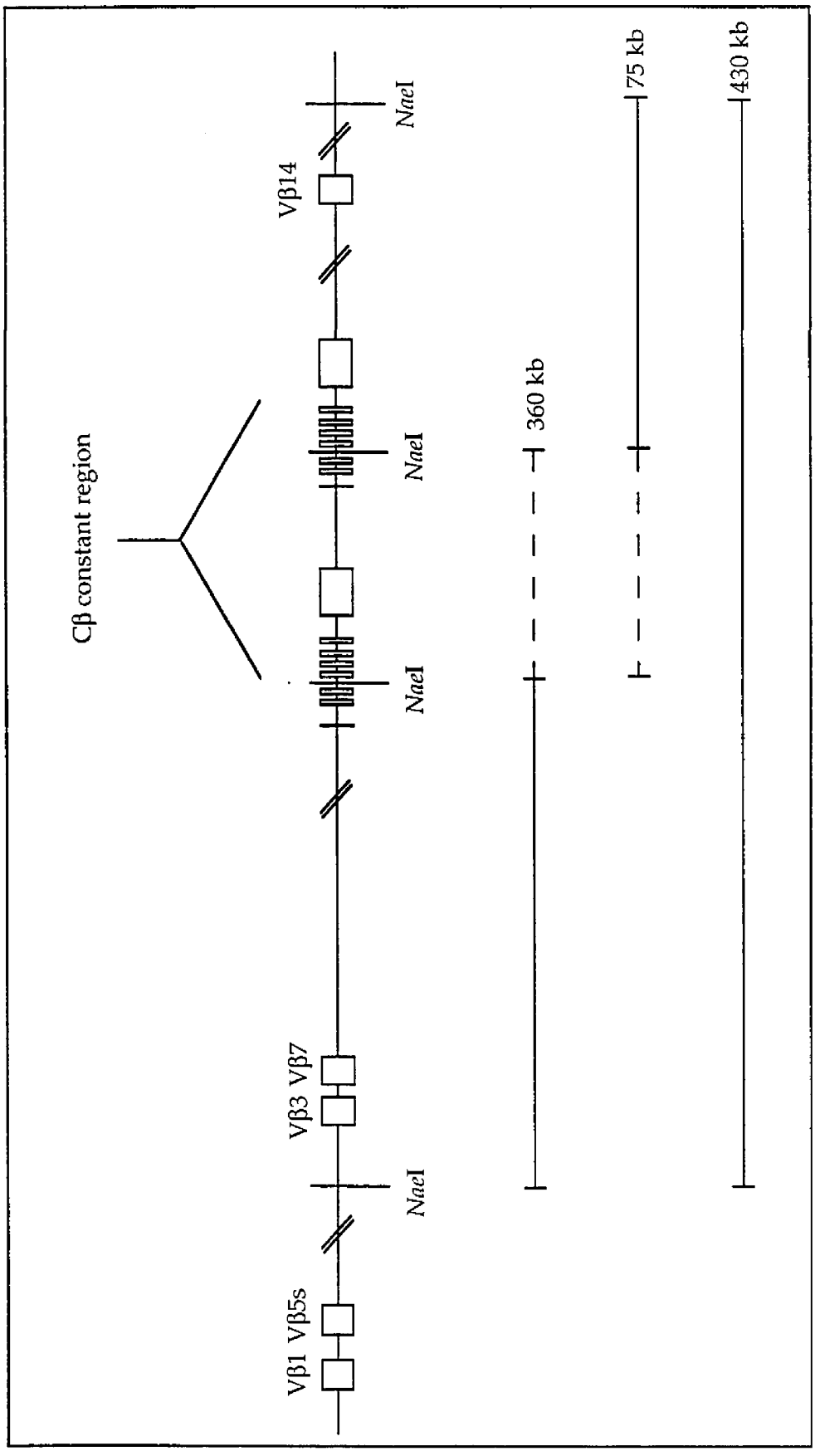
Vβ1 Vβ5s
Vβ3 Vβ7
Vβ14
Cβ constant region
NaeI
NaeI
NaeI
NaeI
360 kb
75 kb
430 kb

Figure 21

Pulsed Field Gel Electrophoresis of the TcRβ locus in *scid* DP T cell lines

DNA from IRNB-SCID DP T cell lines SCTL2, LK8, LK6.2, LK3C and LK3 (panels A-E, respectively) was prepared in agarose blocks as described in the Materials and Methods section. The DNA was digested in the agarose blocks with the enzyme *Nae*I, separated by pulsed field gel electrophoresis, transferred to nylon membrane, and assayed for hybridization to TcR Vβ7, TcR Cβ and TcR Vβ14 DNA probes. The approximate size of each fragment is indicated on the left edge of each row of panels. Detectable fragments are indicated by an arrow on the left edge of each panel. Size approximation was done by comparison with λ phage DNA concatamer size standards. The compression zone (C.Z., zone where DNA migrates independently of electrophoresis parameters) is indicated by a '*' on the left edge of each panel. Phosphorimages were obtained after a 48-72 hour exposure with the use of a Molecular Dynamics imaging system.

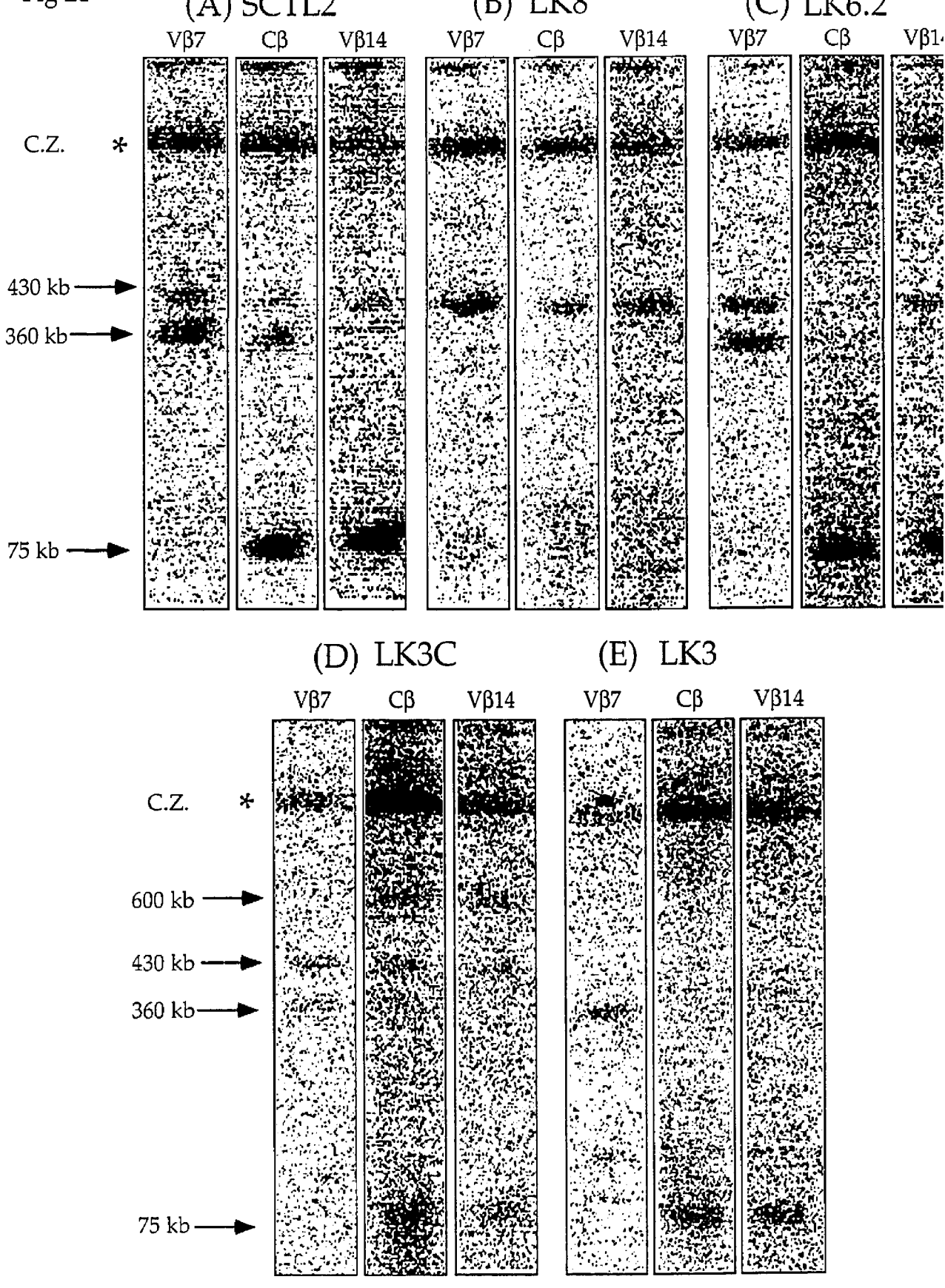
(A) SCTL2
(B) LK8
(C) LK6.2
Vβ7
Cβ
Vβ14
C.Z.
*
430 kb
360 kb
75 kb
(D) LK3C
(E) LK3
600 kb

Figure 22

Restriction maps of the TcRβ constant region in *scid* DP T cell lines

Physical maps of both alleles of the TcRβ constant region in LK3 (A), LK3C (B), LK6.2 (C), LK8 (D), and SCTL2 (E). The approximate positions of restriction enzyme sites in relation to constant region genes are based on the data presented in this study. The size of the restriction fragments hybridizing to the TcR Cβ probe used throughout this study are found beneath each TcRβ allele. TcRβ gene segments are represented by open boxes. Bolded **?** and hatched bars signify that the represented DNA sequence is unknown. H = *Hind*III, P = *Pvu*II restriction sites.

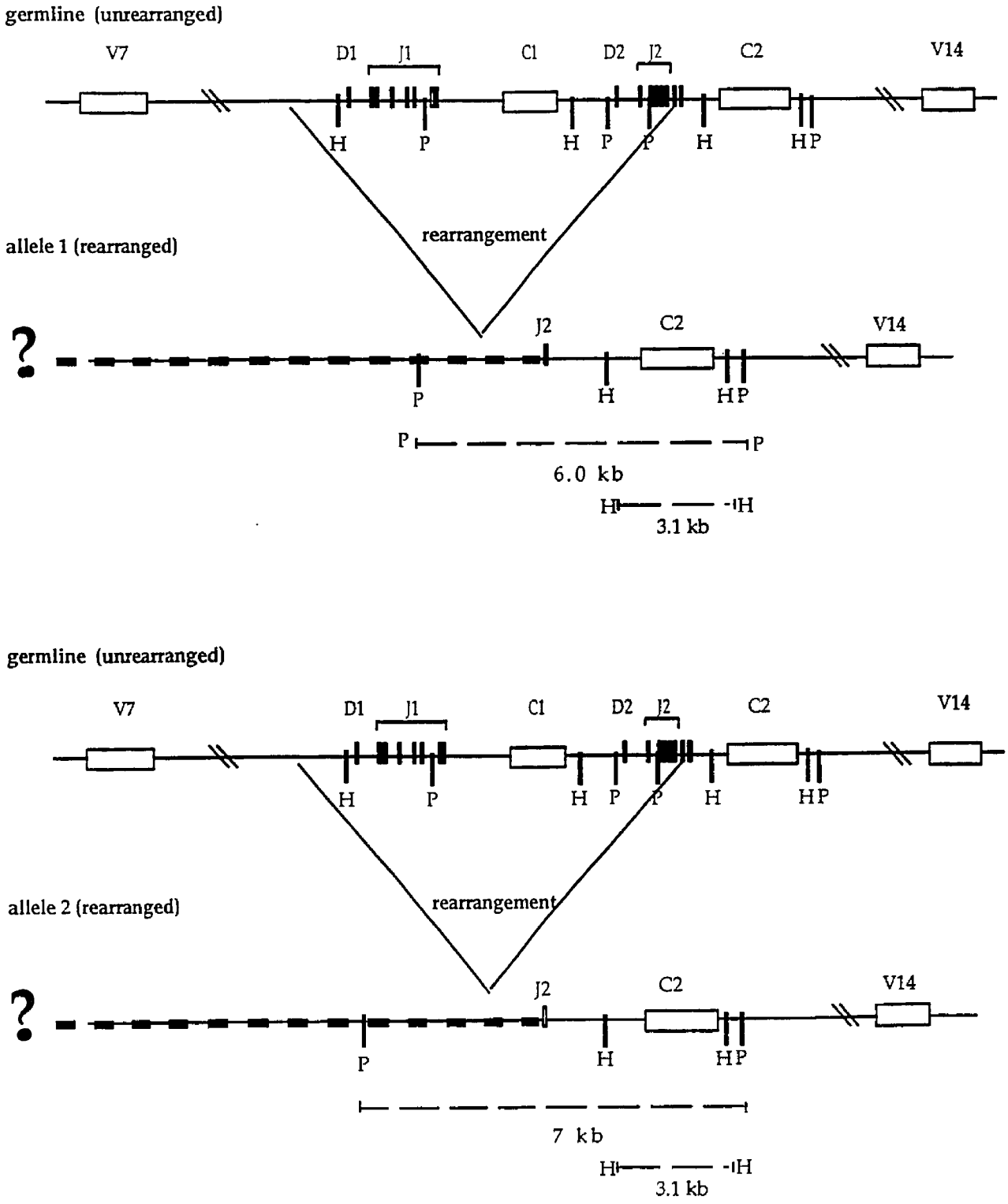
germline (unrearranged)
V7
D1
J1
C1
D2
J2
C2
V14
H
P
H
P
P
H
HP
rearrangement
allele 1 (rearranged)
?
J2
C2
V14
P
H
HP
P
P
6.0 kb
H
H
3.1 kb
germline (unrearranged)
V7
D1
J1
C1
D2
J2
C2
V14
H
P
H
P
P
H
HP
rearrangement
allele 2 (rearranged)
?
J2
C2
V14
P
H
HP
7 kb
H
H
3.1 kb

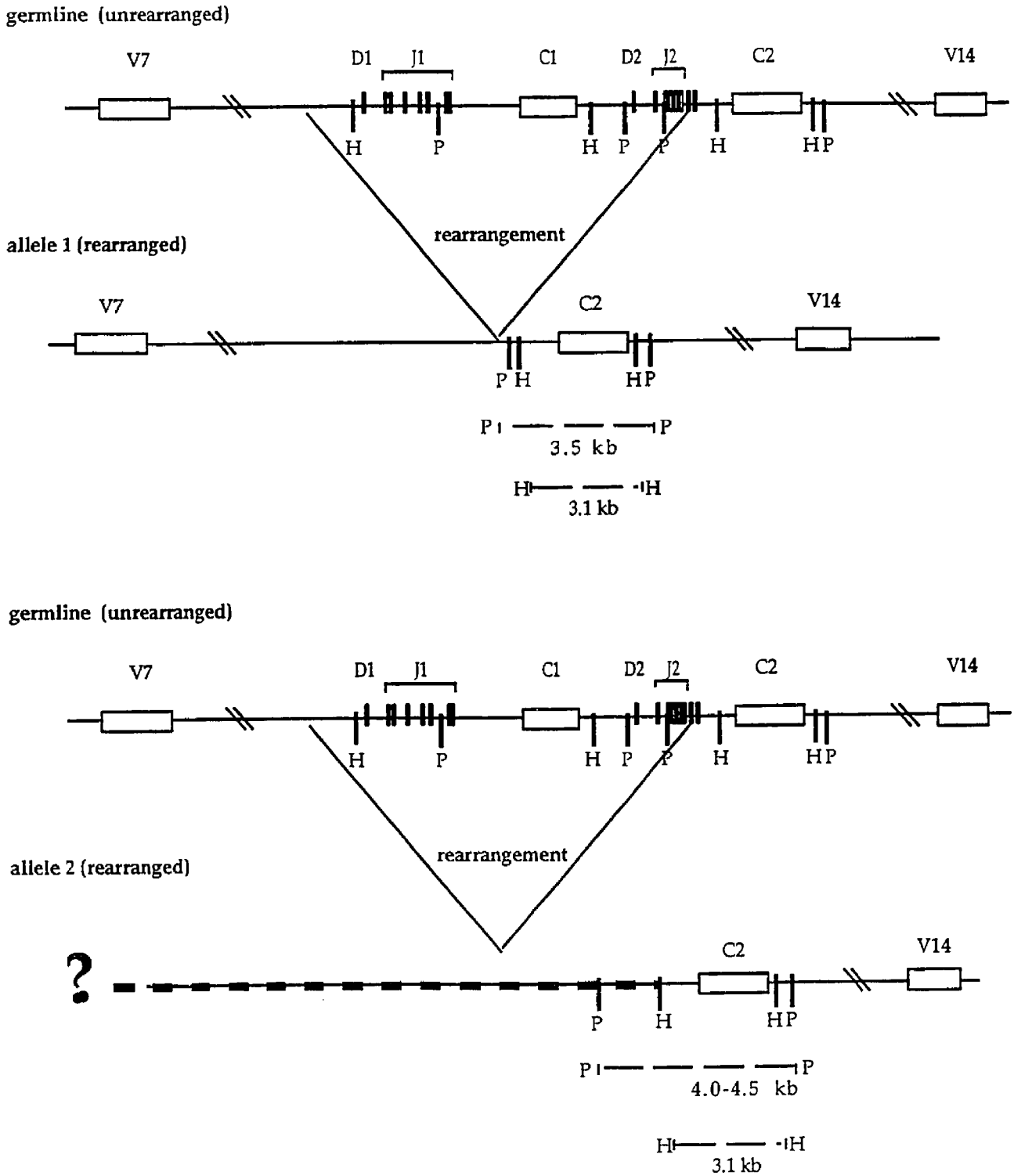
germline (unrearranged)
V7
D1
J1
C1
D2
J2
C2
V14
H
P
H
P
P
H
HP
rearrangement
allele 1 (rearranged)
V7
C2
V14
P H
HP
P
P
3.5 kb
H
H
3.1 kb
germline (unrearranged)
V7
D1
J1
C1
D2
J2
C2
V14
H
P
H
P
P
H
HP
rearrangement
allele 2 (rearranged)
?
C2
V14
P
H
HP
P
P
4.0-4.5 kb
H
H
3.1 kb

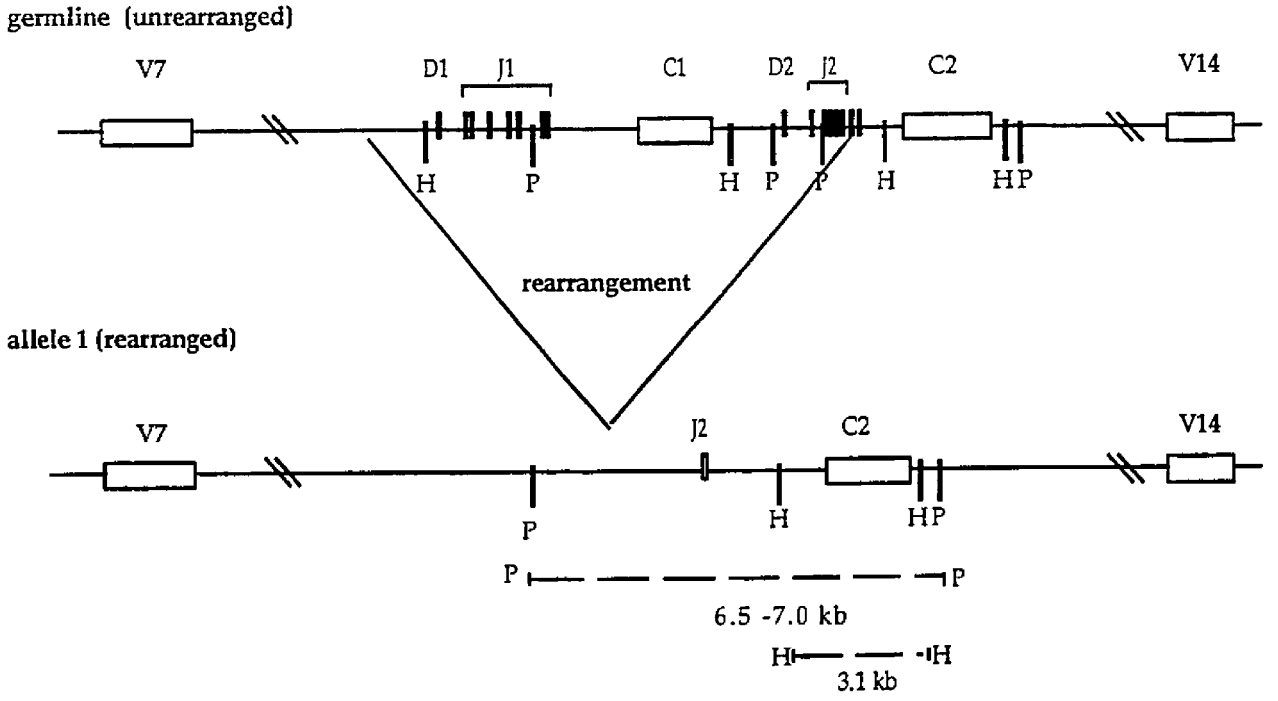
germline (unrearranged)
V7
D1
J1
C1
D2
J2
C2
V14
H
P
H
P
P
H
HP
rearrangement
allele 1 (rearranged)
V7
J2
C2
V14
P
H
HP
P
P
6.5 -7.0 kb
H
H
3.1 kb

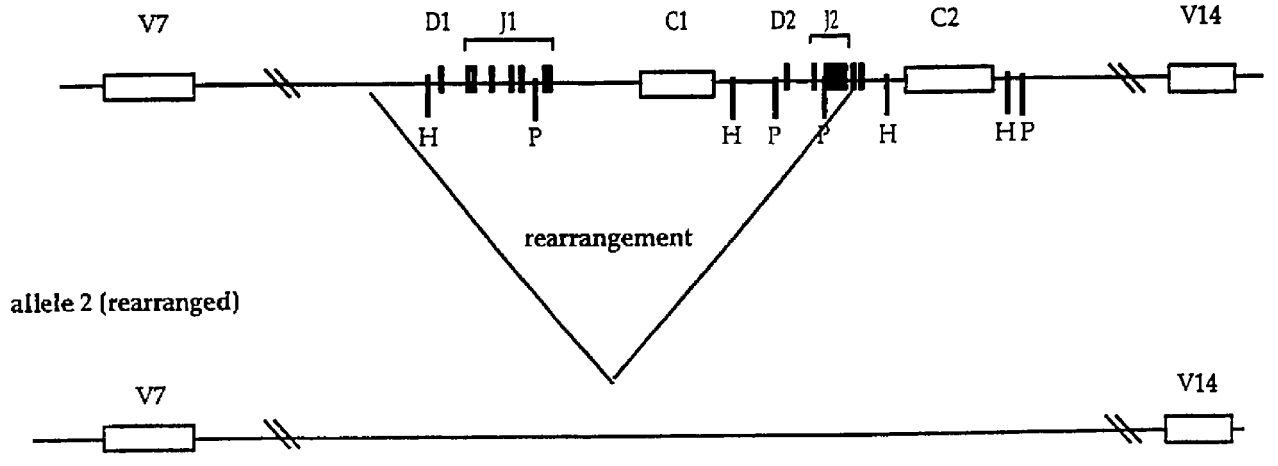
germline (unrearranged)
V7
D1
J1
C1
D2
J2
C2
V14
H
P
H
P
P
H
HP
rearrangement
allele 2 (rearranged)
V7
V14

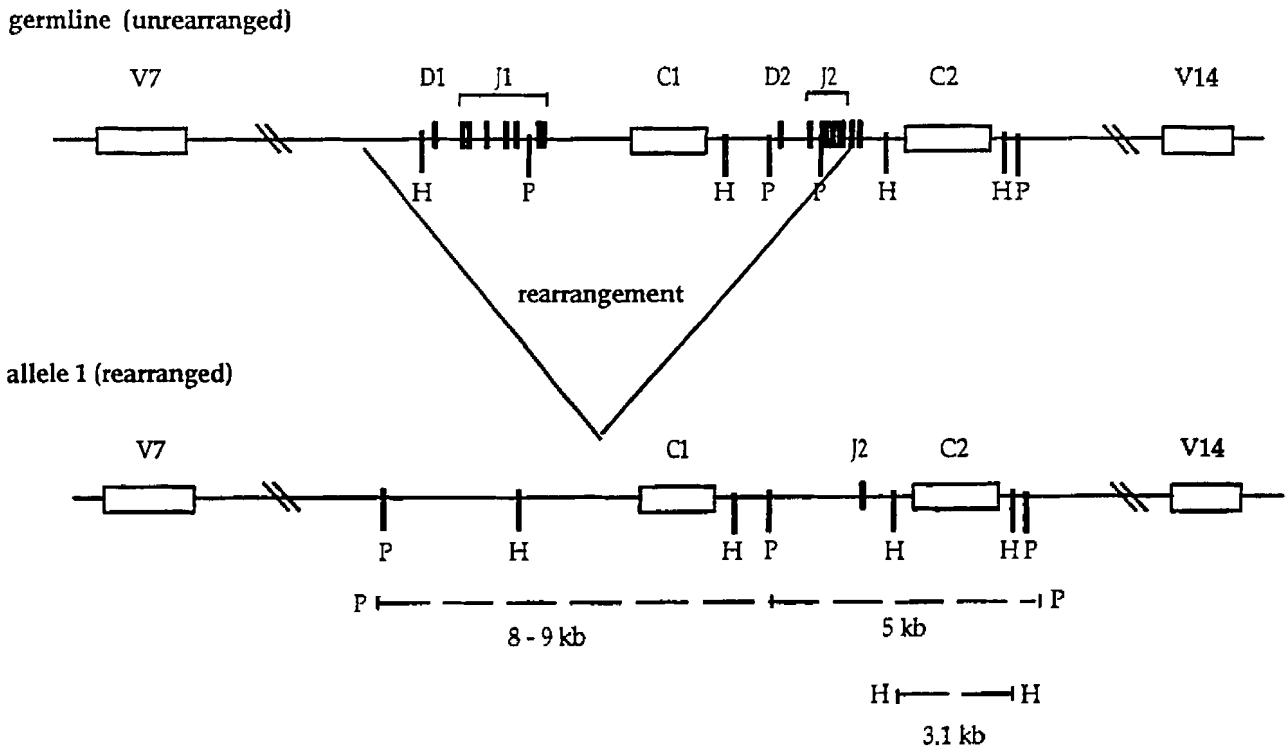
germline (unrearranged)
V7
D1
J1
C1
D2
J2
C2
V14
H
P
H
P
P
H
HP
rearrangement
allele 1 (rearranged)
V7
C1
J2
C2
V14
P
H
H
P
H
HP
P
P
8 - 9 kb
5 kb
H
H
3.1 kb

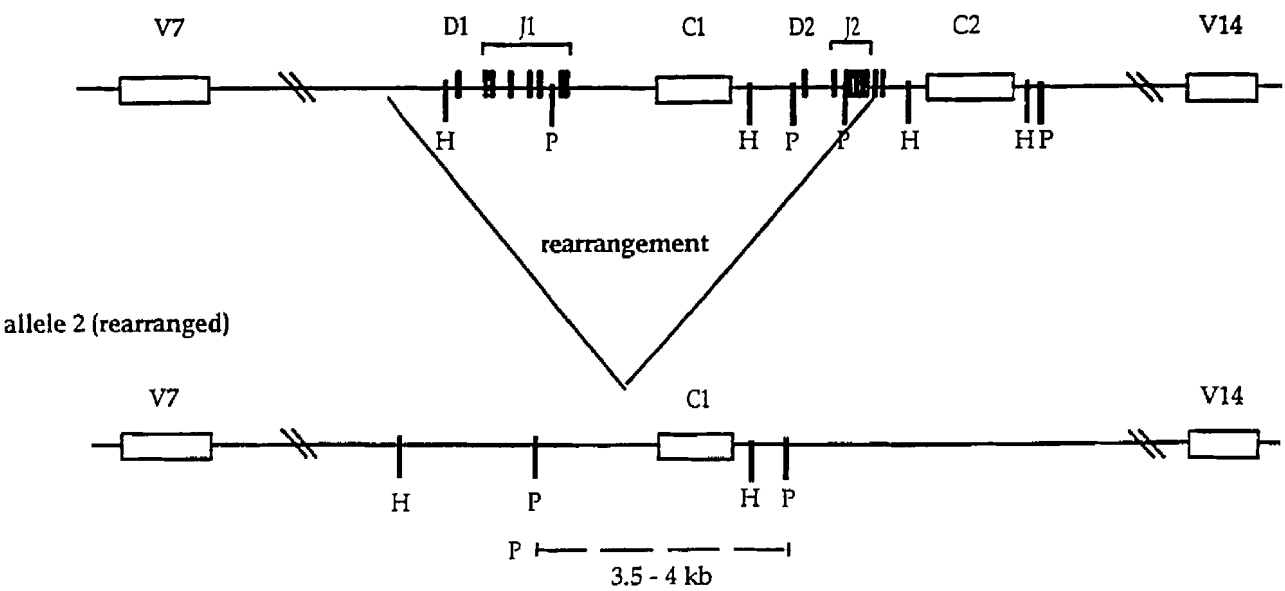
germline (unrearranged)
V7
D1
J1
C1
D2
J2
C2
V14
H
P
H
P
P
H
HP
rearrangement
allele 2 (rearranged)
V7
C1
V14
H
P
H
P
P
3.5 - 4 kb

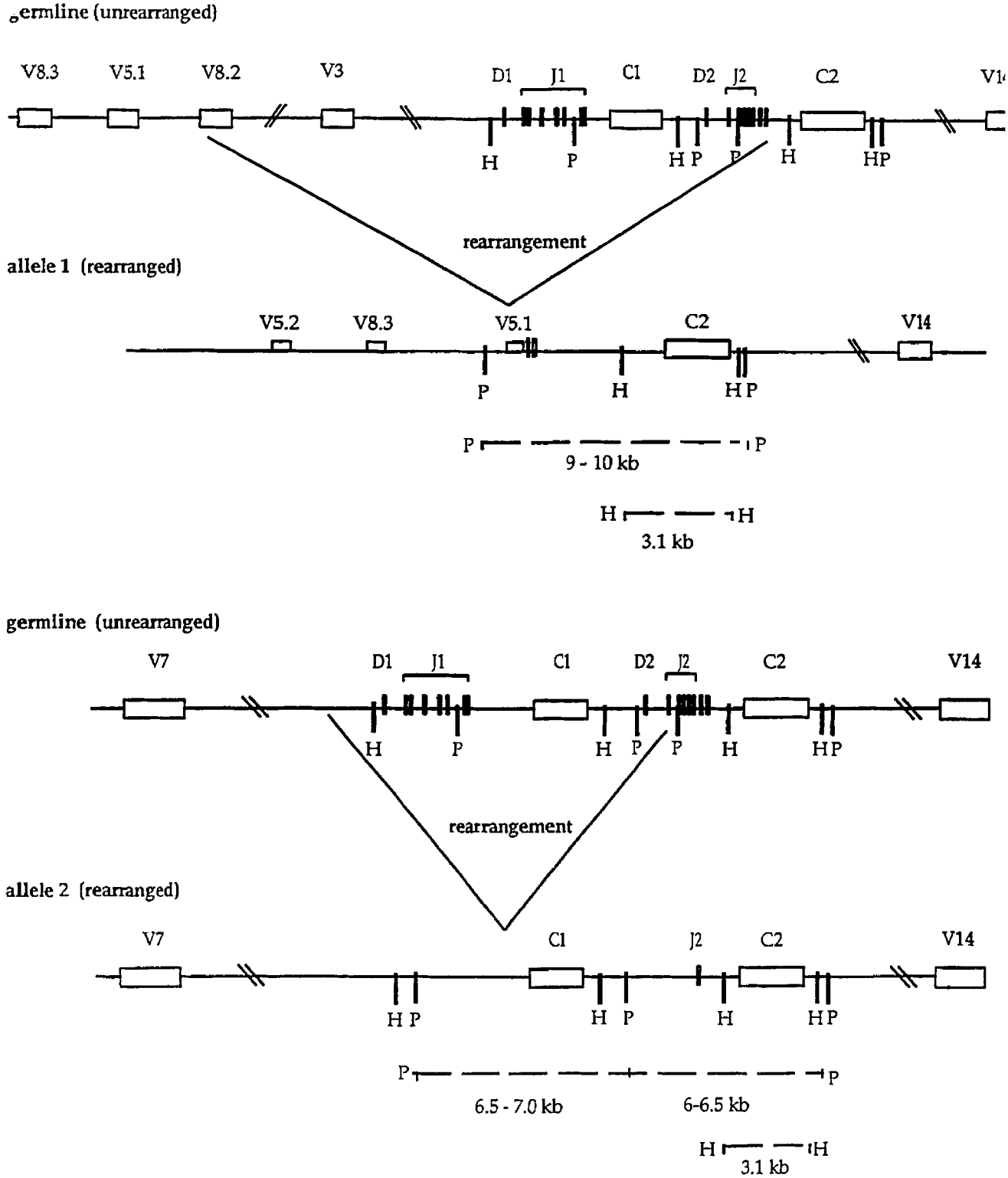
germline (unrearranged)
V8.3
V5.1
V8.2
V3
D1
J1
C1
D2
J2
C2
V14
H
P
H P
P
H
HP
rearrangement
allele 1 (rearranged)
V5.2
V8.3
V5.1
C2
V14
P
H
HP
P
P
9 - 10 kb
H
H
3.1 kb
germline (unrearranged)
V7
D1
J1
C1
D2
J2
C2
V14
H
P
H
P
P
H
HP
rearrangement
allele 2 (rearranged)
V7
C1
J2
C2
V14
H P
H
P
H
HP
P
P
6.5 - 7.0 kb
6-6.5 kb
H
H
3.1 kb

References

1. Lieber, M. R. 1991. Site-specific recombination in the immune system. *FASEB J. 5:2934.*
2. Lewis, S. M. 1994. The mechanism of V(D)J joining: lessons from molecular, immunological, and comparative analyses. *Adv. Immunol. 56:27.*
3. Tonegawa, S. 1983. Somatic generation of antibody diversity. *Nature 302:575.*
4. Oettinger, M. A., D. G. Schatz, C. Gorka, and D. Baltimore. 1990. RAG-1 and RAG-2 adjacent genes that synergistically activate V(D)J recombination. *Science 248:1517.*
5. Mombaerts, P., J. Iacomini, R. S. Johnson, K. Herrup, S. Tonegawa, and V. E. Papaioannou. 1992 RAG-1-deficient mice have no mature B and T lymphocytes. *Cell 68:869.*
6. Shinkai, Y., G. Rathbun, K.-P. Lam, E. Oltz, V. Stewart, M. Mendelsohn, J. Charron, M. Datta F. Young, A. Stall, and F. Alt. 1992. RAG-2 -deficient mice lack mature lymphocytes owing to inability to initiate V(D)J rearrangement. *Cell 68:855.*
7. van Gent, D. C., J. F. McBlane, D. A. Ramsden, M. J. Sadofsky, J. E. Hesse, and M. Gellert. 1995 Initiation of V(D)J recombination in a cell-free system. *Cell 81:925.*
8. van Gent, D. C., D. A. Ramsden, and M. Gellert. 1996. The RAG1 and RAG2 proteins establish the 12/23 rule in V(D)J recombination. *Cell 85:107.*
9. Schatz, D. G., M. A. Oettinger, and M. S. Schlissel. 1992. V(D)J recombination: molecular biology and regulation. *Ann. Rev. Immunol. 10:359.*
10. Desiderio, S. V., G. D. Yancopoulos, M. Paskind, E. Thosma, M. A. Boss, N. Landau, F. W. Alt and D. Baltimore. 1984. Insertion of N regions into heavy-chain genes is correlated with expression of terminal deoxytransferase in B cells. *Nature 311:752.*
11. Gilfillan, S., A. Dierich, M. Lemeur, C. Benoist, and D. Mathis. 1993. Mice lacking TdT: Mature animals with an immature lymphocyte repertoire. *Science 261:1175.*
12. Komori, T., A. Okada, V. Stewart, and F. W. Alt. 1993. Lack of N regions in antigen receptor variable region genes of TdT-deficient lymphocytes. *Science 261:1171.*

13. Roth, D. B., J. P. Menetski, P. Nakajima, M. Bosma, and M. Gellert. 1992. V(D)J recombination: Broken DNA molecules with covalently sealed (hairpin) coding ends in scid mouse thymocytes. *Cell 70:983.*

14. Lewis, S. M. 1994b. P nucleotide insertions and the resolution of hairpin DNA structures in mammalian cells. *Proc. Natl. Acad. Sci. USA 91:1332.*

15. Lieber, M. R., J. E. Hesse, S. Lewis, G. C. Bosma, N. Rosenber, K. Mizuuchi, M. J. Bosma, and M. Gellert. 1988. The defect in murine severe combined immune deficiency: joining of signal sequences but not coding segments in V(D)J recombination. *Cell 55:7.*

16. Bosma, G. C., R. P. Custer, and M. J. Bosma. 1983. A severe combined immunodeficiency mutation in the mouse. *Nature 301:527.*

17. Fulop, G. M., and R. A. Phillips. 1990. The *scid* mutation in mice causes a general defect in DNA repair. *Nature 347:479.*

18. Biedermann, K. A., J. Sun, A. J. Giaccia, L. M. Tosto, and J. M. Brown. 1991. scid mutation in mice confers hypersensitivity to ionizing radiation and a deficiency in DNA double-strand break repair. *Proc. Nalt. Acad. Sci. USA 88:1394.*

19. Hendrickson, E. A., X.-Q. Qin, B. E. A., D. G. Schatz, M. Oettinger, and D. T. Weaver. 1991. A link between double-strand break-related repair and V(D)J recombination: The *scid* mutation. *Proc. Natl. Acad. Sci. USA 88:4061.*

20. Disney, J., A. Barth, and L. Shultz. 1992. Defective repair of radiation-induced chromosomal damage in scid/scid mice. *Cytogenet. Cell. Genet. 59:39.*

21. Schuler, W., I. J. Weiler, A. Schuler, R. A. Phillips, N. Rosenberg, T. W. Mak, J. F. Kearney, R. P. Perry, and M. J. Bosma. 1986. Rearrangement of antigen receptor genes is defective in mice with severe combined immune deficiency. *Cell 46:963.*

22. Malynn, B. A., T. K. Blackwell, G. M. Fulop, G. A. Rathbun, A. J. Furley, P. Ferrier, L. B. Heinke, R. A. Phillips, G. D. Yancopoulos, and F. W. Alt. 1988. The scid defect affects the final step of the immunoglobulin VDJ recombinase mechanism. *Cell 54.*

23. Blackwell, T. K., B. A. Malynn, R. R. Pollock, P. Ferrier, L. R. Covey, G. M. Fulop, R. A Phillips, G. D. Yancopoulos, and F. W. Alt. 1989. Isolation of scid pre-B cells that rearrang kappa light chain genes: formation of normal signal but abnormal coding joins. *EMBO J. 8:735.*

24. Alt, F. W., E. M. Oltz, F. Young, J. Gorman, G. Taccioli, and J. Chen. 1992. VDJ recombination *Immunol. Today 13:306.*

25. Penneycook, J. L., Y. Chang, J. Celler, R. A. Phillips, and G. E. Wu. 1993. High frequency o normal DJH joints in B cell progenitors in severe combined immune deficiency mice. *J. Exp. Med 178:1007.*

26. Ferrier, P., L. R. Covey, S. C. Li, H. Suh, B. A. Malynn, T. K. Blackwell, M. A. Morrow, and F W. Alt. 1990. Normal recombination substrate Vh to DJh rearrangements in pre-B cell lines from *scid* mice. *J. Exp. Med. 171:1909.*

27. Petrini, J. H., A. M. Carroll, and M. J. Bosma. 1990. T-cell receptor gene rearrangements in functional T-cell clones from scid mice: reversion of the scid phenotype in individua lymphocyte progenitors. *Proc. Natl. Acad. Sci. USA 87:3450.*

28. Kotloff, D. B., M. J. Bosma, and N. R. Ruetsch. 1993. V(D)J recombination in peritoneal B cells o leaky scid mice. *J. Exp. Med. 178:1981.*

29. Kienker, L. J., W. A. Kuziel, B. A. Garni-Wagner, W. Kumar, and P. W. Tucker. 1991. T cel receptor γ and δ gene rearrangements in *scid* thymocytes: similarity to those in norma thymocytes. *J. Immunol. 147:4351.*

30. Schuler, W., N. R. Ruetsch, M. Amster, and M. J. Bosma. 1991. Coding joint formation o endogenous T cell receptor genes in lymphoid cells from *scid* mice: unusual P-nucleotid additions in VJ-coding joints. *Eur. J. Immunol. 21:589.*

31. Okazaki, K., S. I. Nishikawa, and H. Sakano. 1988. Aberrant immunoglobulin gen rearrangement in scid mouse marrow cells. *J. Immunol. 141:1348.*

32. Kim, M., W. Schuler, M. J. Bosma, and K. B. Marcu. 1988. Abnormal recombination of Igh D and gene segments in transformed pre-B cells of scid mice. *J. Immunol. 141:1341.*

33. Blunt, T., N. J. Finnie, G. E. Taccioli, G. C. M. Smith, J. Demengeot, T. M. Gottleib, R. Mizuta, A. J. Varghese, F. W. Alt, P. A. Jeggo, and S. P. Jackson. 1995. Defective DNA-dependent protein kinase activity is linked to V(D)J recombination and DNA repair defects associated with the murine *scid* mutation. *Cell 80:813.*

34. Kirchgessner, C. U., C. K. Patil, J. W. Evans, C. A. Cuomo, L. M. Fried, T. Carter, M. A. Oettinger, and J. M. Brown. 1995. DNA-dependent kinase (p350) as a candidate gene for the murine SCID defect. *Science 267:1178.*

35. Peterson, S. R., A. Kurimasa, M. Oshimura, W. S. Dynan, E. M. Bradbury, and D. J. Chen. 1995. Loss of catalytic subunit of the DNA-dependent protein kinase in DNA double-strand break repair mutant mammalian cells. *Proc. Natl. Acad. Sci. USA 92:3171.*

36. Hartley, K. O., D. Gell, G. C. M. Smith, H. Zhang, N. Divecha, M. A. Connelly, A. Admon, S. P. Lees-Miller, C. W. Anderson, and S. P. Jackson. 1995. DNA-dependent protein kinase catalytic subunit A relative of phosphatidylinositol 3-kinase and the ataxia telangiectasia gene product. *Cell 82:849.*

37. Gottlieb, T. M., and S. P. Jackson. 1993. The DNA-dependent protein kinase: requirement for DNA ends and association with Ku antigen. *Cell 72:131.*

38. Gottlieb, T. M., and S. P. Jackson. 1994. Protein kinases and DNA damage. *Trends in Biochem. Sci. 19:500.*

39. Anderson, C. W. 1993. DNA damage and the DNA-activated protein kinase. *Trens Biochem. Sci. 18:433.*

40. Danska, J. S., D. P. Holland, S. Mariathasan, K. M. Williams, and C. J. Guidos. 1996. Biochemical and genetic defects in the DNA-dependent protein kinase in murine *scid* lymphocytes. *Mol. Cell Bio. 16:5507.*

41. Boubnov, N. V., and D. T. Weaver. 1995. scid cells are deficient in Ku and replication protein A phosphorylation by DNA-dependent protein kinase. *Mol. Cell Bio. 15:5700.*

42. Blunt, T., D. Gell, M. Fox, G. E. Taccioli, A. R. Lehmann, S. P. Jackson, and P. A. Jeggo. 1996. Identification of a nonsense mutation in the carboxy-terminal region of DNA-dependent protein kinase catalytic subunit in the *scid* mouse. *Proc. Natl. Acad. Sci. USA 93:10285.*

43. Godfrey, D. I., J. Kennedy, P. Mombaerts, S. Tonegawa, and A. Zlotnik. 1994. Onset of TCRβ rearrangement and role of TCRβ expression during CD3-CD4-CD8- thymocyte differentiation. *J. Immunol. 152:4783.*

44. Dudley, E. C., H. T. Petrie, L. M. Shah, M. J. Owen, and A. C. Hayday. 1994. T cell receptor beta chain gene rearrangement and selection during thymocyte development. *Immunity 1:83.*

45. Saint-Ruf, C., K. Ungewiss, M. Groettrup, L. Bruno, H. J. Fehling, and H. von Boehmer. 1994. Analysis and expression of a cloned pre-T cell receptor gene. *Science 266:1208.*

46. Groettrup, M., and H. von Boehmer. 1993. A role for a pre-T-cell receptor in T-cell development. *Immunol. Today 14:6101.*

47. Ehlich, A., S. Schaal, H. Gu, D. Kitamura, W. Muller, and Rajewsky. 1993. Immunoglobulin heavy and light chain genes rearrange independently at early stages of B cell development. *Cell 72:695.*

48. Reth, M. G., E. Petrac, P. Wiese, L. Lobel, and F. W. Alt. 1987. Activation of Vκ gene rearrangement in pre-B cells follows the expression of membrane-bound immunoglobulin heavy chains. *EMBO J. 6:3299.*

49. Iglesias, A., M. Kopf, G. S. Williams, B. Buhler, and G. Kohler. 1991. Molecular requirements for the μ-induced light chain gene rearrangement in pre-B cells. *EMBO J. 10:2147.*

50. Tsubata, T., R. Tsubata, and M. Reth. 1992. Crosslinking of the cell surface immunoglobulin (μ-surrogate light chains complex) on pre-B cells induces activation of V gene rearrangements at the immunoglobulin κ locus. *Int. Immunol. 4:637.*

51. Melchers, F., H. Karasuyama, D. Haasner, S. Bauer, A. Kudo, N. Sakaguchi, B. Jameson, and A. Rolink. 1993. The surrogate light chain in B-cell development. *Immunol. Today 14:60.*

52. Pearse, M., L. Wu., M. Egerton, A. Wilson, K. Shortman, and R. Scollay. 1989. A murine early thymocyte developmental sequence is marked by transient expression of the interleukin-2-receptor. *Proc. Natl. Acad. Sci. USA 86:1614.*

53. Kishi, H., P. Borgulya, B. Scott, K. Karjalainen, A. Traunecker, J. Kaufman, and H. Von Boehmer. 1991. Surface expression of the β T cell receptor (TCR) chain in the absence of other TCR or CD3 proteins on immature T cells. *EMBO J. 10.*

54. Siu, G., M. Kronenberg, E. Strauss, R. Haars, T. W. Mak, and L. Hood. 1984. The structure, rearrangement and expression of Dβ gene segments of the murine T-cell antigen receptor. *Nature 311:344.*

55. Born, W., J. Yague, E. Palmer, J. Kappler, and P. Marrack. 1985. Rearragement of the T-cell receptor β-chain genes during T cell development. *Proc. Natl. Acad. Sci. USA 82:2925.*

56. Born, W., M. McDuffie, N. Roehm, E. Kushnir, J. White, D. Thorpe, J. Stefano, J. Kappler, and P. Marrack. 1987. Expression and role of the T cell receptor in early thymocyte differentiation in vitro. *J. Immunol. 138:999.*

57. Mombaerts, P., A. Clarke, M. Rudnicki, J. Iacomini, S. Itohara, J. Lafaille, L. Wang, Y. Ichikawa, R. Jaenisch, M. Hooper, and S. Tonegawa. 1992b. Mutations in T-cell antigen receptor genes α and β block thymocyte development at different stages. *Nature 360:225.*

58. Shinkai, Y., S. Koyasu, K.-I. Nakayama, K. Murphy, D. Loh, E. Reinherz, and F. Alt. 1993. Restoration of T cell development in RAG-2-deficient mice by functional TCR transgenes. *Science 259:822.*

59. Spanopoulou, E., C. Roman, L. Corcoran, M. Schlissel, D. Silver, D. Nemazee, M. Nussenzweig, S. Shinton, R. Hardy, and D. Baltimore. 1994. Functional immunoglobulin transgenes guide ordered B cell differentiation in RAG-1 -deficient mice. *Genes Dev. 8:1030.*

60. Karasuyama, H., A. Rolink, Y. Shinkai, F. Young, F. W. Alt, and F. Melchers. 1994. The expression of Vpre-B/λ5 surrogate light chain in early bone marrow precursor B cells of normal and B cell-deficient mutant mice. *Cell 77:133.*

61. Danska, J. S., F. Pflumio, C. Williams, O. Huner, J. E. Dick, and C. J. Guidos. 1994. Rescue of T cell-specific V(D)J recombination in SCID mice by DNA-damaging agents. *Science 266:450.*

62. Murphy, W. J., S. K. Durum, M. R. Anver, D. K. Ferris, D. W. McVicar, J. J. O'Shea, S. K. Ruscetti, M. R. Smith, H. A. Young, and D. L. Longo. 1994. Induction of T cell differentiation and lymphomagenesis in the thymus of mice with severe combined immune deficiency (SCID). *J. Immunol. 153:1004.*

63. Livac, F., S. C. Welsh, G. C.J., I. N. Crispe, J. S. Danska, and D. G. Schatz. 1996. Transient restoration of gene rearrangement at multiple T cell receptor loci in γ-irradiated *scid* mice. *J. Exp. Med. 184:419.*

64. Bogue, M. A., C. Zhu, E. Aguilar-Cordova, L. A. Donehower, and D. B. Roth. 1996. p53 is required for both radiation-induced differentiation and rescue of V(D)J rearrangement in *scid* mouse thymocytes. *Genes Dev. 10:553.*

65. Rabbitts, T. H. 1994. Chromosomal translocations in human cancer. *Nature 372:143.*

66. Kaplan, H. S. 1967. On the natural history of the murine leukemias: Presidential address. *Cancer Res. 27:1325.*

67. Cuypers, H., G. Selten, W. Quint, M. Zijlstra, E. Maandag, W. Boelens, P. van Wezenbeek, C. Melief, and A. Berns. 1984. Murine leukemia virus-induced T-cell lymphomagenesis: Integration of proviruses in a distinct chromosomal region. *Cell 37:141.*

68. Selten, G., H. Cuypers, and A. Berns. 1985. Proviral activation of the putative oncogene *pim-1* in MuLV-induced T cell lymphomas. *EMBO J. 4:1793.*

69. Voronova, A. F., and B. M. Sefton. 1986. Expression of a new tyrosine protein kinase is stimulated by retrovirus promoter insertion. *Nature 319:682.*

70. Lieberman, M., G. A. Hansteen, J. M. McCune, M. L. Scott, J. H. White, and I. L. Weissman. 1987. Indirect induction of radiation lymphomas in mice. *J. Exp. Med. 166:1883.*

71. Hermans, A., N. Heisterkamp, M. von Lindern, S. van Baal, D. Meijer, D. van der Plas, L. M. Wiedemann, J. Groffen, D. Bootsma, and G. Grosveld. 1987. Unique fusion of *bcr* and *c-abl* genes in philadelphia chromosome positive acute lymphoblastic leukemia. *Cell 51:33.*

72. Konopka, J. B., S. M. Watanabe, and W. O.N. 1984. An alteration of the human c-abl protein in K562 leukemia cells unmasks associated tyrosine-kinase activity. *Cell 51:33.*

73. Kamps, M. P., C. Murre, X. Sun, and D. Baltimore. 1990. A new homeobox gene contributes the DNA binding domain of the t(1;19) translocation protein in Pre-B ALL. *Cell 60:547.*

74. Nourse, J., J. D. Mellentin, N. Galili, J. Wilkinson, E. Stanbridge, S. D. Smith, and M. L. Cleary. 1990. Chromosomal translocation t(1;19) results in synthesis of a homeobox fusion mRNA that codes for a potential chimeric transcription factor. *Cell 60:535.*

75. Leiden, J. M. 1993. Transcriptional regulation of T cell receptor genes. *Annu. Rev. Immunol. 11:539.*

76. Zech, L., U. Haglund, K. Nilsson, and G. Klein. 1976. Characteristic chromosomal abnormalities in biopsies and lymphoid-cell lines from patients with Burkitt and non-Burkitt lymphomas. *Int. J. Cancer 17:47.*

77. Dalla-Favera, R., M. Bregni, J. Erikson, D. Patterson, R. C. Gallo, and C. M. Croce. 1982. Human c-myc onc gene is located on the region of chromosome 8 that is translocated in Burkitts lymphoma cells. *Proc. Natl. Acad. Sci. USA 79:7824.*

78. Erikson, J., J. Finan, P. C. Nowell, and C. M. Croce. 1982. Translocation of immunoglobulin VH genes in Burkitt lymphoma. *Proc. Natl. Acad. Sci. U.S.A. 79:5611.*

79. Tycko, B., S. Smith, and J. Sklar. 1991. Chromosomal translocations joining LCK and TCRB loci in human T cell leukemia. *J. Exp. Med. 174:867.*

80. Davey, M., V. Bertness, K. Nakahara, J. Johnson, O. McBride, T. Waldmann, and I. L. Kirsch. 1988. Juxtaposition of the T cell receptor α-chain locus (14q11) and a region (14q32) of potential importance in leukemogensis by a 14;14 translocation in a patient with T-cell chronic lymphocytic leukemia and ataxia-telangiectasis. *Proc. Natl. Acad. Sci. USA 85:9287.*

81. Begley, C. G., A. P.D., M. P. Davey, K. Nakahara, K. Tchorz, J. Kurtzberg, M. S. Hershfield, B. F. Haynes, D. I. Cohen, T. A. Waldmann, and I. R. Kirsch. 1989b. Chromosomal translocation in a human leukemia stem-cell line disrupts the T-cell antigen receptor d-chain diversity region and results in a previously unreported fusion transcript. *Proc. Natl. Acad. Sci. USA 86:2031.*

82. Finger, L. R., J. Kagan, G. Christopher, J. Kurtzberg, M. S. Hershfield, P. C. Nowell, and C. M. Croce. 1989. Involvement of the TCL5 gene on human chromosome 1 in T-cell leukemia and melanoma. *Proc. Natl. Acad. Sci. USA 86:5039.*

83. Aplan, P. D., D. P. Lomardi, A. M. Ginsberg, J. Cossman, V. L. Bertness, and I. R. Kirsch. 1990. Disruption of the Human SCL Locus by "Illegitimate" V-(D)-J Recombinase Activity. *Science 250:1426.*

84. Elisen, L. W., J. Bird, D. C. West, A. L. Soreng, T. C. Reynolds, S. D. Smith, and J. Sklar. 1991. TAN-1, the human homolog of the drosophila notch gene, is broken by chromosomal translocations in T lymphoblastic neoplasms. *Cell 66:649.*

85. Fitzgerald, T. J., N. G.A.M., S. C. Raimondi, and R. M. Goorha. 1991. *c-tal*, a helix-loop-helix protein, is juxtaposed to the T-cell receptor-β chain gene by a reciprocal translocation: t(1;7)(p32;q35). *Blood 78:2686.*

86. Cuomo, C. A., C. L. Mundy, and M. A. Oettinger. 1996. DNA sequence and structure requirements for cleavage of V(D)J recombination signal sequences. *Mol. Cell Bio. 16:5683.*

87. Reynolds, T. C., S. D. Smith, and J. Sklar. 1987. Analysis of DNA surrounding the breakpoints of chromosomal translocations involving the β T cell receptor gene in human lymphoblastic neoplasms. *Cell 50:107.*

88. Cleary, M., J. Mellentin, J. Spies, and S. Smith. 1988. Chromosomal translocation involving the β T cell receptor gene in acute leukemia. *J. Exp. Med. 167:682.*

89. Bernard, O., N. Lecointe, P. Jonveaux, M. Souyri, M. Mauchauffe, R. Berger, C. J. Larsen, and M.-M. D. 1991. Two Site-Specific Deletions and t(1;14) Translocation Restricted to Human T-Cell Acute Leukemias Disrupt the 5' Part of the *tal-1* Gene. *Oncogene 6:1477.*

90. Ye, B. H., S. Chaganti, C. C. Chang, H. Niu, P. Corradini, R. S. K. Chaganti, and R. Dalla-Favera. 1995. Chromosomal translocations cause deregulated BCL6 expression by promoter substitution in B cell lymphoma. *EMBO J. 14:6209.*

91. Begley, C. G., P. D. Aplan, S. M. Denning, B. F. Haynes, T. A. Waldmann, and I. R. Kirsch. 1989. The gene SCL is expressed during early hematopoiesis and encodes a differentiation-related DNA binding motif. *Proc. Natl. Acad. Sci. USA 86:10128.*

92. Aplan, P. D., D. P. Lombardi, and I. R. Kirsch. 1991. Structural Characterization of *SIL*, a Gene Frequently Disrupted in T-Cell Acute Lymphoblastic Leukemia. *Mol. Cell. Bio. 11:5462.*

93. Guidos, C. J., C. J. Williams, G. E. Wu, C. J. Paige, and J. S. Danska. 1995. Development of CD4+CD8+ thymocytes in RAG-deficient mice Through a T cell receptor β chain-independent pathway. *J. Exp. Med. 181:1187.*

94. Zuniga-Pflucker, J. C., D. Jiang, P. L. Schwartzberg, and M. J. Lenardo. 1994. Sublethal γ-irradiation induces differentiation of $CD4^-/CD8^-$ into $CD4^+/CD8^+$ thymocytes without T cell receptor β rearrangement in recombinase activation gene 2-/- mice. *J. Exp. Med. 180:1517.*

95. Fox, C. J., and J. S. Danska. 1997. IL-4 expression at the onset of islet inflammation predicts nondestructive insulitis in nonobese diabetic mice. *J. Immunol. 158:2414.*

96. Chien, Y., D. M. Becker, T. Lindsten, M. Okamura, D. I. Cohen, and M. M. Davis. 1984. A third type of murine T-cell receptor gene. *Nature 312:31.*

97. Galley, K. A., and J. S. Danska. 1995. Peri-islet infiltrates of young non-obese diabetic mice display restricted TCR β-chain diversity. *J. Immunol. 154:2969.*

98. Hurwitz, J., J. Samaridis, and J. Pelkonen. 1989. Immature and advanced patterns of T cell receptor gene rearrangement among lymphocytes in splenic culture. *J. Immunol. 142:2533.*

99. Hedrick, S. M., D. I. Cohen, E. A. Nielsen, and M. M. Davis. 1984. Isolation of cDNA clones encoding T cell-specific membrane-associated proteins. *Nature 308:149.*

100. Groves, T., P. Katis, Z. Madden, K. Manickam, D. Ramsden, G. Wu, and C. J. Guidos. 1995. In vitro maturation of clonal CD4+CD8+ cell lines in response to TCR engagement. *J. Immunol. 154:5011.*

101. Lieberman, M., G. A. Hansteen, J. M. McCune, M. L. Scott, J. H. White, and I. L. Weissman. 1987. Indirect induction of radiation lymphomas in mice. Evidence for a novel, transmissible leukemogen. *J. Exp. Med. 166:1883.*

102. Leo, O., M. Foo, D. H. Sachs, L. E. Samelson, and J. A. Bluestone. 1987. Identification of a monoclonal antibody specific for a murine CD3 polypeptide. *Proc. Natl. Acad. Sci. USA 84:1374.*

103. Guidos, C. J., C. J. Williams, I. Grandal, G. Knowles, M. T. F. Huang, and J. S. Danska. 1996. V(D)J recombination activates a p53-dependent DNA damage checkpoint in *scid* lymphocyte precursors. *Genes Dev. 10:2038.*

104. Cobbold, S. P., A. Jayasuriya, A. Nash, T. D. Prospero, and H. Waldmann. 1984. Therapy with monoclonal antibodies by elimination of T-cell subsets in vivo. *Nature 312:548.*

105. Kubo, R. T., W. Born, J. W. Kappler, P. Marrack, and M. Pigeon. 1989. Characterization of a monclonal antibody which detects all murine αβ T cell receptors. *J. Immunol. 142:2736.*

106. Ortega, G., R. J. Robb, E. M. Shevach, and T. R. Malek. 1984. The murine IL 2 receptor. I. Monoclonal antibodies that define distinct functional epitopes on activated T cells and react with activated B cells. *J. Immunol. 133:1970.*

107. Kanagawa, O., Y. Utsunomiya, J. Bill, E. Palmer, M. W. Moore, and F. R. Carbone. 1991. Conformational difference of a T cell antigen receptor revealed by monoclonal antibodies to mouse Vβ5 T cell receptor antigen determinants. *J. Immunol. 147:1307.*

108. Guidos, C. J., J. S. Danska, C. G. Fathman, and I. L. Weissman. 1990. T cell receptor-mediated negative selection of autoreactive T lymphocyte precursors occurs after commitment to the CD4 or CD8 lineages. *J. Exp. Med. 172:835.*

109. Maniatis, T., E. F. Fritsch, and J. Sambrook. 1982. *Molecular cloning, A laboratory manual.* Cold Spring Harbor Laboratory Press, Cold Spring Harbor, NY.

110. Gubler, U., and B. J. Hoffman. 1983. A simple and very efficient method for generating cDNA libraries. *Gene (Amst.) 25:263.*

111. Sanger, F., S. Nicklen, and A. R. Coulson. 1977. DNA sequencing with chain-terminating inhibitors. *Proc. Natl. Acad. Sci. U.S.A. 74:5463.*

112. Altschul, S. F., W. Gish, W. Miller, E. W. Myers, and D. J. Lipman. 1990. Basic local alignment search tool. *J. Mol. Biol. 215:403.*

113. Southern, E. 1975. Detection of specific sequences among DNA fragements separated by gel electrophoresis. *J. Mol. Bio. 98:503.*

114. Rabbitts, P., H. Impey, A. Heppell-Parton, C. Langford, C. Tease, N. Lowe, D. Bailey, M. Ferguson-Smith, and N. Carter. 1995. Chromosome specific paints from a high resolution flow karyotype of the mouse. *Nature Genetics 9:369.*

115. Telenius, H., A. H. Pelmear, A. Tunnacliffe, N. P. Carter, A. Behmel, M. A. Ferguson-Smith, M. Nordenskjold, R. Pfragner, and B. A. J. Ponder. 1992. Cytogenetic analysis by chromosome painting using DOP-PCR amplified flow-sorted chromosomes. *Genes Chrom. and Cancer 4:257.*

116. Muto, M., E. Kubo, and T. Sado. 1987. Development of prelymphoma cells committed to thymic lymphomas during radiation-induced thymic lymphomagenesis in B10 mice. *Cancer Res. 47:3469.*

117. Kubo, E., M. Muto, T. Sado, S. Takeshita, T. Shimizu, and H. Yamagishi. 1992. Novel TCR gene rearrangements and expression in radiation-induced thymic lymphomas. *J. of Rad. Res. 33:227.*

118. Shimizu, T., M. Muto, E. Kubo, T. Sado, and H. Yamagishi. 1993. Mutiple pre-neoplastic events and clonal selection of radiation induced mouse thymic lymphomas shown by TCR gene rearrangements. *Leuk. Res. 17:959.*

119. Baer, R., K.-C. Chen, S. Smith, and T. Rabbitts. 1985. Fusion of an immunoglobulin variable region and a T cell receptor constant gene in the chromosome 14 inversion associated with T cell tumors. *Cell 43:705.*

120. Denny, C., Y. Yoshikai, T. W. Mak, S. Smith, G. Hollis, and I. R. Kirsch. 1986. A chromosome 14 inversion in a T cell lymphoma is caused by site-specific recombination between immunoglubuling and T cell receptor loci. *Nature 320:549.*

121. Cleary, M. L., S. D. Smith, and J. Sklar. 1986. Cloning and structural analysis of cDNAs for bcl-2 and a hybrid bcl-2/immunoglobulin transcript resulting from the t(14;18) translocation.. *Cell 47:19.*

122. Lipkowitz, S., M.-H. Stern, and I. R. Kirsch. 1990. Hybrid T cell receptor genes formed by interlocus recombination in normal and Ataxia-telangiectasia lymphocytes. *J. Exp. Med. 172:409.*

123. Raulet, D. H., R. D. Garman, H. Saito, and S. Tonegawa. 1985. Developmental regulation of T-cell receptor gene expression. *Nature 314:103.*

124. Snodgrass, H. R., Z. Dembic, M. Steinmetz, and H. von Boehmer. 1985. Expression of T-cell antigen receptor genes during fetal development in the thymus. *Nature 315:232.*

125. Kronenberg, M., J. Goverman, R. Haars, M. Malissen, E. Kraig, L. Phillips, T. Delovitch, N. Suciu-Foca, and L. Hood. 1985. Rearrangement and transcription of the β-chain genes of the T-cell antigen receptor in different types of murine lymphocytes. *Nature 313:647.*

126. Malissen, M., C. McCoy, D. Blanc, J. Trucy, C. Devaux, A. M. Schmitt-Verhulst, F. Fitch, L. Hood, and B. Malissen. 1986. Direct evidence for chromosomal inversion during T-cell receptor beta- gene rearrangements. *Nature 319:28.*

127. Carter, N. P. 1994. Cytogenetic analysis by chromosome painting. *Cytometry 18:2.*

128. Smith, C. L., P. W. Warburton, A. Gaal, and C. R. Cantor. 1986. Analysis of genome organization and rearrangements by pulsed field gel electrophoresis. *Genetic Engineering 8:45.*

129. van Omnen, G. J. B., J. M. H. Verkerk, M. H. Hofker, A. P. Monaco, L. M. Kunkel, P. Ray, R. Worton, B. Wieringa, E. Bakker, and P. L. Pearson. 1986. A physical map of 4 billion bp around the Duchenne muscular dystrophy gene on the human X-chromosome. *Cell 47:499.*

130. Compton, D. A., M. W. Weil, C. Jones, V. M. Riccardi, L. C. Strong, and G. F. Saunders. 1988. Long range physical map of the Wilm's tumour-Aniridia region on human chromosome 11. *Cell 55:827.*

131. Hermann, B. G., D. P. Barlow, and H. Lehrach. 1987. A large inverted duplication allows homologous recombination between chromosomes heterozygous for the proximal t complex inversion. *Cell 48:813.*

132. Lindsten, T., N. E. Lee, and M. M. Davis. 1987. Organization of the T-cell antigen-receptor B locus in mice. *Proc. Natl. Acad. Sci. USA 84:7639.*

133. Chou, H. S., C. A. Nelson, S. A. Godambe, D. D. Chaplin, and D. Y. Loh. 1987. Germline organization of the murine T cell receptor β-chain genes. *Science 238:545.*

134. Yang, C. C., and M. D. Topal. 1992. Nonidentical DNA-binding sites of endonuclease NaeI recognize different families of sequences flanking the recognition site. *Biochemistry 31:9657.*

135. Beecham, E. J., G. M. Jones, C. Link, K. Huppi, M. Potter, J. F. Mushinski, and V. A. Bohr. 1994. DNA repair defects associated with chromosomal translocation breaksite regions. *Mol. Cell. Biol.Mol Cell Biol 14:1204.*

136. Beecham, E. J., J. F. Mushinsski, E. Shacter, M. Potter, and V. A. Bohr. 1991. DNA repair in the c-myc proto-oncogene; possible involvement in a susceptibilty or resistance to plasmacytoma induction in BALB/c mice. *Mol. Cell Bio. 11:3095.*

137. Nadel, B., and A. J. Feeney. 1995. Influence of coding-end sequence on coding-end processing in V(D)J recombination. *J. Immunol. 155:4322.*

138. Schuler, W., A. Schuler, G. G. Lennon, G. C. Bosma, and M. J. Bosma. 1988. Transcription of unrearranged antigen receptor genes in *scid* mice. *EMBO J. 7:2019.*

139. Furley, A. J., S. Mizutani, K. Weilbaecher, H. S. Dhaliwal, A. M. Ford, L. C. Chan, H. V. Molgaard, B. Toyonaga, T. Mak, P. van den Elsen, D. Gold, C. Terhorst, and M. F. Greaves. 1986. Developmentally regulated rearrangement and expression of genes encoding the T cell receptor-T3 complex. *Cell 46:75.*

140. Woodland, D. L., B. L. Kotzin, and E. Palmer. 1990. Functional consequences of a T cell receptor Dβ2 and Jβ2 gene segement deletion. *J. Immunol. 144:379.*

141. Kotzin, B. L., V. L. Barr, and E. Palmer. 1985. A large deletion within the T-cell receptor beta-chain gene complex in New Zealand white mice. *Science 229:167.*

142. Jacobs, H., F. Ossendorp, E. de Vries, K. Ungewiss, H. von Boehmer, J. Borst, and A. Berns. 1996a. Oncogenic potential of a pre-T cell receptor lacking the TCRβ variable domain. *Oncogene 12:2089.*

143. Jacobs, H., J. Iacomini, M. van de Ven, S. Tonegawa, and A. Berns. 1996b. Domains of the TcRb-chain required for early thymocyte development. *J. Exp. Med. 184:1833.*

144. Kraker, W. J., T. J. Borell, C. R. Schad, M. J. Pennington, P. S. Karnes, G. W. Dewald, and R. B. Jenkins. 1992. Fluorescent in situ hybridization: use of whole chromosome paint probes to identify unbalanced chromosome translocations. *Mayo Clin. Proc. 67:658.*

145. Jenkins, R. B., M. M. Le Beau, W. J. Kraker, T. J. Borell, P. G. Stalboerger, E. M. Davis, L. Penland, A. Fernald, R. Espinosa, D. J. Schaid, and e. al. 1992. Fluorescence in situ hybridization: a sensitive method for trisomy 8 detection in bone marrow specimens. *Blood 79:3307.*

146. Poirel, H., H. Rack, E. Delabesse, I. Radford-Weiss, X. Troussard, C. Debert, D. Leboeuf, C. Bastard, F. Picard, A. Veil-Buzyn, G. Flandrin, O. Bernard, and E. Macintyre. 1996. Incidence and characterization of MLL gene (11q23) rearrangements in acute myeloid leukemia M1 and M5. *Blood 87:2496.*

147. Los, F. J., D. Van Opstal, M. P. Schol, J. L. Gaillard, H. Brandenburg, A. M. Van Den Ouweland, and P. A. Veld. 1995. Prenatal diagnosis of mosaic tetrasomy 12p/trisomy 12p by fluorescent in situ hybridization in amniotic fluid cells; a case report of Pallister-Killian syndrome. *Prenatal Diagnosis 15:1155.*

148. Collins, C., W. L. Kuo, R. Segraves, J. Fuscoe, D. Pinkel, and G. J.W. 1991. Construction and characterization of plasmid libraries enriched in sequences from single human chromosomes. *Genomics 11:997.*

149. Ibberson, M. R., J. P. Copier, and A. K. So. 1995. Genomic organization of the human T-cell receptor variable alpha (TCRAV) gene cluster. *Genomics 28:131.*

150. Timmerman, V., A. Lofgren, E. Le Guern, P. Liang, P. De Jonghe, J. J. Martin, D. Verhalle, W. Robberecht, R. Gouider, A. Brice, and C. Van Broeckhoven. 1996. Molecular genetic analysis of the 17p11.2 region in patients with hereditary neuropathy with liability to pressure palsies (HNPP). *Hum. Genet. 97:26.*

151. Lippert, M. J., J. A. Nicklas, T. C. Hunter, and R. J. Albertini. 1995. Pulsed field analysis of hprt T-cell large deletions: telomeric region breakpoint spectrum. *Mut. Res. 326:51.*

152. Olsson, P. G., H. Rabbani, L. Hammarstrom, and C. I. Smith. 1993. Novel human immunoglobulin heavy chain constant region gene deletion haplotypes characterized by pulsed field electrophoresis. *Clin. Exp. Imm. 94:84.*

153. Barr, F. G., R. J. Davis, L. Eichenfield, and B. S. Emanuel. 1992. Structural analysis of a carcinogen-induced genomic rearrangement event. *Proc. Natl. Acad. Sci. USA 89:942.*

154. Zion, M., D. Ben-Yehuda, A. Avraham, O. Cohen, M. Wetzler, D. Melloul, and Y. Ben-Neriah. 1994. Progressive de novo DNA methylation at the bcr-abl locus in the course of chronic myelogenous leukemia. *Proc. Natl. Acad. Sci. U.S.A. 91:10722.*

155. Antequera, F., J. Boyes, and A. Bird. 1990. High levels of de novo methylation and altered chromatin structure at CpG islands in cell lines. *Cell 62:503.*

156. Conrad, M., and M. D. Topal. 1992. Modified DNA fragments activate NaeI cleavage of refractory DNA sites. *Nucleic Acids Res. 20:5127.*

157. Mengle-Gaw, L., D. Albertson, P. Sherrington, and T. Rabbitts. 1988. Analysis of a tumor-specific breakpoint cluster at human chromsome 14q32. *Proc. Natl. Acad. Sci. USA 85:9171.*

158. Korsmeyer, S. J. 1992. Chromosomal translocations in lymphoid malignancies reveal novel proto-oncogenes. *Annu. Rev. Immunol. 10:785.*

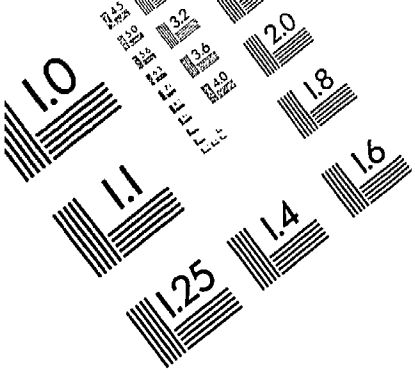

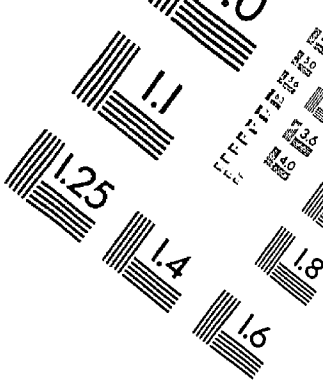

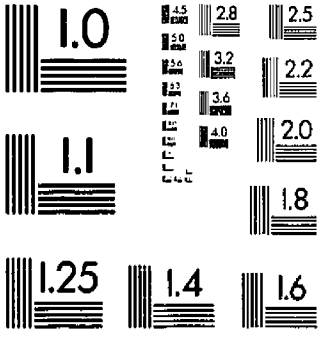

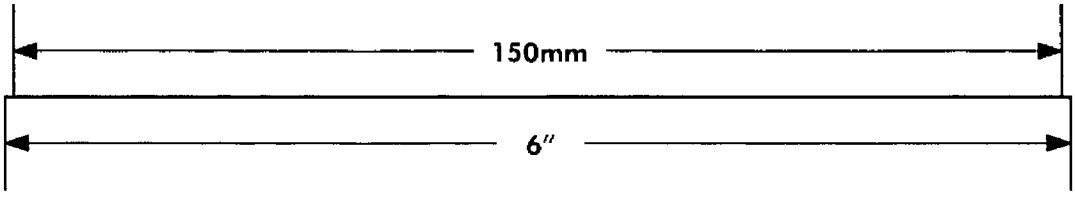

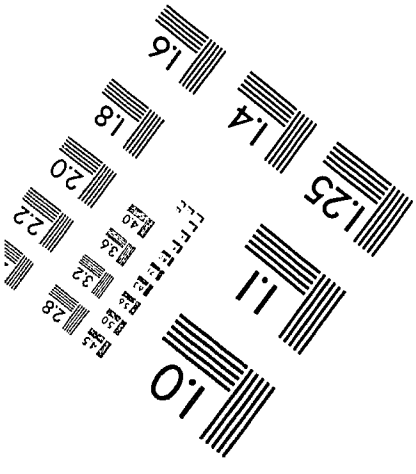

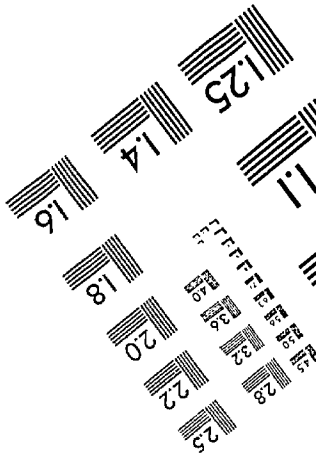

APPLIED IMAGE, Inc
1653 East Main Street
Rochester, NY 14609 USA
Phone: 716/482-0300
Fax: 716/288-5989

© 1993, Applied Image, Inc., All Rights Reserved